Geochemistry of Fossil Lake:
Limnogeologic controls on accumulation of REEs and Th in fossils and sediments

A Thesis Presented

by

Brian Christopher Titone

to
The Graduate School
in Partial Fulfillment of the Requirements
for Degree of
Master of Science

In

Department of Geosciences

Stony Brook University

December, 2004

Stony Brook University
The Graduate School

Brian Christopher Titone

We, the thesis committee for the above candidate for the Master of Science degree,
Hereby recommend acceptance of this thesis.

_____

E. Troy Rasbury, Advisor, Assistant Professor
Department of Geosciences

_____

Richard. J Reeder, Professor
Department of Geosciences

_____

Gilbert N. Hanson, Distinguished Service Professor
Department of Geosciences

Abstract of the Thesis

Geochemistry of Fossil Lake:
Limnogeologic Controls on Accumulation of REEs and Th in Fossils and Sediments

by

Brian Christopher Titone

Master of Science

in

Department of Geosciences

Stony Brook University

2004

Eocene Fossil Lake provides a high resolution record of sediments, fossils and cycles. Fossils from this ancient lake have been found to contain high amounts of thorium and Rare Earth Elements (REEs). Because these elements are not typically mobile in nature, the environments of deposition were investigated to better understand the controls on mobility of these important trace elements. Carbonate alkalinity is believed to play a key role in the concentration of Th and REEs in Fossil Lake. Changes in REE patterns and concentrations of the REE and Th appear to be related to facies that can be understood in terms of the changing conditions that would be expected during contraction and expansion of the lake.

Rock facies of Fossil Lake can be grouped into four types that reflect water depth: bioturbated micrite (BM), partly burrowed laminated micrite (PBLM), kerogen poor laminated micrite (KPLM), and kerogen rich laminated micrite (KRLM). These sedimentary facies represent stages of lake water as the lake area expands and contracts. Examination of REE patterns of rocks and fossils from Fossil Lake and its Eocene neighbor Lake Gosiute using XRF and ICP-MS analysis, compared with REE patterns from modern lakes from the Great Basin area show a striking similarity. Due to this strong correlation, it is speculated that precipitated minerals reflect the REE abundances of the lake water. Mono Lake water matches closely in REE pattern to fossil bone samples. The fossil bones most likely represent the bottom waters (monimolimnion) of Fossil Lake. Mono Lake is a very alkaline stratified lake similar to what Fossil Lake may

have been like. This is perhaps representative of the deep water highstand stage of Fossil Lake.

REE patterns of Walker Lake water match those of micro-laminated calcite samples. Walker Lake is an alkaline lake that produces calcite stromatolites and has a known fish population that is resistant to the high alkalinity and pH. This is believed to represent the surface water environment (mixolimnion) of Fossil Lake during highstands. Summer Lake is a shallow saline and alkaline lake. The REE pattern from this lake matches up well with dolomitic stromatolites of the Washakie Basin and calcitic oncolite samples of Fossil Lake. It is believed that dolomitic samples require a saline environment to form. This would place these samples in the lowstand shoreline deposits.

Mobility of Th and REEs is due to complexation with aqueous carbonate species. Modeling confirms that the dominant aqueous species in the expected pH range of Fossil Lake was carbonate. Incorporation into fossil bones is believed to be facilitated through local environmental changes around decaying fish, which may allow efficient incorporation of Th and REEs in both the carbonate and phosphate phase.

Table of Contents

List of Figures

List of Tables

Acknowledgements

I would like to first thank the helpful advice and availability of my advisor Troy Rasbury throughout my time spent here at Stony Brook. She was always available and eager to talk about my research and had so much enthusiasm. Without all of her invaluable help I wouldn't have had the confidence to complete this work and I will always be indefinitely grateful. She always had her door open and I can't even count how many hours I spent talking (and at times arguing) about the GRF. She always had an intuitive view on something and was always coming up with new ideas that made working with Troy very dynamic and exciting. Thank you so much!

I would like to thank Rich Reeder for helping me understand geochemistry and encourage me to do experiments. Even though the experiments we planned out didn't transpire, I am still thankful for his willingness to talk about my research and the help in designing our un-realized experiments. He was also very helpful in putting the final touch-ups on the final work.

Gil Hanson really showed me what being a geologist is all about. He is so involved with the department and cares so much about all of his students. He runs a very difficult class, but it taught me what it was to be a graduate student. I call Gil's class "graduate initiation", kind of a form of hazing. It definitely helped me build character as a graduate student.

Bill Holt worked me hard as his TA for two semesters, but it was worth it. He reviewed my grant proposal which was accepted and did it at the last possible minute (in the style of Bill anyway). That was a big help to me in getting that grant and allowing my research to get where it has gone.

Great thanks go out to Arvid Aase of Fossil Butte National Monument for being my guide in the field and taking time to answer questions. He also provided me with really neat samples! Paul Buchheim of Loma Linda University was also a big help in supplying samples and a lot of helpful feedback on my work.

Thanks also to Bob and Bonny Finney of Kemmerer, Wyoming who let me collect samples in their quarry. They are tremendously nice and generous people and if you like fossils you should visit www.fossilfishco.com and buy some of their specimens.

Thank you to the Geological Society of America for their generous grant award I received in 2003 to carry out my field work in Wyoming.

Thank you to Matt Whitaker, because without him, I wouldn't have even come to Stony Brook and have gotten as far as I have. Thank you from the bottom of my heart. Thanks for not giving up and believing in me. Stay well and best of luck in the future.

Thanks to Nick Tosca, Joel Hurozitz, Andy Winslow, Jenna Cole-Celestian, Aaron Celestian for helping me with getting started when I arrived at SB. Thanks to Dave Martin and Jennie Munster-Martin for being great friends and sharing with me lots of good conversation and internet game play. Also I'd like to give a shout out to Corey Cohn, my nemesis on the handball court and tour guide to underground LI.

Thank you to the rest of the geosciences department grad students, staff and friends that took time to chat and share stories. I'll never forget the times spent in the beer room.

Thanks to Jim Quin of Materials Science for the SEM work. Thank you also to Don Lindsley for his skill in operating the electron microprobe.

Thank you to Amy Bentow for taking time out for helpful reviews and edits.

Thank you to Danielle Odette for lending me her computer when crunch time hit.

I would also like to thank my family (Mom, Dad, Grandma and Grandpa, Aunt Diane, and my brother James) and my friends (Adam Duckworth, Chris Raineri (and Amanda), Dave Crudele (and Brenda), TJ Sitrin, Mike Gosiewski, Mike Naclerio Mike Sivilli and others). They teased me for being the last one left in school, but they always took an interest in what I was doing despite not having a clue what I was talking about. They always supported me and encouraged me to do well and to never give up. Thank you all for your love and support.

I would like to lastly thank my very close and dear friend Rebecca H. Vogt. Without her love, encouragement, and intense grasp of the English language, I wouldn't have been able to put this thesis together. She was a loyal and trusting field assistant and followed me wherever I went, not knowing what might be ahead, through all of those long unknown bumpy dirt roads, off-roading in my Honda Accord. I am greatly indebted to her dedication and support through all the tough times. Because of her emotional support and careful edits, I can consider this work to be hers in every way that it is mine. This thesis could not be possible without her and words cannot describe how truly and utterly thankful I am to her.

Introduction

The Green River Formation (GRF) of the western United States has a plethora of economically important natural resources. It can also supply a wealth of knowledge about geochemical processes, lake dynamics, and evolutionary changes in animals. There are still many things to learn from this extraordinary lacustrine sequence.

Workers have tried to understand lake sequences to better understand how oil forms, how climate has changed, and how anthropogenic factors affect lake sedimentation in a modern lake setting. It is the intent of this study to understand the geochemistry of Th and Rare Earth Elements (REEs) present in the Eocene Green River Formation of Fossil Lake for the purpose of environmental and sedimentological reconstruction.

Th and REEs are elements that are not typically mobile in nature. It is because of this understanding that finding anomalous concentrations of these elements indicates an unusual environment. This research was initiated when a small fossil fish from the GRF was discovered to have levels of Th in its bone material (figure 1). By understanding the conditions that could lead to the anomalous enrichment in Th, we could learn more about sequestering and storing harmful waste elements similar in behavior to Th and the REEs using natural materials (bone) and "natural environmental conditions". Much can be learned in a laboratory, but the forces of nature are difficult to reproduce in a lab and the geologic timescale is impossible to endure in a lab setting. Instead, studying the fossils and authigenic sediments of the GRF and making links to modern lakes can allow us to glean much about a lake that existed some 50 million years ago.

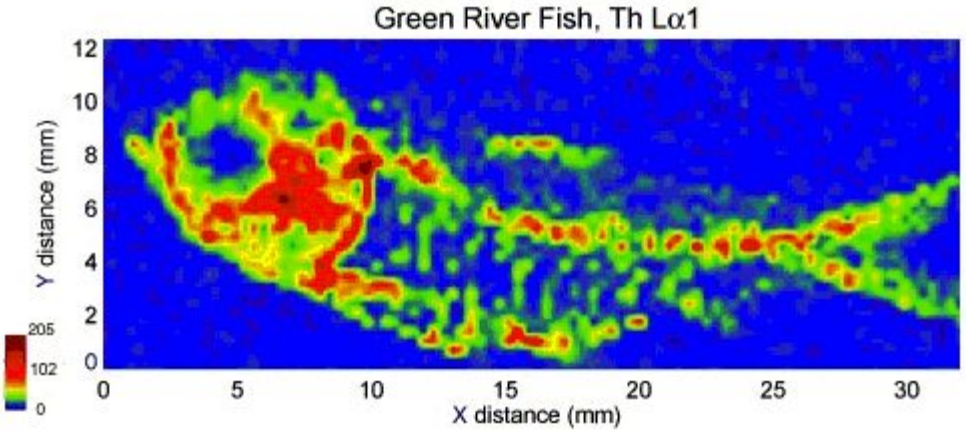

Figure 1. Synchrotron X-ray fluorescence map of a fossil fish from the Fontanel Member of the GRF. Warm regions depict high concentrations of Th.

Geologic and Limnogeologic Background

Geologic History

The Green River Formation (GRF) is the bulk name for all of the lacustrine rocks formed in the Eocene which range from southwest Wyoming to northeastern Utah and western Colorado (figure 2). The two large lakes that formed the rocks of the GRF were Lake Gosiute of Wyoming (figure 3) and Lake Uinta of Utah and Colorado. These lakes were separated into two basins each by tectonic uplifts. The Green River Basin and Washakie Basin were the northern basins, and the Uinta Basin and Piceance Creek Basin were the southern basins (figure 2). These pairs of basins may have been connected at one time in the lakes' history, perhaps more than once. The basins, however, were independent enough to have their own unique deposits. Off to the western edge of the Green River Basin is a small basin, which is often not included with Lake Gosiute, called Fossil Basin. This is one of the most famous areas of the GRF because of the vast deposits of fossils that are found there (Buchhiem and Eugster 1998).

The climate of the Early and middle Eocene was much different compared to what we see today. Levels of CO_2 were slightly higher on average than present day (Pearson and Palmer 1999) but peaked to 700-900ppm between 54-50 Mya (Pearson and Palmer 2000) with even higher estimates up to 2500ppm proposed by others (Demicco, Lowenstein and Hardie 2003). Though it is not clear how this had an impact on the environment directly, the combination of these factors made this epoch a very unique depositional environment, especially in the upper Lost Cabinian time.

It is believed that the Paleocene-Eocene Thermal Maximum (PETM) occurred at the end of the Tipton and into the Wilkins Peak. It was at this time that ocean temperatures rose significantly and caused the release of methane hydrates from the ocean floor (Thomas 2002). This caused surface temperatures to rise which may have been the cause of the evaporation of the lakes during the Wilkins Peak. This may have caused the buildup of alkalinity in the lake over the preceding time allowed the Wilkins Peak to produce the unusual suite of minerals we find today. Many of the rare minerals found in the GRF have been found only in the GRF (Milton 1971) which only reiterates that this was a unique environment in geographic location and in climate.

Prior to the sedimentation of the GRF, a major tectonic event, the Sevier Orogeny took place starting around 150 million and ending around 55 million years ago (Lageson and Spearing 1991). This major tectonic event was responsible for the Wyoming overthrust belt that separated Fossil Basin from the larger Lake Gosiute. The event closed just prior to the filling of Fossil Lake, but further tectonic deepening of the lake or uplift of surrounding of terrain from this event could have kept the accommodation space in the lake available for the duration of the lakes life.

The basins of the GRF were separated by these tectonic uplifts that closed the basins from any major drainage to the sea. This allowed the sediments in the lakes to accumulate and inevitably cause the demise of the lake. The lateral extent of the lake and uplifted regions which separated the GRF into the various basins can be seen quite well in figure 3. The Rock Springs uplift is the prominent pink and orange feature near the lower center. The Wyoming thrust belt can be seen to the left side of the figure showing a contrast of older lithologies suggesting how isolated Fossil Lake was during the early

Eocene. Fossil Basin, which is the focus of this study, is believed to be equivalent to Tipton in age and spans approximately one million years (Grande 1984 figure 4).

The sedimentary deposits of Lake Gosiute are broken up into three main members: Tipton, Wilkins Peak, and Laney (figure 4) (Desborough 1978, Grande 1984). The Tipton member is the oldest of the formation and represents a wet, semi-tropical period of time where the lakes were filling up and were fairly deep. The Wilkins Peak member represents an evaporitic time in the lake's history where the lake saw its smallest lateral extent and became shallow. This member is where the famous deposits of trona and other sodium-carbonate evaporite minerals such as shortite formed. These deposits are some of the richest in the world. The Laney member is the youngest of the three and is again the representative of a wet semi-tropical time where lake levels increased and freshened. At the very close of the Laney, the lacustrine rocks grade into fluvial deposits as the lake basin became shallow to a negligible depth because of substantial infilling with sediments (Desborough 1978).

The mineralogy and resources found in the GRF are quite vast. The formation is renowned for its "oil shale" which is defined as rock that yields two or more gallons of oil per ton from distillation (Desborough 1978). The "oil" is in the form of kerogen and has been described to have been formed from the accumulation of blue-green algae remains (Bradley 1948). Estimates suggest that reserves of 75 billion barrels of crude oil are possible from the GRF (Bradley 1948) but trillions are estimated now. The other mineralogical riches found in the GRF are the sodium-carbonate minerals as described above. These deposits, some of the largest in the world, are found in the subsurface near Green River, Wyoming.

Limnogeology

The GRF have facies that could be interpreted to have formed in a stratified lake or in a playa lake (Eugster and Surdam 1973, Surdam and Wolfbauer 1975, Boyer 1982, Fischer and Roberts 1991). Boyer (1982) and Fischer and Roberts (1991) argue that Lake Gosiute went through both of these types, or modes. On the large scale, the Tipton and Laney members represented the stratified mode while the Wilkins Peak represented playa mode.

Playa Lake Model

The Playa lake model was proposed by Eugster and Surdam (1973), Eugster and Hardie (1975), and Surdam and Wolfbauer (1975). These authors infer that the micro-laminated sediments of the Tipton and Wilkins Peak of the GRF were created in a playa setting. Surdam and Wolfbauer (1975) suggest "Lake Gosiute is an ancient lake without modern analog." However, they still use a modern analog for comparison, Deep Springs playa which does not have micro-laminated sediments in the center but instead has evaporitic sediments. They propose a three facies system where the distribution pattern is independent of water depth (Surdam and Wolfbauer 1975). Their three facies do not support a playa-type lake because a key part of their ideal playa lake is an evaporitic salt in the center, which is absent in the Tipton. They fail to explain why there is oil shale in the center of the Tipton rather than trona. The playa lake model fails to consider biologic

factors that appear to be an integral part of oil shale production (Desborough 1978). Other flaws in the playa lake model are believed to be fossil assemblages, similarities to modern meromictic lake lamination and examples of Quaternary playas that become meromictic lakes with increased flow (Boyer 1982).

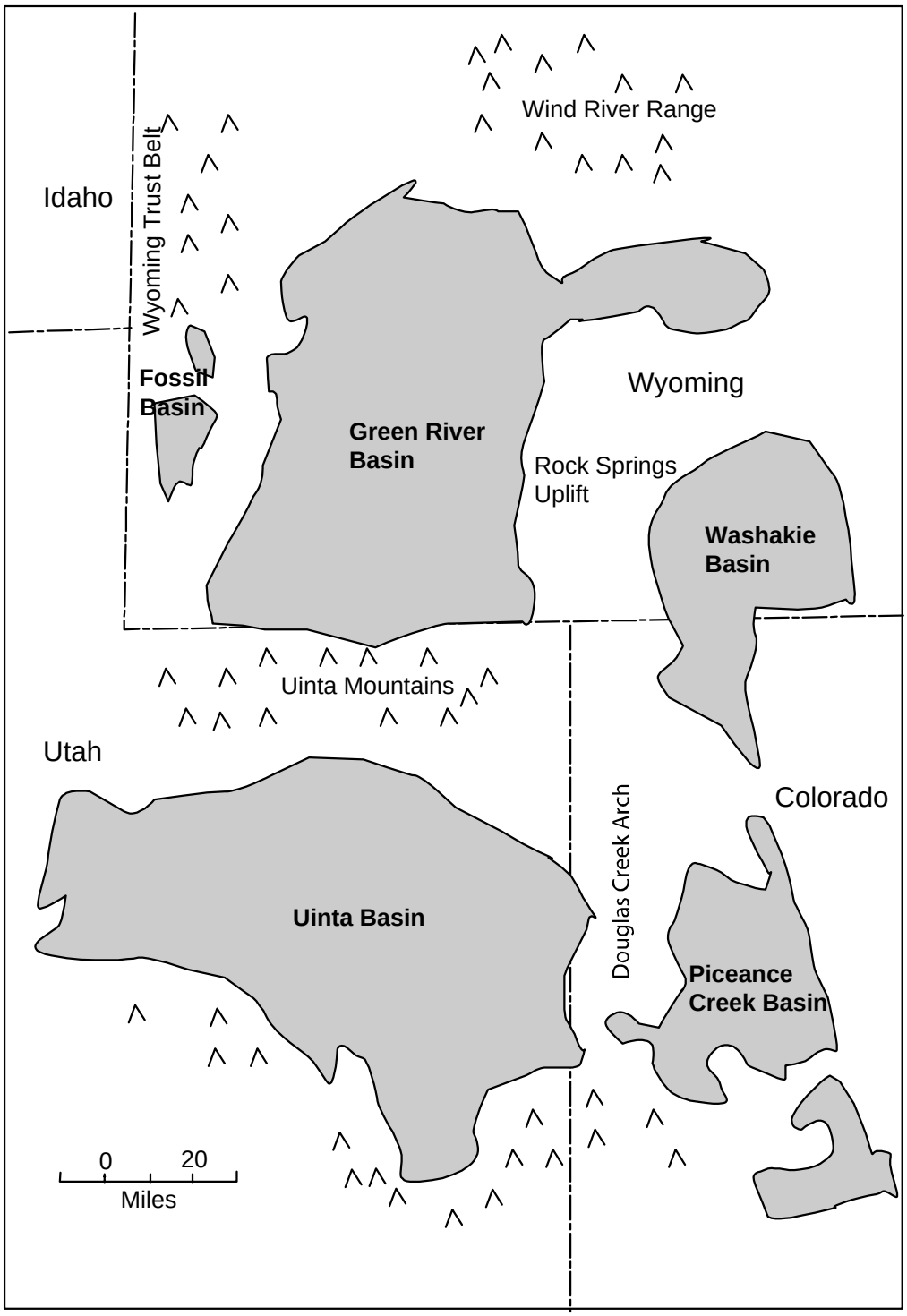

Figure 2. Simplified map of the geographic outcrop locations of the Green River Formation. Fossil Basin is the area to the left of the Green River Basin (After Shanks et al. 1976).

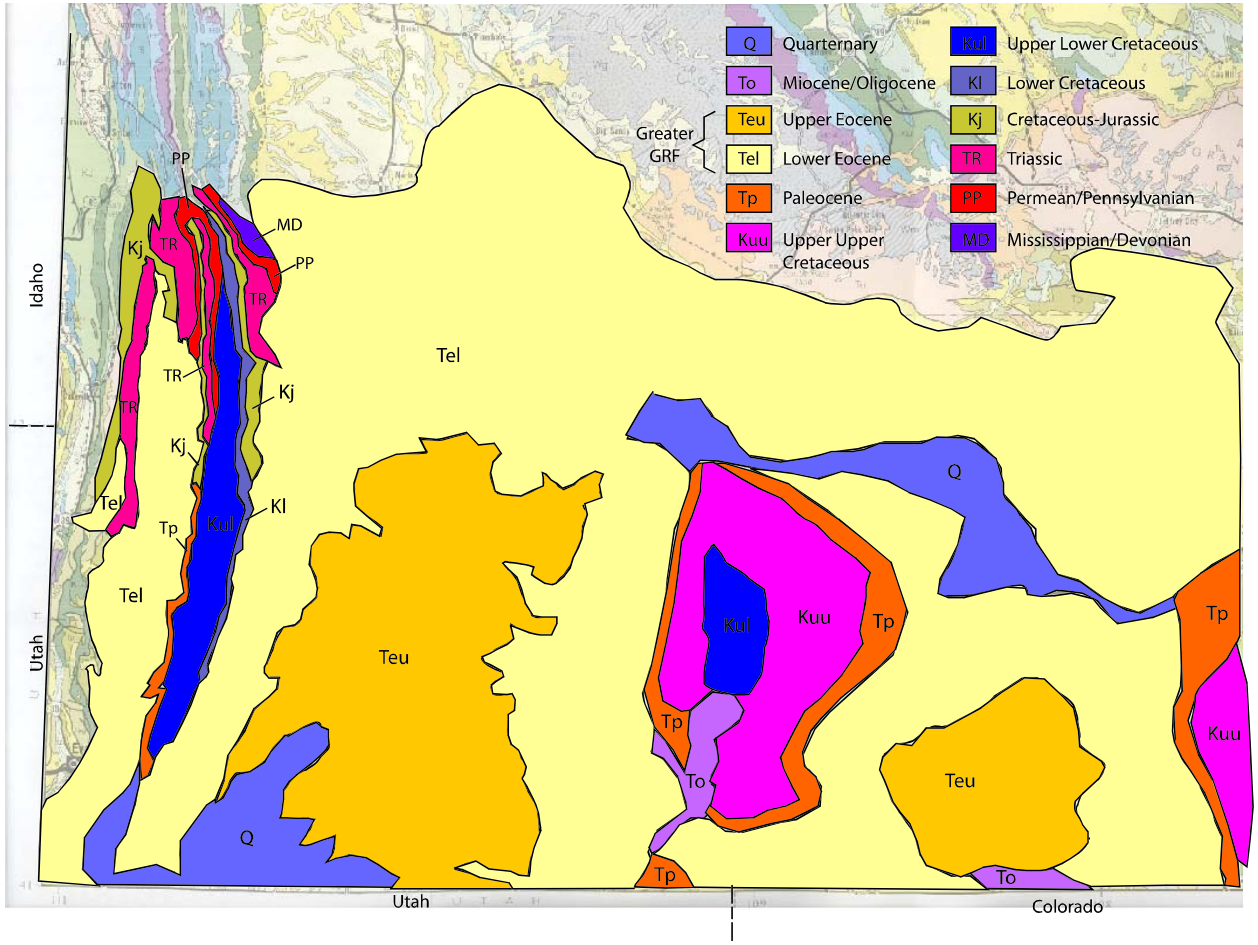

Figure 3. Simpilfied geologic map of the Green River Formation Lake Gosiute area. The GRF lithologies are depicted in the key at the top. Uplifted areas are clearly seen where older rocks appear on the surface. After Christiansen 2001.

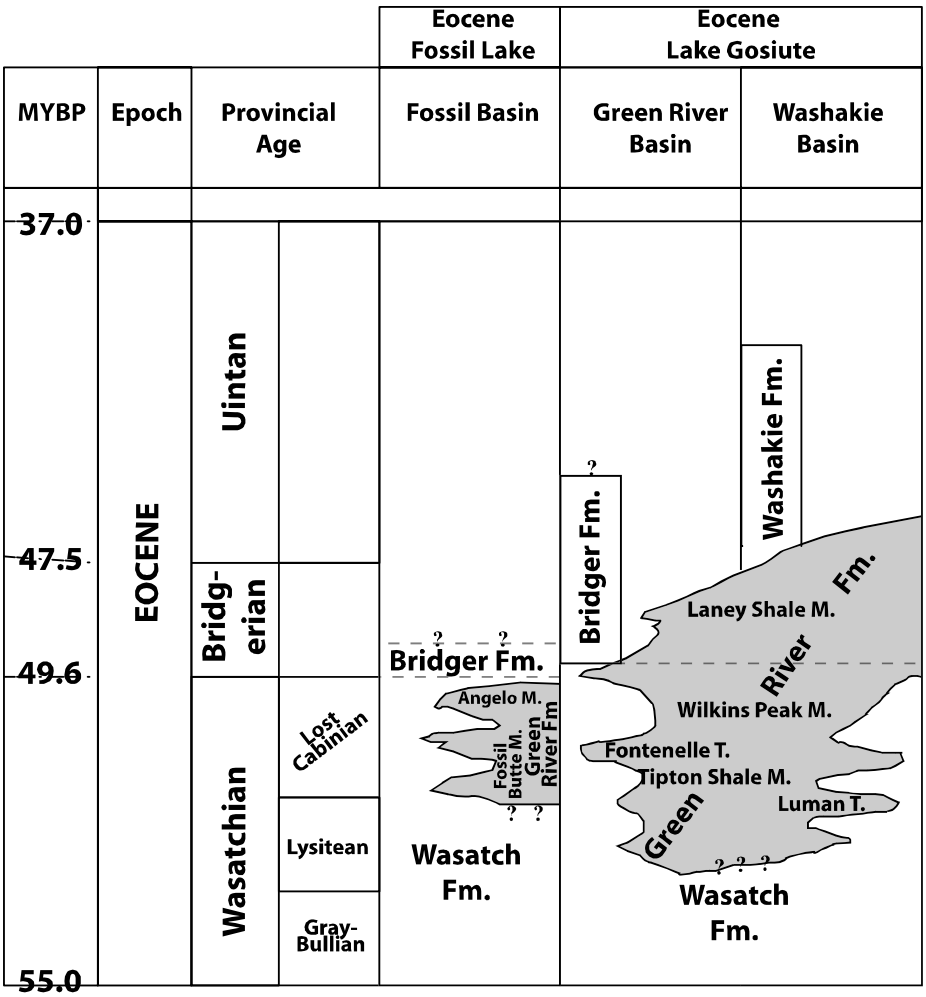

Figure 4. Age relation of Fossil Basin and Lake Gosiute Basins (after Grande 1984). Samples collected are from the Fossil Butte Member of Fossil Basin and some from areas in the Green River and Washakie Basins.

Though the playa lake model as a whole seems to have flaws, it still has qualities that can be embraced in meromictic models. The idea that the Tipton began as shallow ponds and lakes on a subsiding plain and then began to fill up seems to be valid. But this only explains the initial stage. A model of a playa being "drowned" to become meromictic seems plausible due to the density contrast between fresh and saline water (Boyer 1982). This is called ectogeneic meromixis. Fluctuating lake levels play a key role in the small-scale cyclitic of the sedimentation of the GRF in all basins that cycle between a stratified highstand and lowstand (Surdam and Wolfbauer 1975). The interpretation of the Wilkins Peak member being a playa lake seems to be quite reasonable because of the extensive trona deposits that are present in about 60 different distinct layers (Eugster and Surdam 1973). Trona requires very unique environmental conditions to form suggesting that the basins of GRF were unique during evaporitic times and through the duration of the lakes' history. Tuttle and Goldhaber (1987) estimated the pH of the GRF to be near 11, which is not typical of natural modern environments.

The sediment facies produced in the playa lake are defined by Surdam and Wolfbauer (1975) as (1) marginal silts and sands, which are comprised of calcite concretions and calcareous cement, (2) carbonate mudflat, which is comprised of calcite and/or dolomite, and (3) lacustrine which is made up of trona or oil shale. The first two types of sediments, however, can be easily found in deep water lacustrine systems along the lake fringes. Any lake that has gently sloping ramps leading to the lake would have sediments such as these. This is especially true for Fossil Lake which formed in a long narrow north-south oriented basin. Fluctuating lake water would allow wetting of the surrounding area and decreased inflow which would lead to mud cracks. Trona formation is the main argument behind the playa lake model. There are no evaporitic minerals that form in Fossil Basin until the final infilling of the basin in the Angelo Member (Buchheim and Eugster 1998), but yet there are still mudflat and calcite deposits throughout the entire lake history. This suggests that the deposits mentioned by Surdam and Wolfbauer (1975) do not require a playa environment to form, or that a playa-like environment was present as part of the stratified lake system.

Stratified Lake Model

The stratified lake model for the GRF has been around since the pioneering work of Bradley (1948) and workers have continued to embrace it (Bradley 1963, Bradley and Eugster 1969, Desborough 1978, Boyer 1982). This model explains nearly all of the features of the GRF.

Stratification in a lake can involve one or both of two main factors: thermal stratification or chemical stratification (Wetzel 2001). The type of lake that may best describe the GRF lakes is a meromictic lake.

A meromictic lake is a type that does not undergo complete circulation and the primary upper stratum of water does not mix with the lower (Wetzel 2001). This type of lake has an upper zone of mixing (mixolimnion) which overlies the stagnant saline layer (monimolimnion). These layers are separated by a chemocline, similar to how a thermocline separates density layers in a thermally stratified lake. This condition can exist even without a high amount of salinity because water density increases 0.0008g/ml with the addition of 1g/L of salt (Wetzel 2001). A change in temperature from 4 to 5 degrees C changes water density by 0.000008g/ml. Because of this, it would take a formidable change in temperature in upper waters to mix with saline strata below. Meromixis can last permanently or can persist for long periods of time but depends on the stability of the stratification, which is a function of surface area, depth of water, and wind circulation.

Bradley (1948) showed how lakes can become stratified, remain stratified and ways they can mix. His justification for speculating stratification of the GRF was the abundance of carbonate minerals (calcite and dolomite) and the preservation of organic matter. He argued that organic matter needed an oxygen-free environment at the bottom of a lake to be preserved (Bradley 1948). Boyer (1982) proposed a model that utilized both a playa and a stratified lake in an ectognic-meromixis case. This lake type begins with a playa lake and is then drowned under increased freshwater input preserving the playa waters as the monimolimnion.

Sedimentation in a lake is governed by a variety of things. Lake water chemistry, stream input rates, wind strength and bottom topography are some factors that can control sedimentation. A limnogeologic model has been proposed for Fossil Basin based on rock facies relations (Buchheim and Eugster 1998) (figure 5). The sediments closest to the lake margin are dominated by stream input including conglomerates, sandstones and mudstones. Further away from the lake shore is the biturbated micrite (BM) facies. These are typically thick because they are closest to the shore and incoming Ca rich waters that precipitate calcite. While these facies contain fossils, the preservation is poor because of scavengers. The next furthest out are partly burrowed laminated micrite facies (PBLM). These contain high amounts of fossils most likely because this zone borders where the chemocline resides. The next facies is the kerogen-poor laminated micrite (KPLM). This is somewhat thinner than the previous facies because of its distance from the lake margin. Calcite is derived from surface waters near the shore and thus accumulation of calcite slows with further distance from the shore. This facies contains abundant articulated fossil fish. Because this region may be within the monimolimnion, laminations remain intact due to the lack of bioturbating fauna. The final, deepest, and thinnest facies of the lake sequence is the kerogen-rich laminated micrite (KRLM). This type is still dominated by calcite, which is derived from shore and surface precipitation but contains a significant amount of dolomite and a minor fraction of unidentified alumino-silicate minerals. The presence of dolomite suggests in-situ diagenetic formation from interaction with saline monimolimnion pore water. Some workers have suggested that the dolomite is allocthanous and forms on the playa (Boyer 1982). The actual source of the dolomite has not yet been determined. The alumino-silicate minerals may be detrital in origin and most likely due to slow settling of water-borne clay particles which settle out slowly (Boggs 2001). This allows detrital components to reach the lake center. Because there is less accumulation of calcite in this facies relative to detritus, the dilution effect of the calcite is somewhat less significant. These minerals also may be autochthonous and form from the concentrated monimolmnion waters.

Some of the sediments of Fossil Lake resemble playa-type facies as defined by Surdam and Wolfbauer (1975). The geometry of the lake suggests that playa-like fringe sediments easily formed on the low angle flanking slopes. The lake formed in a long valley with one deep area centered south of Fossil Butte National Monument (figure 8). The rest of the lake remained fairly shallow, especially to the north and south where mudflats were common. Fluctuating lake levels caused the wetting and desiccation of these areas. The fossil taphonomy and rock facies are clear evidence that a portion of Fossil Lake was, for most of its life, a stratified lake.

Modern Lake Characteristics

An effective way to evaluate a limnogeologic model to an ancient deposit is to examine modern analogs. Some of the modern lakes that will be used for comparison to Fossil Basin will be briefly discussed. No one single lake can be a perfect analog. It is a well-known fact that like snowflakes, no two lakes are completely alike. They can change over time and from place to place within a lake. Though no one lake will be completely analogous, we can extract aspects of certain analogs and make a composite model. Based on the geology of the GRF, we can make some assumptions about the

environment of deposition. Once these main assumptions are made, analogs that fit similar descriptions can be examined and compared.

The Great Basin lakes are a group of lakes that span from southern Oregon to Nevada and eastern California. These lakes have no outlet to the sea, which has allowed the lakes to become considerably more saline and alkaline as their surface area shrank after the close of the Pleistocene Lake Lahontan. These lakes remain isolated from each other and any outlet to the sea. The surrounding rocks and source water may have an influence on the lake chemistry. Some of these lakes are supplied by underground springs that in turn produced tufa columns of massive proportion.

Mono Lake is a reasonable analog in some respects because of the high amount of actinides found in the water (Simpson et al. 1982), particularly Th. This lake has elevated alkalinity, phosphate and chloride, all of which seem appropriate for what the GRF may have exhibited. Johannesson, Lyons, and Bird (1994) studied REE patterns in Mono Lake and other Great Basin Lakes and showed relationships in HREE enrichment with carbonate complexes (figure 5). The lakes that exhibited this quality were lakes with a pH greater than 9.5. Carbonate complexation seemed to be a driving mechanism for concentrating aqueous species of REEs, especially HREEs, while LREEs are limited by precipitation of amorphous phosphate (Johannesson and Lyons 1994). Activity product calculations show for REE phosphate coprecipitates in Mono Lake indicate that saturation may be reached and that these coprecipitates limit the maximum dissolved REE complexes in the lake (Johannesson and Lyons 1994). Mono Lake was unstratified at the time of sampling in Johannesson's study due to anthropogenic effects of water input diversion. Because of this unnatural mixing and decreased inflow it is reasonable to assume that the water chemistry strongly reflects slightly diluted monimolimnion water chemistry. Mono Lake has such an elevated alkalinity that water entering the lake with any calcium content nearly immediately forms calcite. This has been evident from the tufa columns that formed from fresh water springs that entered the lake from the bottom (Buchardt, Seaman, Stockmann, et al. 1997). Calcite also does not seem to be precipitating from the center of the lake, but on the margins where fresh water input takes place. In water that has alkalinity that far exceeds calcium, the water will be alkaline and calcium and magnesium free (Cohen 2003). Waters of this type are not likely to precipitate any Ca-bearing minerals without the introduction of Ca to the system (Cohen 2003). As of today, Mono Lake fluctuates between being a monomictic and meromictic stratified lake ("Profile of Monomixis…" 2003.)

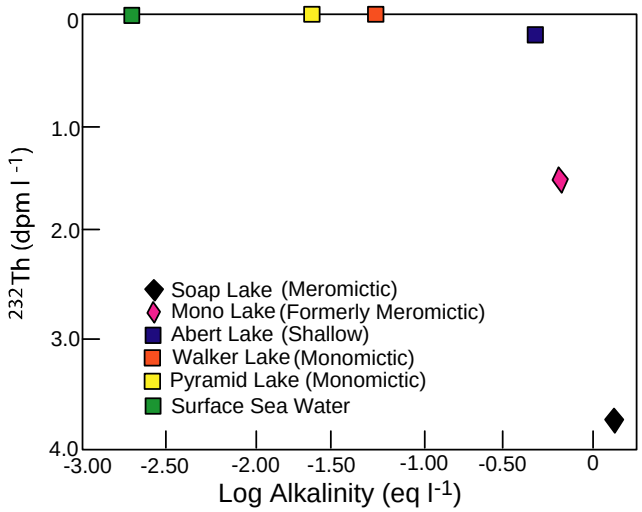

Figure 5. Alkalinity vs thorium content of some Great Basin Lakes. There is a clear trend between alkalinity and Th content of the lakes. Points are average values. AfterLaFlamme and Murray (1987)

Soap Lake is another similar analog stratified lake of note because of the observations of thorium-carbonate species forming in natural environments (LaFlamme and Murray 1987). In the study, LaFlamme and Murray noted how Soap Lake had a distinct chemocline where the alkalinity showed a drastic increase. At the same depth that the alkalinity increased, so did the amount of Th isotopes in the lake water which was up to four times greater than seawater (figure 6). The typical residence time for Th in seawater is approximately 75 days because of the particle reactability (Huh 1995). This causes the content of Th in seawater to be quite low. LaFlamme's conclusion was, based on observation and experiment, that thorium forms carbonate species in the water at high pH and alkalinity, thus resulting in higher concentrations in solution. Although REE patterns are not published from this lake, we can surmise that they would show patterns similar to those observed by Johannesson et al. (1994) because of the stratification.

Abert Lake is a shallow alkaline body of water which is no greater than 16' deep. It has a pH of 9.6 and is dominated by Na, Cl and CO_3 (Banfield, Jones and Veblen 1991). This lake has an abundance of calcite forming in the lake with calcite sediment percentage of over 40 in the lake center (Deike and Jones 1980). This is an example of a playa type lake precursor that may have been drowned by freshwater inflow causing ectogenic meromixis as in the model proposed by Boyer (1982). This could represent what Fossil Lake may have been like prior to lake deepening.

Walker Lake in Nevada is a monomictic (Cooper and Koch 1984) stratified alkaline lake that is noted for its stomatolites that are common on the shores (Osborne, Licari and Link 1982). This lake also contains three species of fish which show that even highly alkaline environments can sustain life for these animals. Calcite is not forming in the center of Walker Lake (Osborne, Licari, and Link 1982), probably because of the small amount of inflow carrying Ca into the alkaline lake and is quickly precipitated on the margins.

These modern analog alkaline lakes will be compared to Fossil Lake in greater detail in the results and conclusions sections.

Geochemistry

Behavior of Th in natural environments

A study of the mobility of Th in natural waters at low temperatures showed that Th was mobile in the hydroxide aqueous species form and bound to organic complexes in seawater (Langmuir and Herman 1980). Th forms strong complexes with F, SO4 and PO_4 in acidic conditions and OH species above pH 7.5. Organic acids played a role in the dissolution of thorianite. This study was not able to consider thorium carbonate complexes because of the lack of thermodynamic data at the time.

Simpson et al. (1982) and Anderson et al. (1982) reported high levels of actinides in Mono Lake, especially Th. They attributed this enrichment to CO_3^{2-},which was an important discovery for complexation of actinides and REEs.

Another important study observing Th in a lacustrine environment was by LaFlamme and Murray (1987) who observed that the Th content in Soap Lake was due to carbonate complexation. The solubility of thorianite was observed to increase with increasing alkalinity. The limiting factor for thorianite solubility seems to be the amount of alkalinity present in the water. Alkalinity also has an effect on the adsorption of Th (LaFlamme and Murray 1987). The higher the alkalinity of the water, the less adsorption to colloids in the water.

More recent studies by Östhols, Bruno and Grenthe (1994) and Östhols and Malmström (1995) presented more thermodynamic data on the formation of thorium carbonate species. These studies examined the solubility of ThO_2 in CO_2-H_2O media, and the dissolution kinetics of ThO_2 in acid and carbonate media respectively. These works, as well as data presented by Ingmar Grenthe from personal communication, were the basis for Th modeling in PHREEQCi presented in the modeling section.

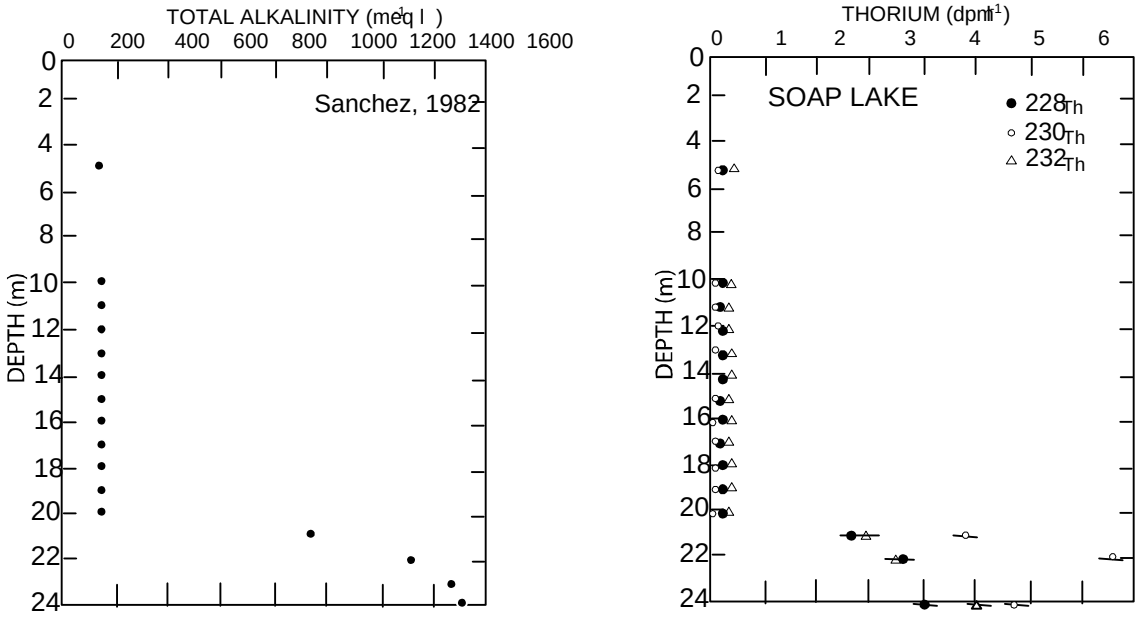

Figure 6. Alkalinity profile of Soap Lake (left) and Th profile of Soap Lake (right) after LaFlamme and Murray (1987) showing an association between alkalinity and Th content of the lake.

REEs in Natural Environments

REEs have behavior similar to that of Th in that they are very particle reactive and typically immobile in natural environments (Taylor and McLennan 1985). McLennan, Nance, and Taylor (1980) show a correlation in the La/Th ratio with fine-grained sedimentary rocks of various ages in Greenland and Australia. McLennan and Taylor (1979) showed mobility of REEs is due to carbonate complexing during metamorphism. Johannesson and Bird (1994) and Johannesson, Lyons and Bird (1994) observed REEs in Mono Lake and other Great Basin lakes. Observations were made that the main control of REE solubility is carbonate complexing. Mono Lake is enriched in HREEs, which is not indicative of the signature from the surrounding rocks which are LREE enriched. The HREE enrichment is due in part by the higher affinity for HREEs to complex with carbonate and the saturation of the water with respect to phosphate precipitates which limit the dissolved REE concentrations in the lake (Johannesson and Lyons 1994). This finding was similar to four other lakes found in the Great Basin region (Johannesson, Lyons, and Bird 1994). Carbonate complexing is still important because carbonate remains in the water as an aqueous species while phosphate is believed to precipitate out.

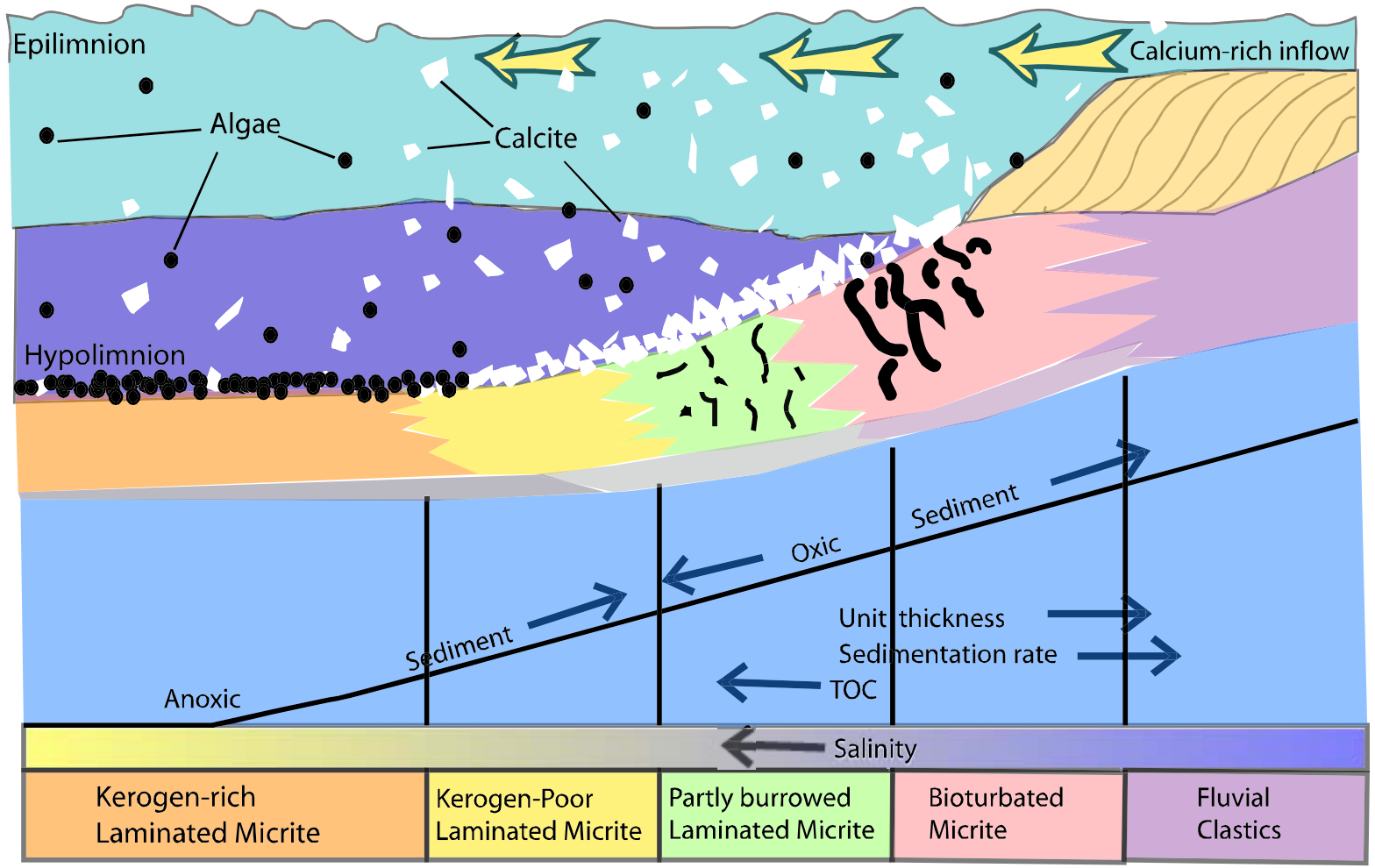

Figure 7. Facies relations of Fossil Basin based on the rock record. Organic content increases toward the lake center while unit thickness and sedimentation rate increase toward the shore. The accumulation of algae is more prominent in the deep lake center because of less dilution form calcite. Modified from Buchheim and Eugster (1998).

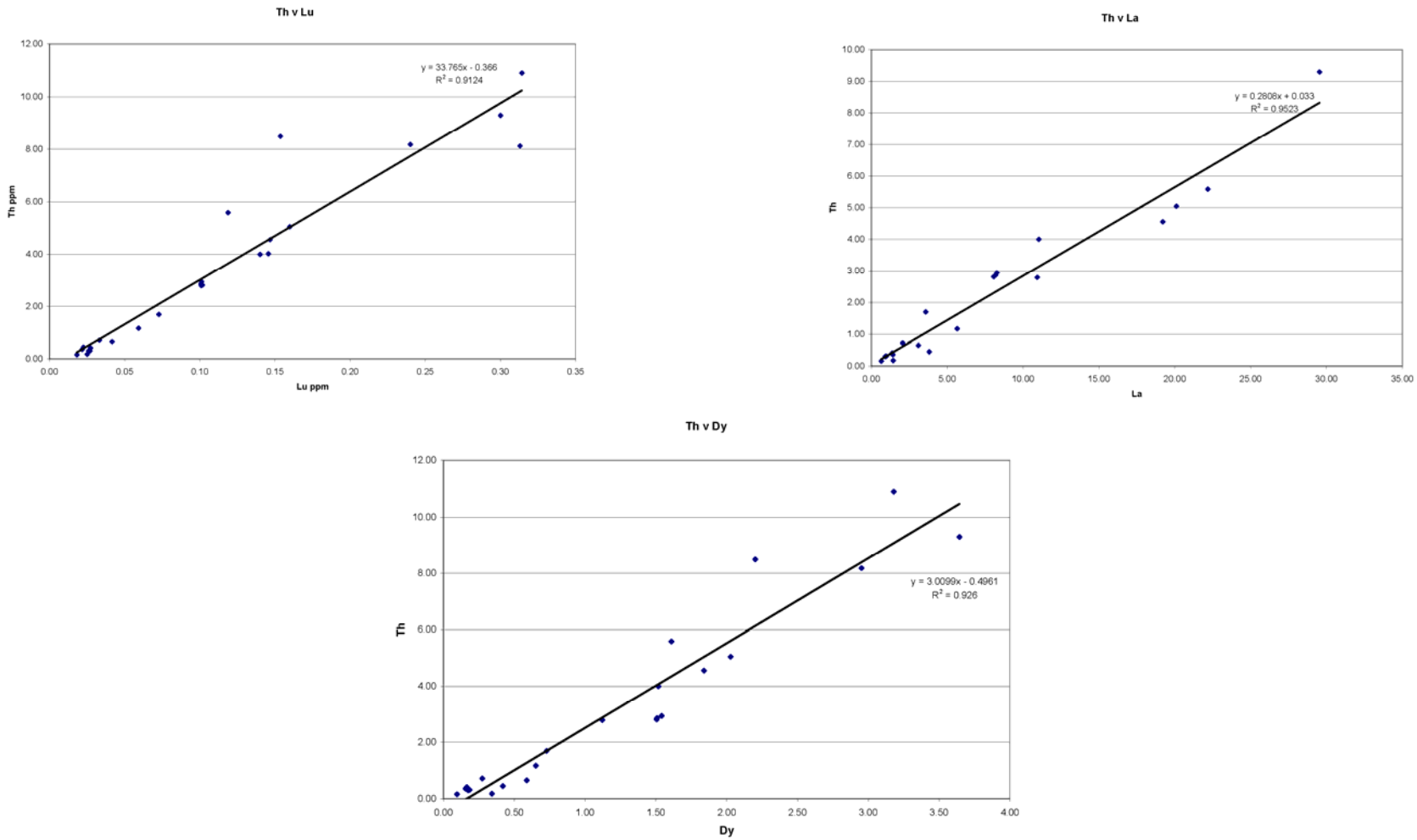

Figure 8. Th v Lu, Th vs. La, and Th vs. Dy plots of samples from table 2. Samples GR4, S3-B, D3-B, and TS1 are not represented in these plots. These all show very linear trends between them suggesting that the behavior of Th an REEs are similar.

Methods

Rock Sampling for Trace Element Analysis

In order to understand how REEs behave, it is essential to have a model that allows us to understand how facies might be related to changing lake chemistry. In this study, the samples chosen were based on criteria that were thought to fit the originally incepted model. A hypothesis was formulated based on observations in Soap Lake by LaFlamme and Murray (1987) that there would be differences in Th and REE enrichment in fossils found in the mixolimnion or the monimolimnion. Sample locations were therefore chosen to represent deep water deposits and shallow water deposits. There can be limitations to this approach. The actual depths of the lake water that produced the sediments are difficult to determine but can be estimated with reasonable certainty. It is important to realize that fossils of different fish can have varying densities and compositions based on the local water chemistry in the lake. It is there fore possible to find a small thin fossil that may have higher concentrations than larger fossils in close vicinity. Fossilization happens over a time span that would reflect an average so if a small fossil began forming in a time rich in aqueous species, this may reflect a high overall concentration. If a larger fossil began at the same time it may only reflect some of that time rich in aqueous species and more time lean in aqueous species.

Field Selection

Samples of fossils and accompanying rocks were collected from varying depth facies from the Fossil Basin in Lincoln County, in the state of Wyoming. Sample locations are noted on map figures 2 and 9 and in table 1. Sample photos and autoradiography of the samples are shown in Appendix D.

The first site of sample acquisition was “Smith Hollow Quarry” (figure 9, labeled SHQ) which is a commercial quarry that mines fossil fish from the 18” “sandwich” layer. This quarry is due south of Fossil Butte National Monument (FBNM). This deposit represents KRLM type samples (Buchheim and Eugster 1998). Abundant fish fossils are found at this location, many of which are large and well preserved. The samples collected here are from 10 cm below the 18” layer and consisted of a few small pieces of fish bone and some micro-laminated carbonate (“shale”).

The second sample location was another commercial fossil quarry (figure 9, labeled FIN) owned by Bob and Bonnie Finney which is east of FBNM. This quarry is interpreted to represent shallow water lake environment because of the abundance of small and juvenile fish and the presence of turtles, birds and palm fronds (Buchheim and Surdam 1981). The rock found here is generally buff and is finely laminated with alternating layers of organic material and micrite. These are considered KPLM by Buchheim and Eugster (1998). Fossil samples here were generally plentiful. Also collected here were two layers of ash that were above the main body of fossils (samples AU1 and AL1).

Oncolites were collected further to the north towards the margin of Fossil Lake (see figure 9 and table 1 for detailed location). The oncolites were found in a gray weathered outcrop of limestone. The oncolites are spherical to elliptical in shape ranging in size

from a hazelnut to a grapefruit. Alternating medium dark gray and dark gray concentric rings can be seen throughout the samples in cross section. Some samples were in matrix which is a hard contrasting lighter gray limestone. These samples would represent the lake shore environment. These are believed to be part of the lower Road Hollow unit which is the lower of the three units in Fossil Basin (Buchheim personal communication) (refer to Appendix E for stratigraphic column of Fossil Basin).

XRD and SEM Analysis

Powder XRD analysis was performed on a Scintag X-ray diffractometer. All of these analyses were done using Cu Kα radiation and at a step rate of 0.5 degrees/min in a 2θ orientation. Minerals were determined by matching 2-theta values from the PDF (Powder Diffraction File) database (figure 10). Thin sections of the two fossil bones were made and analyzed with a scanning electron microscope. These samples were carbon coated and observed through the SEM using backscattered electrons (figures 11-12). Energy Dispersive X-ray analysis (EDX) was done to aid in determination of the minerals present in the samples.

Geochemical Analysis

Samples collected were initially screened for further analysis by autoradiography techniques (Cole et al. 2003). This allowed spatial and quantitative approximations of the concentrations of Th and U in the samples (Appendix D). Based on the data, samples were selected for more detailed spatial analysis at Brookhaven National Lab. National Synchrotron Light Source Beamline X26A (figure 1).

Analysis of major and trace elements was performed by the Geoanalytical Laboratory of Washington State University. Analysis of 27 major and trace elements was done using a Rigaku automated X-ray fluorescence spectrometer (XRF) analysis (Johnson, Hooper, and Conrey 1999). REE analysis was done using a Hewlett-Packard inductively coupled plasma mass spectrometer (ICP-MS). Loss On Ignition (LOI) was recorded for each sample prior to the XRF process. The percentage recorded is a measure of all volatiles that are lost during heating of the sample which includes organics, water or volatile elements like F or Cl. Analytical data is presented in appendix A.

Samples, prior to outside analysis at WSU, were first crushed using either a steel mortar or a ceramic mortar to obtain a usable size. The samples were then powdered in an agate shatterbox. Each grinding was “pre-contaminated” prior to sample grinding. “Pre-contamination” is a practice of powdering a small amount of the new sample in the grinding container and eliminating that fraction, then powdering the bulk sample. This reduces contamination by diluting any material from pervious samples. The shatterbox was completely washed out with running water and dried after each grinding.

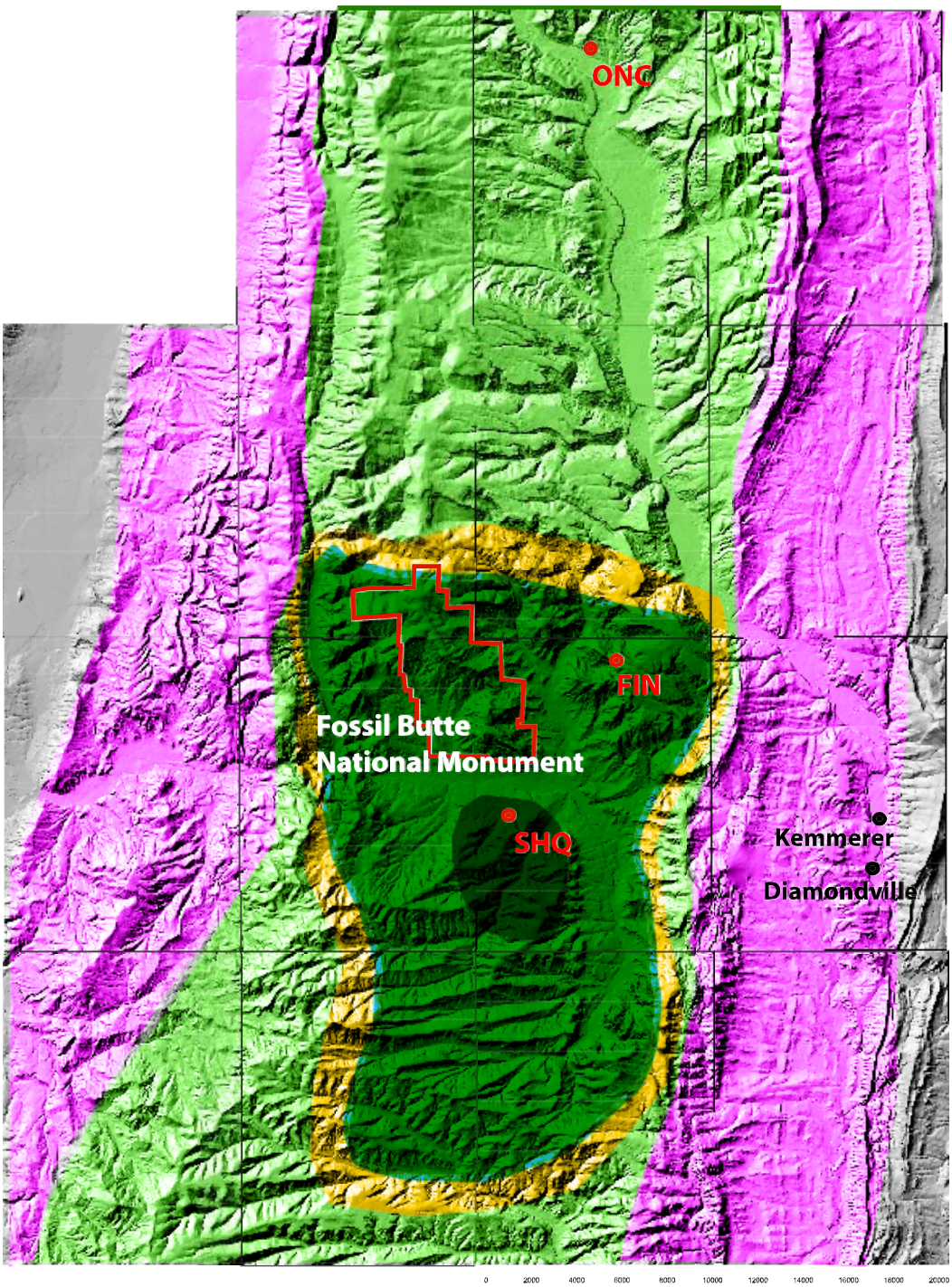

Figure 9. Shaded relief Digital elevation model with environment overlay of sample collection locations during time of sedimentation of "D" samples. FIN samples are samples S1, S2, S3B. SHQ samples are D1, D2, and D3B. ONC is the O1 sample location. Dark green is the permanently stratified lake region. The green color is a shallow, oxygenated perennial lake. The yellow represents the ephemeral lake mudflats and the light green is the flood plain areas. The pink represents the surrounding mountainous terrain.

Sample ID	Rock Formation	Rock Type	State	County	Lattitude/Longitude or Township/Range Locations
S1	Green River Formation	Carbonate	WY	Lincoln	N41 51.9 W110 40.5
S2	Green River Formation	Carbonate	WY	Lincoln	N41 51.9 W110 40.5
AL	Green River Formation	Ash/Carbonate	WY	Lincoln	N41 51.9 W110 40.5
AU	Green River Formation	Ash/Carbonate	WY	Lincoln	N41 51.9 W110 40.5
D1	Green River Formation	Carbonate	WY	Lincoln	N41 46.3 W110 47.82
D2	Green River Formation	Carbonate	WY	Lincoln	N41 46.3 W110 47.82
D3-B	Green River Formation	Francolite/fossil	WY	Lincoln	N41 46.3 W110 47.82
S3-B	Green River Formation	Francolite/fossil	WY	Lincoln	N41 51.9 W110 40.5
O1	Green River Formation	Carbonate/Oncolite	WY	Lincoln	N42 6.62 W110 41.34
O2	Green River Formation	Dolomite/Stromatolite	WY	Lincoln	N41 34.2 W108 23.84
FG-A15	Green River Formation	silisiclastic	WY	Sweetwater	N41 20.1 W109 24.79
FG-B2	Green River Formation	silisiclastic	WY	Sweetwater	N41 20.1 W109 24.79
M1	Green River Formation	oil shale	WY	Sweetwater	T14N R99W18
O3	Green River Formation	Dolomite/Stromatolite	WY	Sweetwater	N41 34.2 W108 23.84
S4	Green River Formation	Carbonate	WY	Sweetwater	N41 51.9 W110 40.5
TS1*	Green River Formation	Turtle Shell	WY	Sweetwater	SE1/4 sec. 18 and NW1/4 sec. 19, T14N, R99W
F1**	Green River Formation	Shale	WY	Sweetwater	N42 10 W109 45
U1*	Green River Formation	Carbonate	WY	Sweetwater	41.77 deg N, 110.55 deg W
GR1*	Green River Formation	Varved Carbonate	WY	Sweetwater	NW1/4 sec31 T16N R107W
GR2*	Green River Formation	Shaly Varved Carbonate	WY	Sweetwater	T16N R108W, NE1/4SW1/4 of section 7
GR3*	Green River Formation	Carbonate	WY	Sweetwater	T3S R100W sections 13,14,24 and T3S R99W sec 19
GR4*	Green River Formation	Fossil Fish Scales	WY	Sweetwater	T3S R100W sections 13,14,24 and T3S R99W sec 19
GR5*	Green River Formation	Shale	WY	Sweetwater	NW1/4 sec31 T16N R107W
GR6*	Green River Formation	Dolomitic Stromatolite	WY	Sweetwater	SE1/4 sec. 18 and NW1/4 sec. 19, T14N, R99W
GR7*	Green River Formation	Oolitic LS	WY	Sweetwater	SE1/4 sec. 18 and NW1/4 sec. 19, T14N, R99W
GR8*	Green River Formation	Pisolitic LS	WY	Sweetwater	SE1/4 sec. 18 and NW1/4 sec. 19, T14N, R99W

Table 1. Sample locations. Notes: *Approximate locations. ** Gross approximation based solely on rock type and fossil.

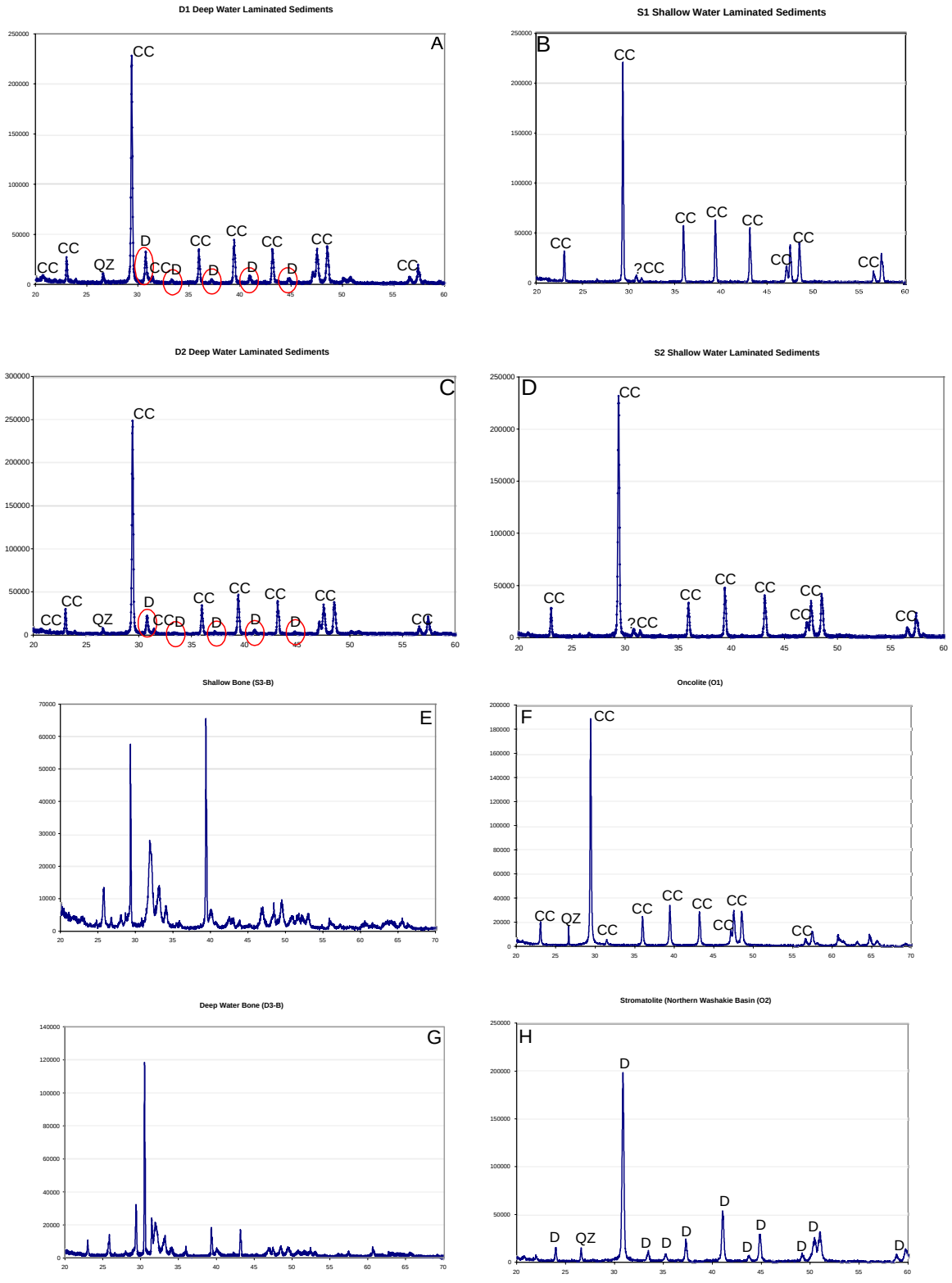

Figure 10. Powder XRD patterns of samples. Patterns A, B, C, D and F show peaks representing calcite, but samples A and C (left two) show a small dolomite component (circled in red). Patterns E and G are phosphatic fish patterns. These patterns show fluorapatite mineral but SB3 has calcite and another unidentified dominant phase. Sample H is dolomite. CC = calcite, D = Dolomite, QZ = Quartz

Modeling

Modeling of aqueous species of Th and REEs was done using PHREEQCi (Charlton et. al. 1987). The lack of published data on Th aqueous species was an initial problem. Thermodynamic data were collected from a variety of sources (Joao, Bigot and Fromage 1986, LaFlamme and Murray 1987, Östhols, Bruno, and Grenthe 1994, Östhols and Malmström 1995, Grenthe Personal Communication) and added to the existing LLNL database provided with PHREEQCi. Simulation parameters for the various models and log K values for carbonate, phosphate and hydroxyl species are reported in Appendix B.

Models were simplified from "real" lake conditions. This is because some lakes contain so much dissolved constituents that the equations used in simulations do not work. PHREEQCi uses ion-association and Debye Hückel expressions to calculate aqueous solution chemistry (Charlton et. al. 1987.) The Debye-Hückel expression fails at higher ionic strengths at and above seawater. Model results present percent species of aqueous Th out of total Th input of 10^{-5}mol (figure 19). REE models are based on data collected by Johannesson and Lyons (1994). Because Mono Lake is so highly concentrated, concentrations of elements, other than REEs, were reduced by half to cut down on the total ionic strength. The modeling of REEs is to understand what form the REEs are in the aqueous phase in the water. The result of Eu in the modeling was difficult to report because the LLNL database contains carbonate species unique only to Eu. The modeling results produced many carbonate species, none of which amounted to values that fit the other REEs. Because of this uncertainty in the result, Eu was omitted from the modeled pattern. Because shape of the pattern is not affected by the lack of Eu, it does not detract from the overall result.

Limnogeologic features play an important role in the resulting geochemistry of lake sediments. Precipitated GRF lake sediment REE patterns reflect a facies relation and the water conditions at the relative time of formation. Comparison modeling was done by examining REE patterns from modern lakes from the Great Basin region (Johannesson et al. 1994) and REE patterns from GRF samples. It is possible to use lake sediment REE patterns and Th content to better understand the lake chemistry from which it formed. Sholkovitz and Shen (1995) report that corals uptake REEs proportional to seawater abundances. The assumption can be made that this is true for most precipitated carbonates in Fossil Basin and especially true of phosphatic fossils. This will be illustrated in the results section. Though the Kd values differ from aragonite to calcite, dolomite, and phosphate, we can speculate that if the elemental concentration of the water was high enough, the REE patterns would directly reflect the water conditions. By comparing the modern lake water and GRF precipitates it would then be possible to hypothesize what type of water may produce that sediment. It is important to note that diagenetic and post-diagenetic alteration may have changed the REE composition of these precipitated sediments, but is unlikely.

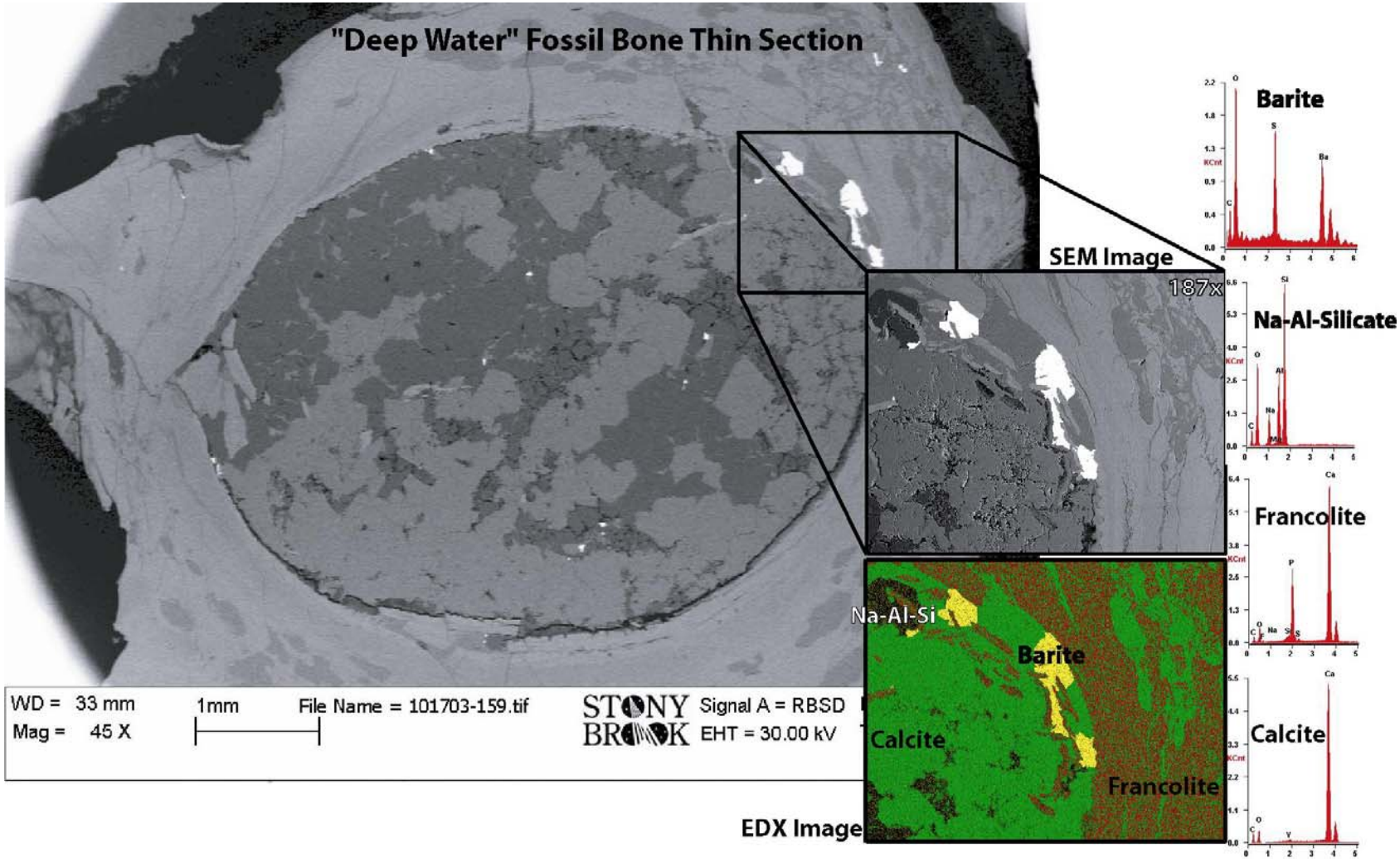

Figure 11. SEM and EDX images of a cross section of the D3B bone samples. Barite can be seen in the center bone cavity suggesting the possibility of microbial induced conditions (Senko, Campbell, and Henriksen 2004).

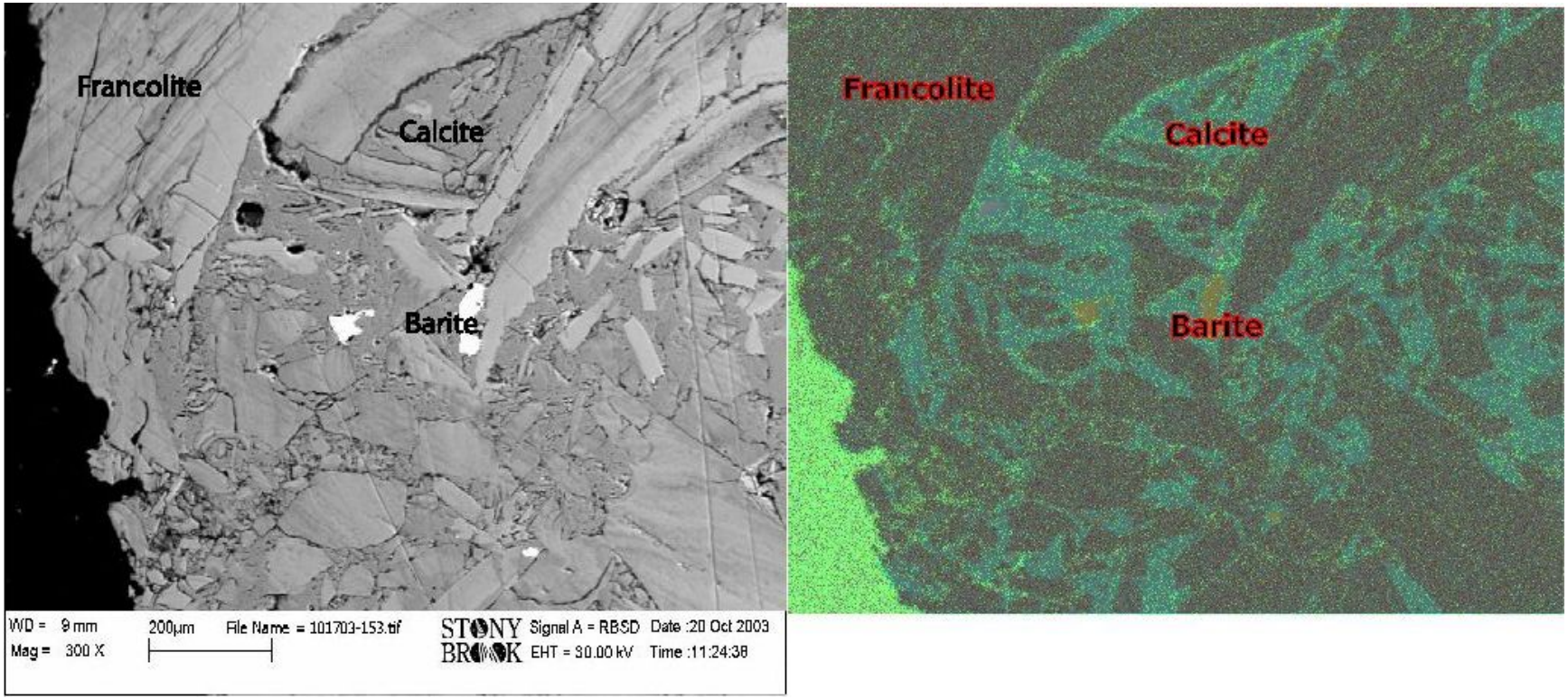

Figure 12. SEM and EDX images of a cross section of the S3B bone samples. Barite can be seen in the fractured center bone cavity suggesting the possibility of microbial induced conditions (Senko, Campbell, and Henriksen 2004)

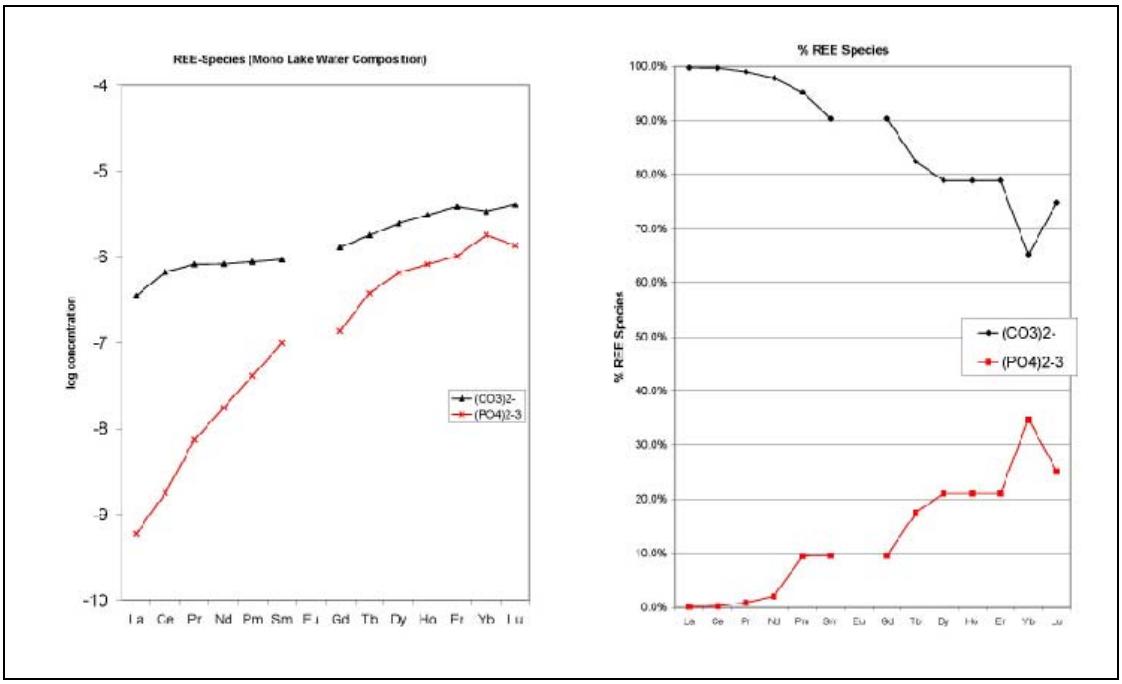

Figure 13. Modeling Results of REEs after data from Johannesson and Bird (1994). These plots show theoretical estimates computed in PHREEQCi of the amount of dominant aqueous species in Mono Lake water. Carbonate species are dominant for all REEs but phosphate species contribute a more significant role towards the HREEs. Eu values are absent because Eu exists in a variety of carbonate species other than $(CO_3)^{2-}$. It was difficult to quantify the actual Eu-carbonate concentration because the number of carbonate species is much higher than that of the other REEs in the database.

Results

Major Element Chemistry

Samples were separated based on dominant mineralogy into groups using major element and XRD data (table 2 and figure 10). Calcite samples were identified by sample compositions that contained 46% CaO by mass. Pure calcite by stoichometry is 56.03% CaO (Barthelmy, D. 2004). Because of impurities in the samples, a lower threshold of 46% was chosen with the help of XRD patterns. Dolomite samples were chosen by the MgO/CaO ratio because major elements analysis results are presented in this form. Pure dolomite has a MgO/CaO ratio of 0.72 (Barthelmy, D. 2004). Because of impurities in the samples, a threshold of 0.42 was chosen. XRD confirmed the bulk mineral was dolomite. Because the MgO/CaO weight percent ratio could be similar in shales with low abundances of both Ca and Mg, a detrital composition (Al_2O_3 + SiO_2) of <8.5% was chosen. Al_2O_3+SiO_2 was chosen to represent the detrital composition because it is assumed that the bulk of silica and alumina compounds are not authigenic precipitates

from the water. Rock texture and appearance is also taken into consideration for this separation. The phosphate group is based on a composition of at least 21.3% P_2O_5. This was chosen because stoichometrically, fluorapatite has 36.45% P_2O_5 (Barthelmy, D. 2004). Because the bone material is not pure fluorapatite, a minimum threshold of 21.3% was chosen with the aid of XRD for bulk mineral composition. Shale samples were chosen by the (Al_3O_2+SiO_2) content. A threshold of 31% normalized (Al_3O_2+SiO_2) was chosen because XRD data was not helpful in identifying any minerals in these samples.

	Calcite Group						Dolomite Group			
content	U1	S1	S2	D1	D2	O1	GR6	GR7	GR8	O2
Al2O3	0.53	0.28	0.52	0.93	0.58	0.15	1.10	0.81	0.36	0.92
CaO	52.22	58.37	55.71	46.35	53.47	55.33	30.32	34.48	32.37	29.70
FeO*	0.16	0.00	0.00	0.02	0.00	0.00	2.31	1.76	1.12	0.72
K2O	0.21	0.00	0.00	0.10	0.08	0.03	0.23	0.09	0.02	0.24
MgO	1.34	0.70	0.97	3.73	2.78	0.70	15.71	14.56	17.78	20.62
MnO	0.005	0.003	0.004	0.005	0.004	0.311	0.083	0.121	0.055	0.099
Na2O	0.06	0.14	0.30	0.51	0.27	0.04	0.35	0.35	0.27	0.19
P2O5	0.054	0.067	0.091	0.204	0.121	0.211	0.042	0.053	0.036	0.096
SiO2	2.51	0.00	0.37	2.52	1.28	0.00	7.39	4.08	2.07	3.37
TiO2	0.025	0.018	0.026	0.068	0.034	0.016	0.062	0.021	0.005	0.061
sum	57.12	59.59	58.00	54.44	58.63	56.78	57.60	56.33	54.09	56.01
Mg/Ca	0.026	0.012	0.017	0.080	0.052	0.013	0.518	0.422	0.549	0.694
ca%	91.43%	97.96%	96.05%	85.12%	91.20%	97.45%	52.64%	61.21%	59.84%	53.01%
Al+Si%	5.33%	0.47%	1.54%	6.34%	3.18%	0.27%	14.73%	8.69%	4.49%	7.66%
P2O5%	0.10%	0.11%	0.16%	0.38%	0.21%	0.37%	0.07%	0.09%	0.07%	0.17%

	Shale Group								Phosphate (fossil) Group			
content	F1	GR1	GR2	GR3	GR5	sco-1	sgr-1	M1	GR4	D3B	S3B	TS1
Al2O3	16.16	3.71	8.03	7.18	13.81	13.68	6.52	3.80	1.05	2.28	0.16	0.32
CaO	3.03	37.32	5.42	18.72	3.35	2.62	8.38	37.64	44.58	49.80	52.49	52.04
FeO*	5.04	1.24	3.39	2.48	3.87	4.67	2.73	1.18	1.87	0.00	0.00	0.29
K2O	2.62	1.25	2.97	4.18	4.19	2.77	1.66	0.70	0.25	1.77	0.50	1.12
MgO	3.22	1.53	3.51	8.11	2.25	2.72	4.44	1.43	2.98	0.35	0.54	3.30
MnO	0.057	0.087	0.049	0.032	0.027	0.053	0.034	0.059	0.026	0.042	0.004	0.045
Na2O	5.35	0.78	1.08	0.68	3.74	0.90	2.99	1.53	1.30	0.06	0.00	0.02
P2O5	0.212	0.203	0.242	0.062	0.175	0.206	0.328	0.623	24.11	21.382	28.560	25.971
SiO2	56.36	15.45	36.70	29.71	50.49	62.82	28.24	16.85	4.53	3.87	0.00	0.00
TiO2	0.571	0.124	0.317	0.269	0.477	0.628	0.264	0.145	0.085	0.026	0.035	0.027
sum	92.61	61.70	61.73	71.43	82.38	91.07	55.58	63.95	80.79	79.58	82.29	83.13
Mg/Ca	1.062	0.041	0.648	0.433	0.672	1.038	0.530	0.038	0.067	0.007	0.010	0.063
ca%	3.27%	60.50%	8.79%	26.21%	4.07%	2.88%	15.08%	58.85%	55.18%	62.58%	63.79%	62.59%
Al+Si%	78.31%	31.05%	72.47%	51.65%	78.05%	84.00%	62.54%	32.29%	6.91%	7.73%	0.19%	0.38%
P2O5%	0.23%	0.33%	0.39%	0.09%	0.21%	0.23%	0.59%	0.97%	29.85%	26.87%	34.71%	31.24%

Table 2. Ratios and percentages of elements of collected samples. Ratios allowed separation of samples into the four colored groups: carbonates (CaO weight % >46), dolomites (MgO/CaO ratio of >.72), phosphates (P_2O_5 weight % of >21.3), and shales (Al+Si weight % >31). Amounts below dashed line reflect normalized percentages to the sum of the major components.

SEM and XRD Results

Ratios of calcite to dolomite were estimated by dividing the 100 percent peak intensities of the two minerals. Of all of the laminated samples analyzed by XRD, only samples D1 and D2 were composed of a mix of calcite and dolomite. Samples D1 and D2 had calcite:dolomite ratios of approximately 7:1 and 11:1 respectively. It can be seen that there are variations within the bone material that reflect compositional differences most likely due to infilling of bone pores with calcite during fossilization (figures 11 and 12). An unknown Na-Al-Si mineral is present inside the bone cavity. This is believed to be authigenic and can potentially give further clues to what the conditions of formation were.

REE Chemistry

REE patterns were normalized to various standards and internal samples. The standards used to normalize were Chondrite (C-1), Standard Green River Shale (SGR-1), Cody Shale (SCo-1), Post Archean Average Shale (PAAS) reported in Taylor and McLennan (1985) and McLennan and Taylor (1980) and from analysis of USGS standards via ICP-MS.

Sample separation can be made by major elements and also REE patterns into four categories. The first category is calcite rich rocks which show similar patterns (figures 14-16). These patterns show LREE enrichment relative to C-1 but show a slight HREE enrichment relative to SGR-1 (figure 14 and 15). Calcite is believed to form in fresh and brackish water (Buchheim and Eugster 1998). Buchheim and Eugster (1998) calls samples in this group kerogen-poor laminated micrite (KPLM) and kerogen-rich laminated micrite (KRLM).

The second group is the dolomitic samples. This group displays a general enrichment of REEs relative to the calcite group and HREE enrichment relative to shale standards (figures 14 and 16).

The next group is the “shale” samples. This group has moderate relative REE compositions compared with the calcite group, with a pattern resembling crustal REE signatures. Because the detrital composition of these samples dominates the REE patterns of these rocks, the effect of the lake water chemistry has a lesser impact. The average concentration of REEs is directly proportional to the amount of “detrital” component. Samples with low detrital components had a large amount of CaO which suggests a dilution effect by calcite.

The final group are the phosphates. This group is composed of fossil samples of fish parts and a turtle shell. These samples have the highest abundance of REEs, especially the HREEs. The material of these samples was found to be fluorapatite by XRD. The nature of this material allows it to obtain many different elements in its crystal structure while forming.

REE Geochemistry Modern Lakes and Fossil Basin

Comparisons of the REE patterns of waters of Mono, Summer, Abert, Goose, Walker and Pyramid Lakes (data of Johannesson et al. 1994) and chemical precipitate rocks of the GRF show that there are some close matches between modern alkaline lake waters and GRF precipitates. This is consistent with the hypothesis that the REE patterns of inorganically precipitated calcite may reflect the water from which it precipitated. Modern lake waters compare to precipitated rock types representing a specific facies: near shore-highstand, transgressive-lowstand, basinal-highstand and basinal-lowstand. The following is a model that attempts to depict this relationship.

Modern lake REE patterns compare very well with REE patterns obtained from the GRF (figure 17). The hypothesis is made that we can use this to unravel the chemistry of the fluids for precipitation of authigenic minerals in the various facies. One representative sample from each facies “group” was compared with modern lake water to match the closest pattern. Using uniformitarianism modern lakes

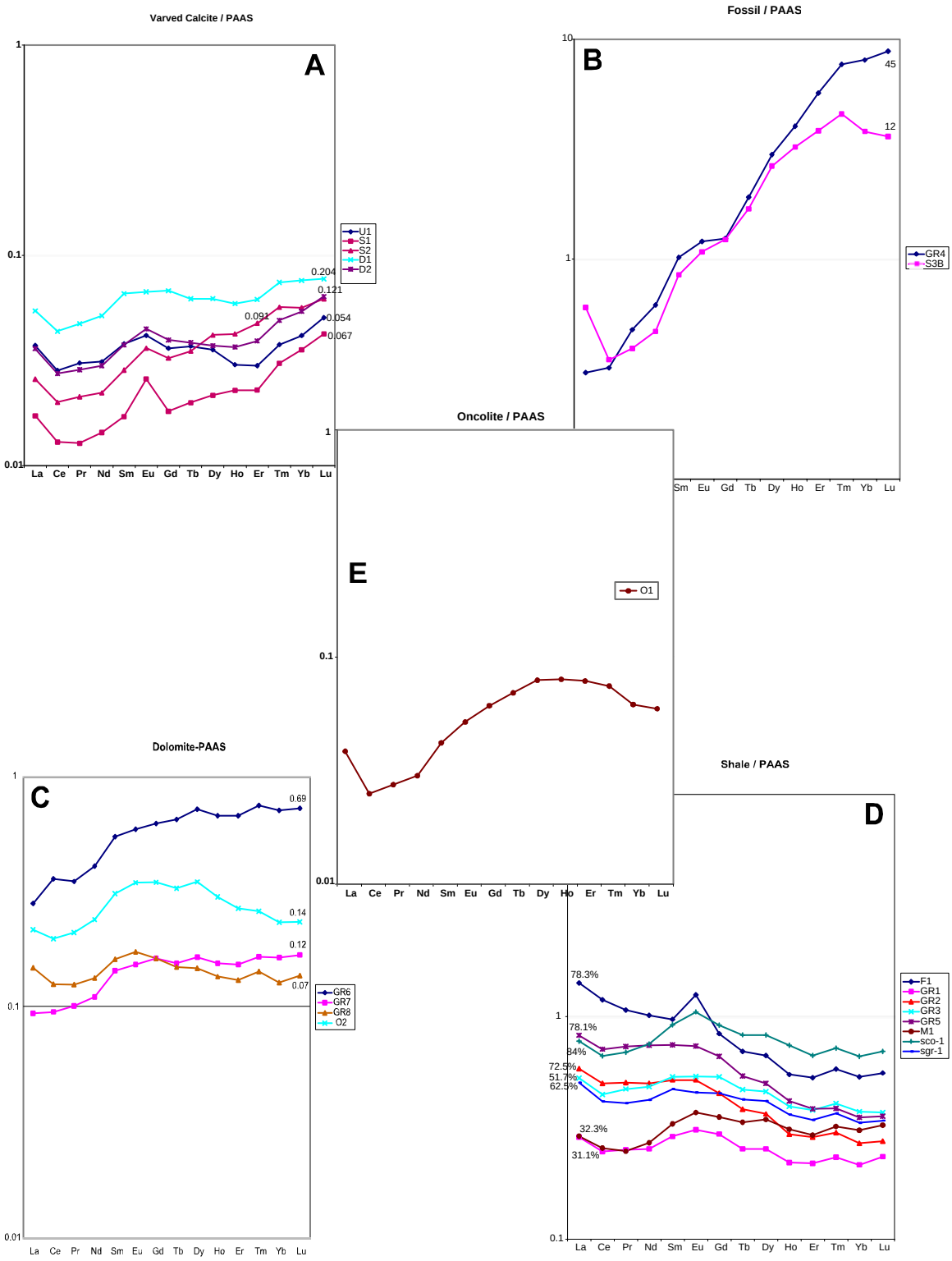

Figure 14. REE patterns normalized to PAAS for comparison. Numbers represented in: A- weight percent phosphate, B- Th ppm, C- Mg/Ca ratio, D- weight percent (Si + Al).

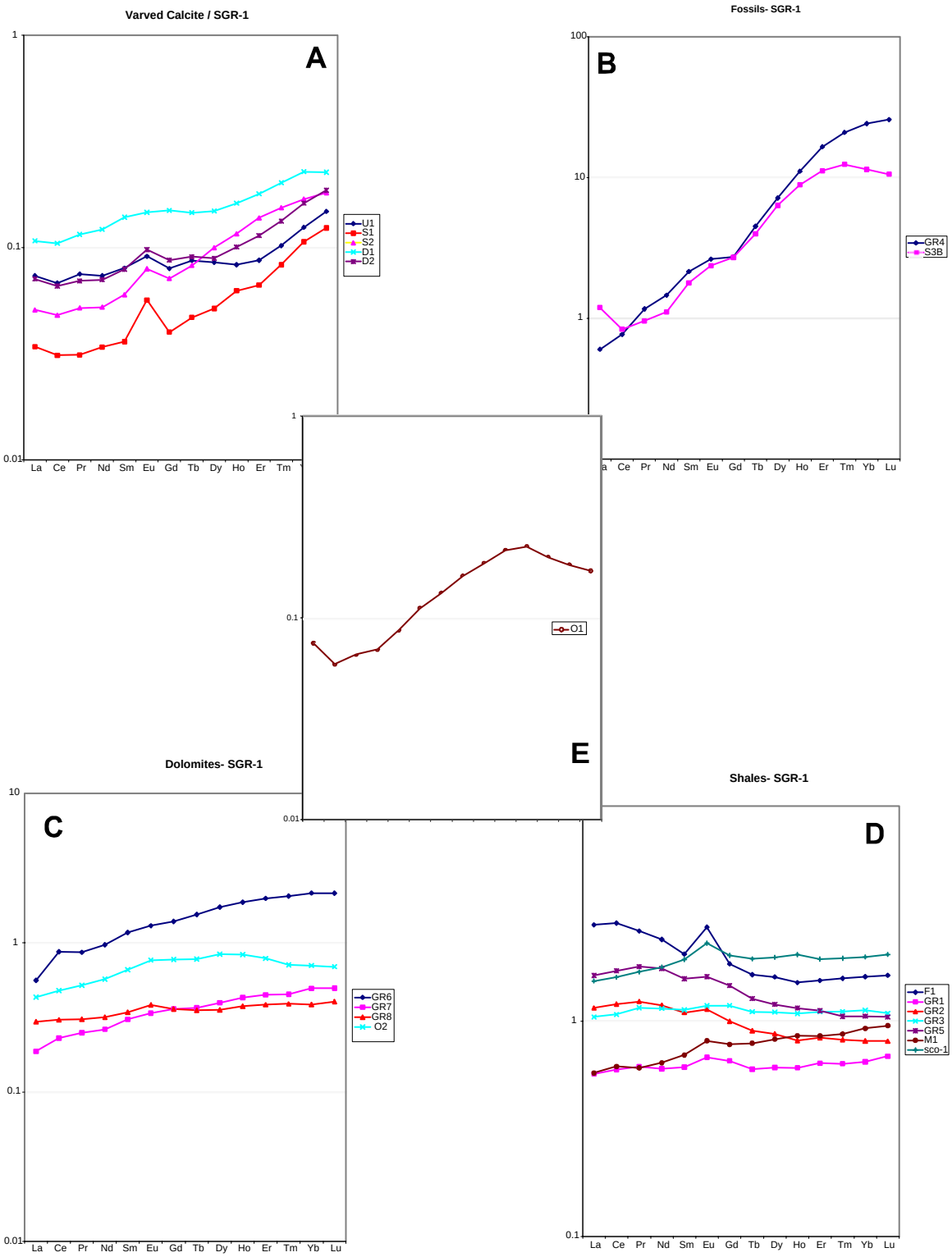

Figure 15. SGR-1 normalized patterns for comparison.

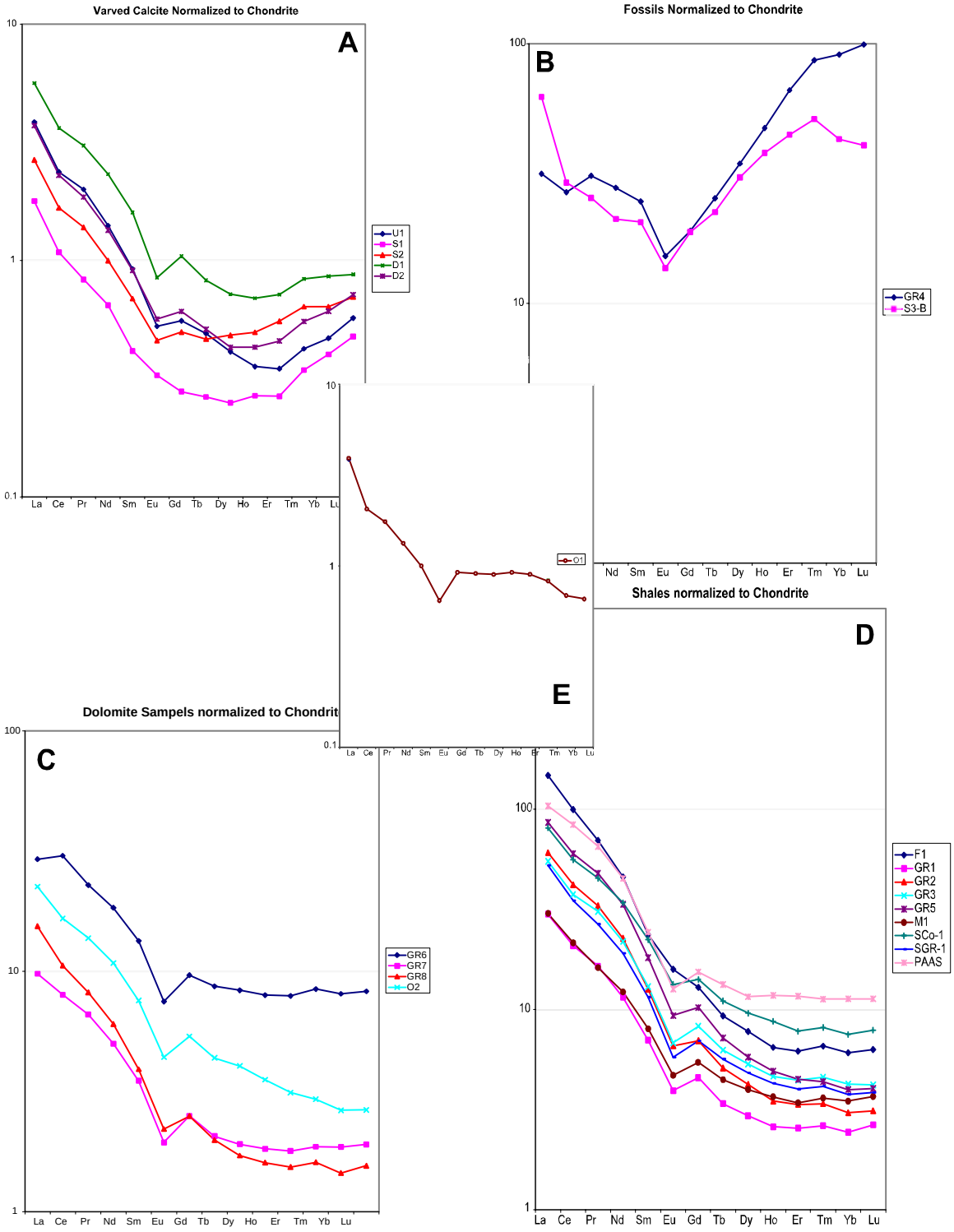

Figure 16. Chondrite normalized patterns for comparison.

Mono Lake water REE patterns closely resemble the phosphatic fossil samples (figure 17). This is directly related to the concentration of alkalinity and phosphate in the lake and not to the REE signature of the surrounding bedrock (Johanesson et. Al 1994). Mono Lake was stratified prior to sampling by Johannesson et al. (1994) and the bulk lake water most likely reflects the concentrated bottom waters that mixed with the surface waters. This bottom water condition would be responsible for giving fossils in the monimolimnion of Fossil Lake the HREE enriched signature that is similar to Mono Lake water. It is suspected that the fossils formed under the influence of the water REE signature and incorporated this signature over time. It is speculated that the fossil patterns have not been altered by diagenesis.

Walker Lake has a pattern that closely resembles the micro-laminated calcites (figure 17). Walker Lake is an alkaline lake that has many unique qualities including a population of fish that are acclimated to alkaline water and many stromatolites (Osborne, Licari and Link 1982) that are forming along the fringe. This gives Walker Lake similar qualities to represent the shallow near-shore mixolimnion environment of Fossil Lake.

Summer Lake is a shallow (average <2m) saline alkaline lake that is also high in phosphate (Cohen, Palacios-Fest et al. 2000). Though neither stromatolites nor oncolites are forming in modern Summer Lake, the shallow trasgressive shore environment conditions of the lake may mimic that of what formed these in Fossil Lake. It is speculated that stromatolites form in calm saline alkaline conditions in the GRF and oncolites form in shallow water areas near moving water. We know that stromatolites and oncolites form in shallow water environments. Stromatolites need long periods of time where conditions are fairly consistent. Some stromatolites of the GRF are estimated to take 355 years to form (Bradley 1929). The stromatolites represented in this study are not from Fossil Basin, but it is speculated that they would form under similar conditions in there as they did in the Washakie Basin.

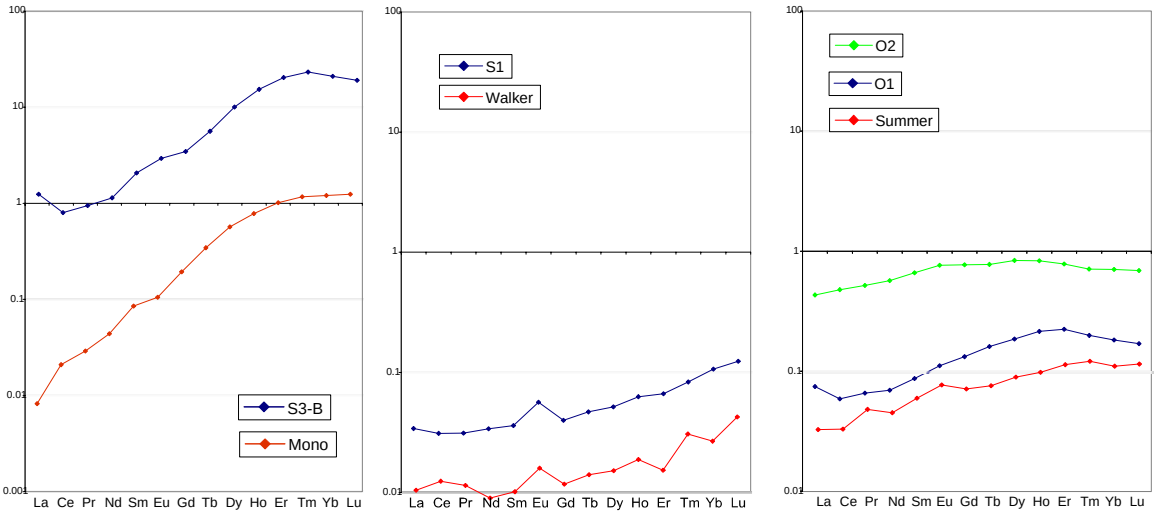

Figure 17. Comparison of modern lake water samples and precipitated sediments of the GRF (normalized to SGR-1). This plot shows how the samples show very close resemblance to modern lake environments suggesting that a link may be made between modern environments and the GRF. Samples are: S3-B (fossil fluorapatite), S1 (micro-laminated calcite), O1 (calcite oncolite), and O2 (dolomitic stromatolite from Laney Member of the Washakie Basin). Lake patterns are: Mono Lake, Walker Lake, and Summer Lake. Lake concentrations are $x10^6$.

Using the hypothesis that sample O1 was formed from lake water after a mixing event, a resulting pattern of mixing "top" and "bottom" waters can be modeled. "Mixolimnion water" responsible for producing the S2 laminated calcite sample was mixed with "monimolimnion waters", represented by Mono Lake water and the result is shown in figure 18a. The resulting pattern, comprised of 0.2x Mono Lake composition and 1.1x S2 composition, is very similar to that of the O1 sample. This suggests that the pattern may reflect mixing of top and bottom waters with two distinct chemistries. Another mixing model shows a mix between S2 and S3-B, the laminated calcite and fossil bone sample from the same quarry (figure 18b). Because these samples are from the same facies, this may show a more realistic mixing result. The ratios are 0.0175x S3-B and 1x S2 for figure 18b..

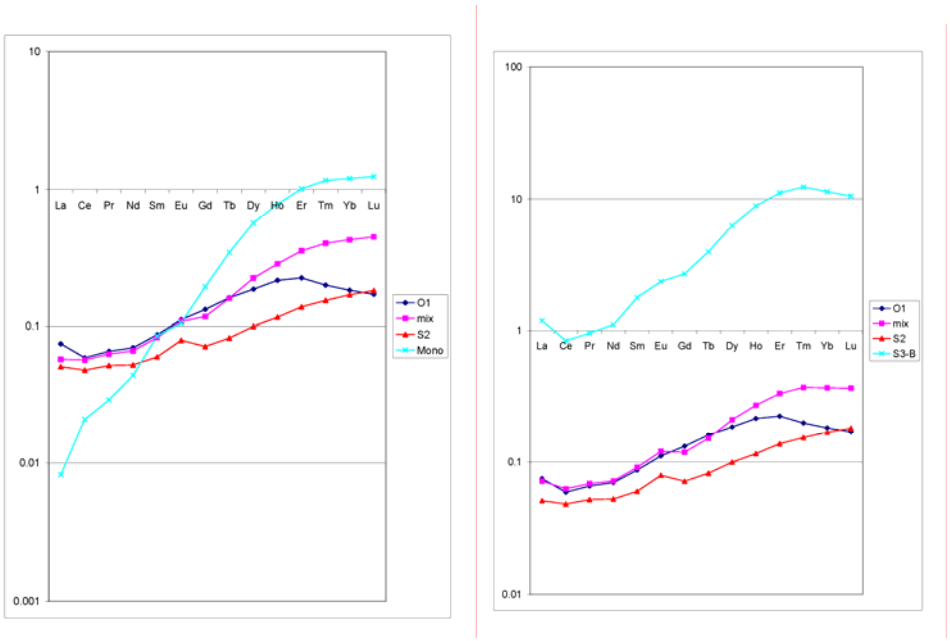

Figure 18a/b. Mixing model of Mono Lake water and sample S2 (left) and fossil Bone S3-B and sample S2 (right). This illustrates how mixing of lake strata could have produced water that was responsible for producing the oncolite sample O1. Because S2 and S3-B are from the same location, this mixing model may show a more realistic representation of a possible mixing. Ratios are: 0.2 Mono Lake : 1.1 S2 and 0.0175 S3-B : 1 S2.

Modeling

A Th speciation model calculated using PHREEQCi and data collected from sources described above is shown in figure 19. This model confirms that aqueous species of Th are dominated by carbonate and phosphate species under all normal pH conditions.

Modeling results using PHREEQCi are based on data from Johannesson and Lyons (1994). Alkaline lakes show that the two dominant aqueous species of REEs would be CO_3^{2-} and $(PO_4)_2^{3-}$ of which the patterns can be seen in figure 13.

Organics are not considered in this model because humic acids were considered by Tang and Johannesson (2003) to be insignificant for high pH. Carbonate makes up around 100 percent of total amount of species in the light REEs and around 80 percent for

the HREEs. Phosphate amounts to only a trace in the LREEs and around 20 percent for the HREEs (figure 13).

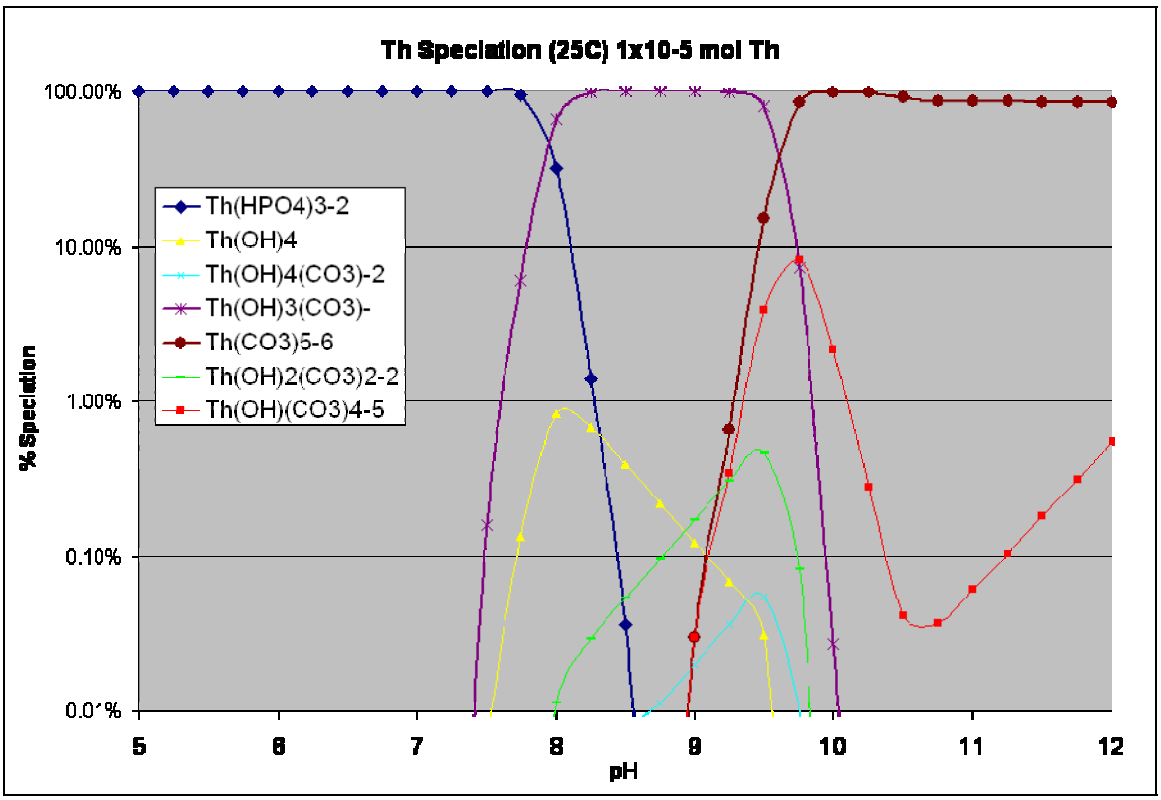

Figure 19. Th speciation diagram of 10^{-5} mol Th in an alkaline system in equilibrium with atomospheric CO_2. See Appendix B for details on PHREEQCi model. Estimates of pH for mixolimnion based on modern lakes could be 8.5 to 10 and pH for monimolimnion could be 10-11.5. Modern lakes range from 8.5 to 10. This means the predicted species for Fossil Lake would be Th(CO3)5-6 and Th(OH)(CO3)4-5 species.

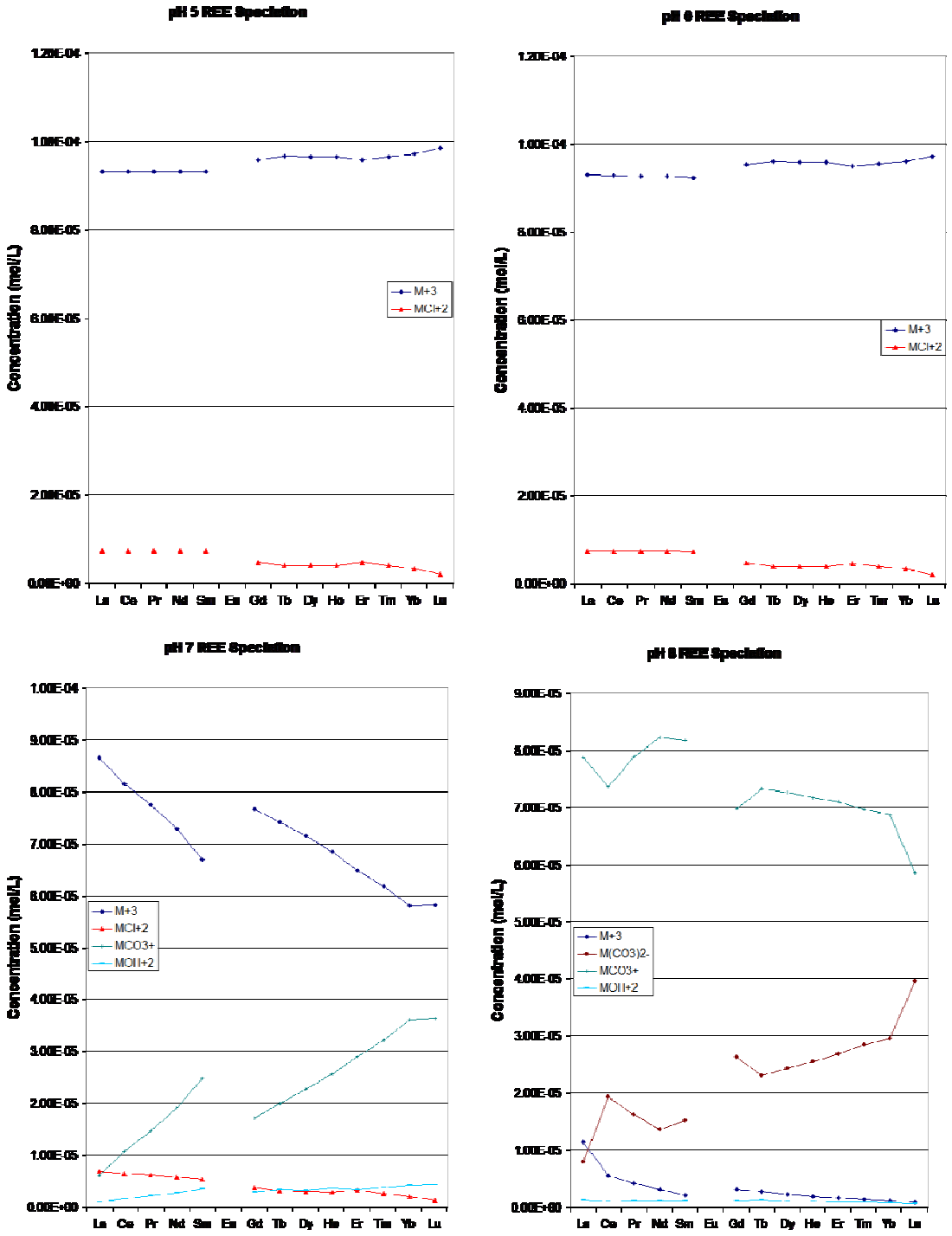

Figure 20. REE speciation at varying pH intervals in equilibrium with atmospheric CO_2. Eu was omitted from this speciation model because of database limitations. Initial input of each REE was 10^{-4} mol/L.

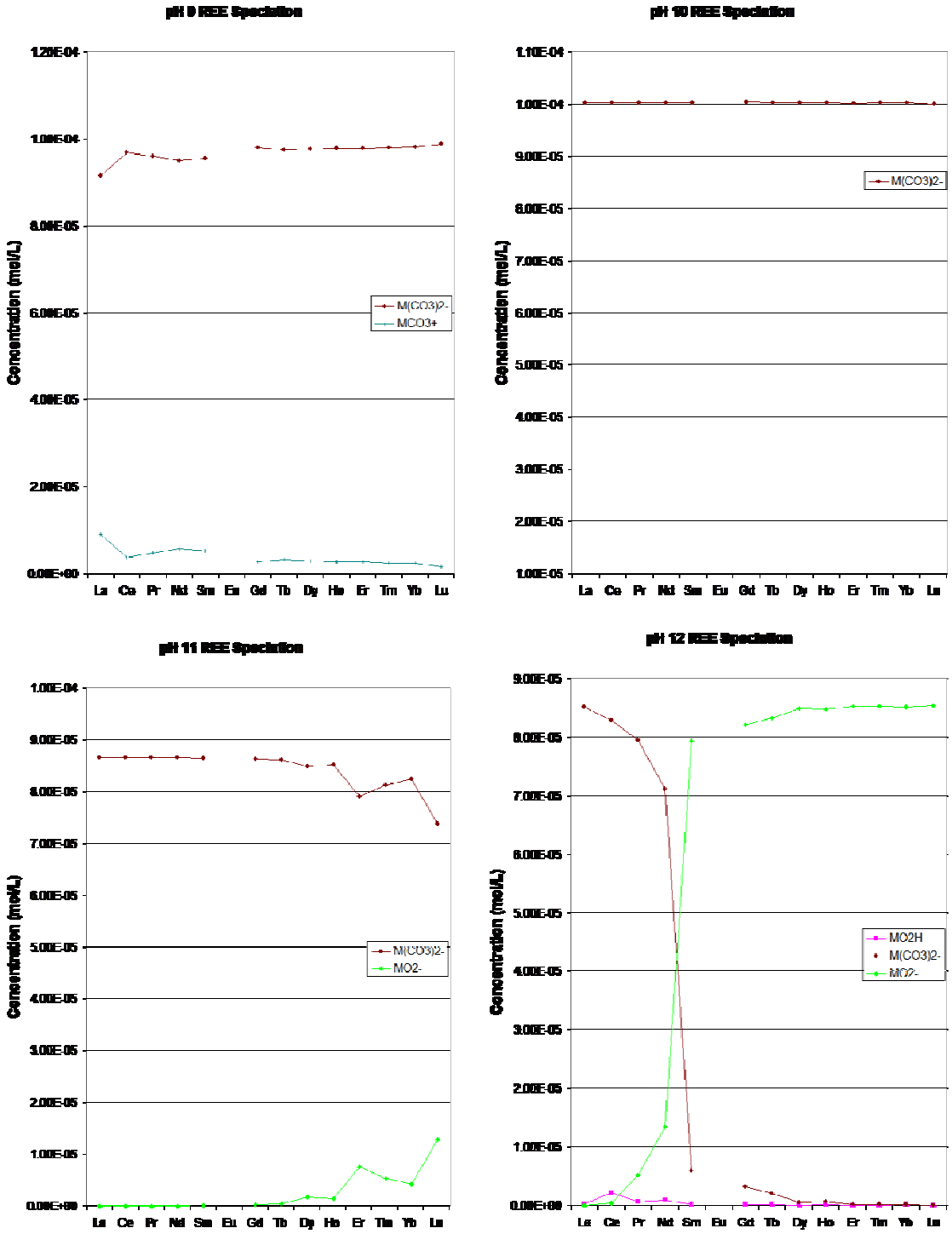

Figure 21 continued. REE speciation at varying pH intervals in equilibrium with atmospheric CO_2. Eu was omitted from this speciation model because of database limitations. Initial input of each REE was 10^{-4} mol/L.

Discussion

Limnogeology

Causes of death of fish and animals, especially mass moralities, can mark significant changes in lake chemistry. Noting and understanding causes in these changes, especially chemical changes, can allow an understanding of how the environment changed.

Fish mortalities can result from major changes in the stratified lake. Grande (1984) proposed two mechanisms that could have caused the massive layers of fossil fish typically called "mass mortalities in the GRF, specifically in Fossil Basin". One theory is that periodically, one or two species of blue-green algae multiply rapidly causing a toxic condition in the lake. The algae in the "superbloom" also produces excessive amounts of $CaCO_3$ which would rapidly cover the fish and prevent harsh decomposition (Grande 1984). This seems reasonable, but if this was the case it would be expected that laterally large scale organic laminae would be found that would be thicker than normal micro-laminations even if the event was short lived.

Another fish mortality mechanism is based on Bradley's (1948) study of the "Fossil Syncline". This model has the lake overturn bringing up anoxic bottom waters which kills most fish and other animals. Because the bottom water of a meromictic lake has a high amount of dissolved CO_2, precipitated $CaCO_3$ that falls down into the monimolinmion becomes dissolved (Grande 1984). This allows bottom water to be supersaturated with respect to calcite. Precipitation of calcite during lake overturn occurs when the water becomes favorable for calcite precipitation which increases sedimentation rates and preserve fossil specimens. Though dissolution of calcite has been noted in some deep modern lakes (Ramisch et al 1999), this is difficult to prove and unlikely because the suspected depth of Fossil Lake was relatively shallow compared to lakes studied by Ramisch et al (1999). A modified version of this theory explains that lake turnover can resuspend sediment which would cover the fish (Ferber and Wells 1995). They argue that the re-oxygenating of the water would cause immediate scavenging of the bottom so this may not be the most plausible theory.

A third possibility for fish mortalities was proposed by Ferber and Wells (1995). This hypothesis is a summertime loss of habitable zone. This is when ascending isopleths of salinity and anoxia meet lethal maximum isotherms (Ferber and Wells 1995). Toxicity of the water can be caused by ammonia from dying fish, decreased available oxygen, increased alkalinity or increased salinity. This model works well for the GRF because the taphonomy of fossils reflects species and size selective death assemblages. This could be facilitated through contraction of the lake margins during lowstands (analogous to playa lake contractions).

Fossil Basin Facies

Calcite is believed to form in fresh and brackish water (Buchheim 1998). Buchheim (1998) calls samples in this group kerogen-poor laminated micrite (KPLM) and kerogen-rich laminated micrite (KRLM). Of the laminated calcite samples analyzed, samples U1, S1, and S2 are KPLM while samples D1, and D2 are KRLM. KRLM samples are believed by Buchheim (1994) to represent deeper, oxygen-poor lake center environments

which fit into the model of a stratified lake. Because calcite does not form in the center of most alkaline lakes, it is believed that calcite forming these samples was derived from near shore and was carried out to the lake center through lake currents.

Kerogen poor laminated micrite samples are considered to be near shore-highstand deposits and have relatively flat REE patterns that have a subtle HREE enrichment normalized to shale, perhaps due to the small amount of phosphate present in these rocks (figure 20 and table 2). These carbonate facies sediments, represented by S1, S2 and U1, match most closely with the water from Walker Lake. These carbonates are rapidly deposited and thus dilute any detrital component that may enter the lake. They are far enough from the shore line to transport in dead fish and in the right location to catch precipitating $CaCO_3$ depositing from biogenic and inorganic means from the surface waters.

The basinal-highstand facies (represented by D1 and D2) are deposited at lesser rate because they are further from the shore (figure 20). Calcite precipitates near the shore where streams input Ca into the lake and the calcite settles out closer to where it forms. Although these carbonates almost certainly form in the mixolimnion, they are slowly deposited in the monimolimnion, the anoxic region at the lake bottom which is free from scavengers and oxygen.

Samples D1 and D2 have a small dolomite component (figure 10). This is most likely because of this facies forming in the hypolimnion where saline conditions occur. Buchheim and Eguster (1998) observes that dolomite forms in hypersaline and alkaline environments which would be representative of lake bottom waters. Boyer (1982) also believes that dolomite was probably formed by sublacustrine authigenesis or chemical precipitation off the playa. It is also possible for the dolomite to be formed from calcite influenced by pore fluids during diagenesis.

Dolomitic stromatolites were grouped into the transgressive-lowstand deposits (figure 21). These samples were not from Fossil Basin but were from the Laney of the Washakie Basin. It is assumed that samples of this type would have formed similarly in fossil basin. These samples represent the lowstand and evaporitic times of the lake's history similarly to Summer Lake. Because these samples are on the fringe of the lake they had to have experienced a more concentrated mix of water from when the lake was lowest. This may be a period where fresh waters and bottom waters mix creating a pattern that appears to be a mix between the mixolimnion and monimolimnion waters of the expansion stage of the cycle causing lake turnover (figures 18a and b).

It is possible that the dolomite samples were formed as calcite initially and then dolomitized and that this may have had an effect on the REE signatures. It has been shown, however, that dolomitization of calcite does not change the REE signature of the rock (Banner, Hanson, and Meyers 1988). It can be assumed, therefore, that even if the dolomite is primary or secondary, the dolomitic samples still reflect the original water chemistry that produced the initial material.

Samples that would have formed in the monimolimnion are the fossil fish bones (samples D3B, S3B, and GR4). It is important to distinguish however, that fossils and calcite samples have very different compositions and develop different REE patterns because of differing K_d values. Fossil samples show pronounced HREE enrichment that is likely caused by increased alkalinity and increased elemental concentrations which is noted in the monimolimnion of modern lakes (like Soap Lake). Mono Lake water

matches up fairly nicely with the fossil patterns. Mono Lake has had a history of being a stratified lake and though the water samples taken from the study by Johannesson and Bird (1994) were collected at an unstratified time, the water chemistry reflects the concentrated bottom waters that had been mixed with the upper waters. Because fossilization occurs on the same relative time scale as typical lake cycles (10Ky – 100 Ky (Trueman and Tuross 2003)), it is therefore necessary to consider that the REE patterns of these type of samples reflect an average water condition over a span of time including concentrated highstand and mixed lowstand water chemistries.

In the bone samples, S3-B, and D3-B, using EDX, it is believed that some minerals can be identified as fluorapatite, calcite, barite, and an undetermined sodium-aluminum silicate which is believed to be authigenic (figures 11 and 12). The minerals contained in the fossils, if identifiable, may help understand the conditions in which they were formed. It has been suggested by Senko, Campbell, and Henriksen (2004) that microbial action can help precipitate barite in sedimentary environments.

The phosphate group is composed of fossil samples of fish parts and a turtle shell. These samples have the highest abundance of REEs, especially the HREEs. The material of these samples was found to be flourapatite by XRD. The nature of this material allows it to obtain many different elements in its crystal structure while forming.

Sample O1, although not a dolomitic sample, exhibits enrichment in the MREEs similar to that of the dolomitic samples most likely due to differences in environmental conditions that formed the oncolites. This sample has a relatively low abundance of REEs but unlike the other pure calcite samples, this sample exhibits a MREE hump. Phosphate may account for the anomalous pattern (table 2). Based on the total chemical analysis of the rock compared to other calcite samples, it appears that the only main difference is the phosphate component of this sample. The waters that formed this sample may have been fresher than these that formed samples O2 and GR6. This sample, based on its origin, being that it is algal like a stromatolite, is most likely representative of the transgressive- lowstand deposit (figure 21). Because of the lack of dolomite in this sample, it is speculated that the conditions were less evaporitic, more fresh and likely to be near stream input. This may have to do with the effect of acidic stream water dissolving phosphate rich sediments and bringing them into the lake analogous to the marginal marine setting reported by Hannigan and Sholkovitz (2001). Lithologic facies relative to the lake margin can be seen in figures 20 and 21. Phosphate composition and position on the lake margin seem to be the driving forces in the middle to heavy REE enrichment. The modern lake that could represent this phase is Summer Lake based on the similar REE patterns.

Oncolites are commonly seen forming in fairly fresh water (Dean and Fouch 1983). Using simple mixing, it is possible to produce a REE pattern similar to the oncolite by mixing Mono Lake water and any laminated calcite sample lake water (figure 17a and b). This may reflect two scenarios: 1. that oncolites form where saline waters are present as a result of the increased salinity of the surface waters due to mixing of the lake strata or 2. perhaps they form in evaporative pools of residual lake water near periodic river input where stream water signatures are responsible for the REE patterns. It is difficult to say for certain in what manner these fossils formed because it is uncertain what the timescale of formation of the fossils and also the duration of the lowstand periods (figure 13b).

The shale group (table 2) has moderate REE compositions with a pattern resembling crustal REE signatures. Because the detrital composition of these samples dominates the REE patterns of these rocks, the effect of the lake water chemistry has a reduced effect. The average concentration of REEs is directly proportional to the amount of "detrital" component. Samples with low detrital components had a large amount of CaO which suggests a dilution effect by calcite.

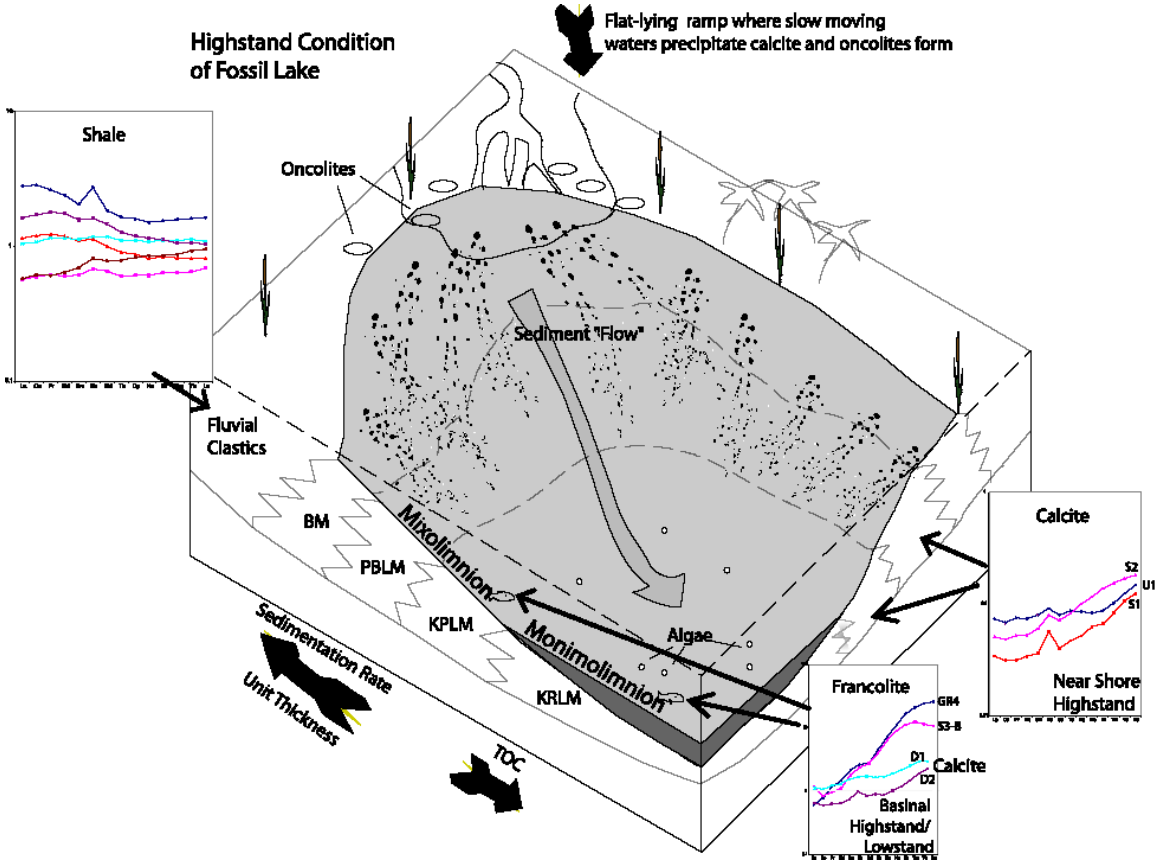

Figure 22. Highstand representation of Fossil Lake. This figure shows how sediment facies are deposited relative to shoreline and lake depth. Inflow from the shore supplies dissolved Ca to force precipitation of calcite in near shore environments. Some of this calcite drifts down into the monimolimnion. Calcite accumulation is slow because of the distance from the shore. Detrital accumulation is slow but slightly more significant because of less dilution for calcite. The algae accumulation rate is higher in the deep water because of the slower dilution by calcite. The formation of protodolomite is also a factor in this region. Oncolites may form along the shore influenced by streams and are composed of calcite mud. Modified after Buchheim (1998) and Ramos et al. (2001).

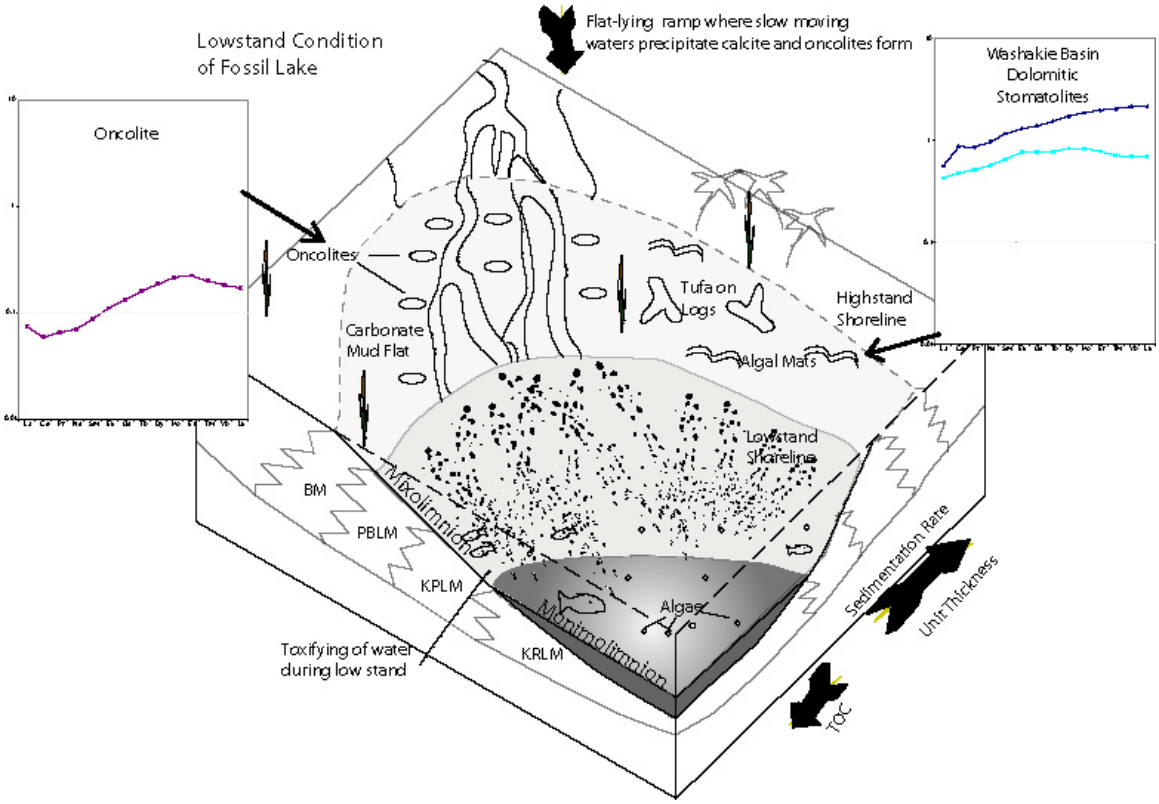

Figure 23. Lowstand representation of Fossil Lake. This figure shows the former highstand shoreline and exposures of sedimentary features formed in this fluctuating zone. Stromatolites, algal tufa and oncolites form in this region during transgression. The stomatolites are from Washakie Basin are presented here as a prediction of how Fossil Basin stomatolites may behave. Oncolites are able to roll more freely on the gentler slopes of the carbonate mudflats accumulating more calcite. Mixolimnion waters may be concentrated due to shrinkage of lake volume leading to mass kills of most fish. The stratification may remain during this period and sedimentation rates may increase because of smaller sedimentation area and concentration of alkalinity in the lake. Modified after Buchheim and Eugster (1998) and Ramos et al. (2001)

Proposed Incorporation of Th and REEs in Fossils

A model was developed for thorium (and REE) incorporation into fossils (figure 22). Fish live in the upper waters and near fresh water stream input. When a fish dies it can descend into bottom waters of a stratified lake that are too harsh for scavengers and there it is digested by anaerobic bacteria in the presence of water rich in Th and REE aqueous carbonate and phosphate species. The rapid breakdown of the fish soft tissue allows the waters local to the fish to become more acidic due to breakdown products of the bacteria. This may provide the ideal conditions for fossilization. Under lower pH conditions, phosphate may be the dominant aqueous species that may be able to combine with the forming fossil. The fossilizing bone is exposed to the water column for all or most of the fossilization process until complete burial and thus would take on a REE pattern reflecting the average water chemistry over the interval of permineralization.

Fossilization can take place over a relatively short period of time on the order of 10K years (Truemann and Tuross 2002).

Mass kills may be caused by periodic drastic summertime lake level changes. These lake level changes may or may not cause mixing of the lake, but may cause increased toxicity in the fresher lake water because of lower water volume. This would "single out" certain species and age fish because of juvenile fishes and species lower tolerances to toxic conditions (Ferber and Wells 2001).

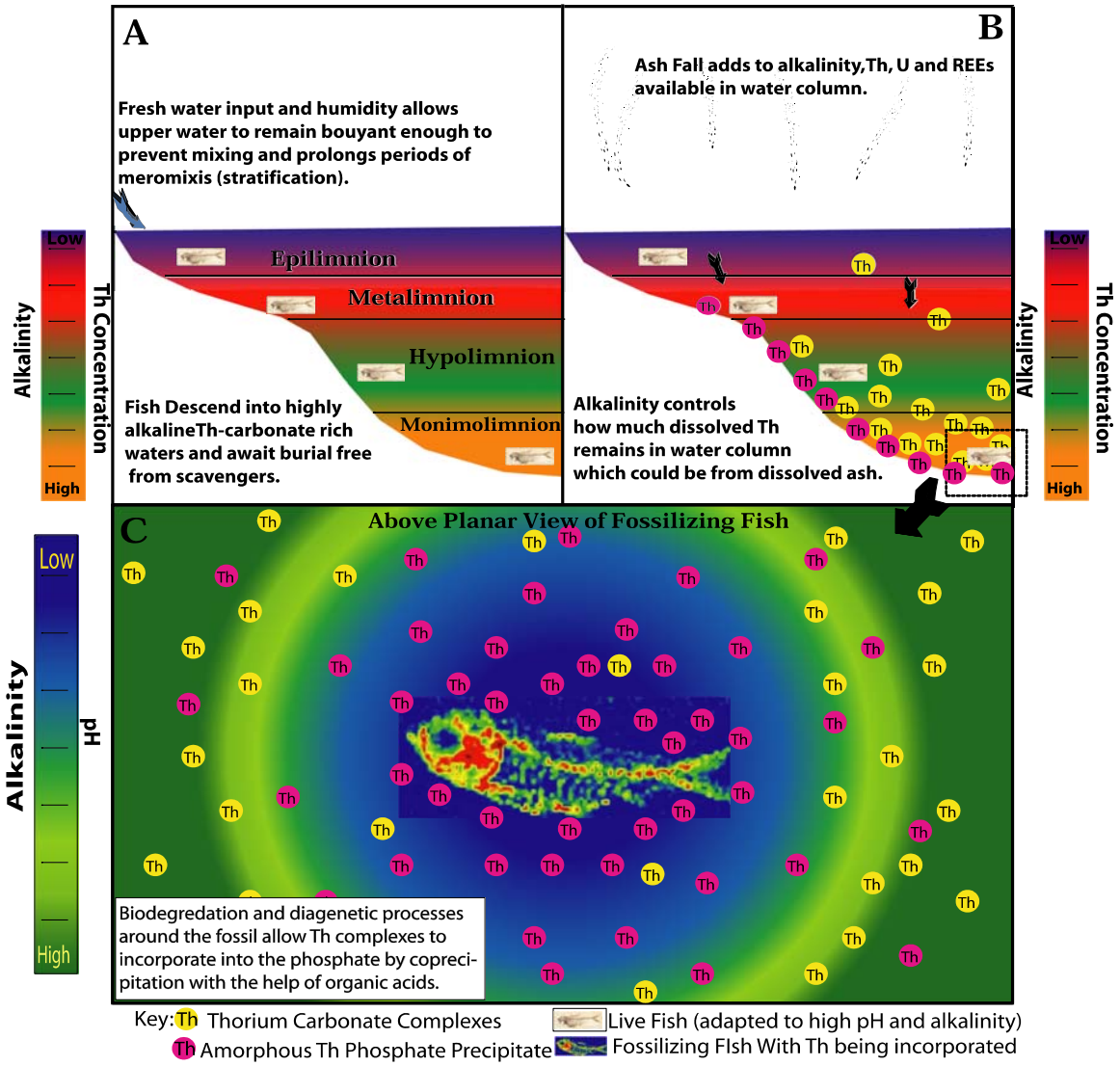

Figure 24. Possible sequence of events leading to enrichment of Th and REEs in fossil fish. The upper left box shows stratification occurring because of sufficient fresh water inflow. The upper right box shows ways that may contribute to increased alkalinity in the lake. The bottom box shows how the decomposition of the fish material may cause local chemical conditions that may allow the recomplexation of carbonate and phosphate species into the fluorapatite structure of the fossil.

Environmental Implications

Apatite minerals have been known to easily incorporate many different size elements in their structure, usually substituting into the Ca site (Pan and Fleet 2002). These samples also contain high amounts of other elements such as Sr, Y, Th and U (see Appendix C). The fact that these elements can be sequestered into bone has workers investigating the use of bone as a sorbing medium for PMBs (permeable reactive barriers) (Fuller, Bargar, and Davis 2003.)

Apatite minerals have long been studied for the possibility of nuclear waste storage (Ewing and Wang 2002). The one problem with studying sequestration of nuclear waste products is the stability of the material over time. The presence of Th, U and other toxic trace and REEs in fossil samples analyzed gives a good probability that under the right conditions theses elements can be retained in a stable form for a long period of time (in this case about 50 million years). This may be used as an example of a "long term study" of how stable materials can be with the relatively high abundances of radioactive and toxic materials.

Conclusions

The GRF has been observed to exhibit characteristics of an alkaline lake complex (Bradley 1948, Surdam and Wolfbauer 1975, Desborough 1978, Boyer 1982, Grande 1984, Buchheim 1994). The popular model of the GRF is a stratified lake model pioneered by Bradley (1948). A playa lake model was proposed by Eugster and Surdam (1973) and was supported by Surdam and Stanley (1981) and Surdam and Wolfbauer (1975). Debate over whether the GRF was formed by a playa lake or stratified lake is still ongoing. Fossil Lake has been interpreted to have been a stratified lake based on sedimentary facies, fossil taphonomy evidence and the presence of organic rich laminated sediments (oil shale). Sedimentary layering thins toward the middle of the lake which is indicative of fossil basin (Buchheim and Eugster 1998). Playa-like mud flat sediments were deposited north and south of the main deep lake area in the long basin but the bulk of the sedimentation was stratified until the close of Fossil Lake where playa-like sediments were deposited in the upper Angelo in the form of bedded chert and evaporitic salts (Buchheim and Eugster 1998) (appendix E).

Precipitated sedimentary rocks from the GRF can be broken up into four main types based on Buchheim and Eugster (1998) and linked to lake depth stages. The fluvial clastic sediments are shales that have at least 30% (Al + Si) content. These sediments surround the lake margins, interfinger with carbonate mud flat sediments and divide the precipitated sediments found in the lake center. The light colored calcite-rich samples which are partly laminated or bioturbated are considered partly burrowed laminated

micrite (PBLM) or bioturbated micrite (BM) respectively. The next facies is kerogen poor laminated micrite (KPLM). These three facies contain the most abundant fossil fish. The lake center is comprised of darker more organic rich sediments that are generally thinner and are considered kerogen rich laminated micrite (KRLM). These contain the larger and best preserved fish specimens and often contain a portion of dolomite because of their formation in deep saline alkaline monimolimnion waters. Samples obtained for this study can be placed into these categories and their REE patterns can be related to modern lake analogs with characteristics that may be similar to the original Fossil Basin environments. REE patterns from three lakes from the Great Basin area match up well with REE patterns of three sedimentary facies found in Fossil Lake.

Modern lakes such as Mono Lake and Soap Lake that have high alkalinities have been shown to accumulate Th (LaFlamme and Murray 1987) and REEs (Johannesson et al. 1994, Johanneson and Bird 1994) in the lake water to much higher abundances that the ocean. LaFlamme and Murray (1987) showed that the presence of alkalinity is the key to keeping Th in the aqueous phase from their study on Soap Lake because of carbonate complexing. Modeling in PHREEQCi confirmed that the dominant species of Th would be carbonate at high pH (figure 19). Other alkaline lakes of the Great basin region were examined to fit GRF sample REE patterns. Because of these relations, it can be assumed that the samples reflect similar water chemistries of modern lakes.

Walker Lake, Summer Lake, and Mono Lake REE patterns matched up closely in shape to the patterns of precipitated rocks from Fossil Lake (figure 13). Because of this close match, it is speculated that the calcite, dolomite and phosphate that formed in Fossil Lake would directly reflect lake water chemistry. The environments of deposition of the Fossil Lake samples may have been analogous to the compared Great Basin Lake.

Based on the environments of the Great Basin Lakes and the compared REE patterns, a model of deposition was formed to show the possible conditions of formation of the rocks of Fossil Basin (figures 20 and 21). A model of incorporation of Th and REEs was developed. It is hypothesized that changes in pH and chemistry local to the fossilizing fish play a role in the incorporation of these elements into these materials (figure 22).

Knowledge of ancient lake environments can help us better handle problems in modern lake environments. It can also help understand how materials can behave over long periods of time which is especially helpful for engineers designing long term storage facilities for harmful nuclear and other waste products.

This study has allowed us to relate the present with the past. Sediments of Fossil Lake and possibly other ancient lakes can be compared to modern lakes and with careful observations of these modern lakes, environments of ancient lakes may be understood. Lakes of past and present tell a hidden story in their sediments, living and dead flora and fauna and water.

Future Work

Much detailed research can still be done on this study. Based on results formulated, it would be worthwhile to do REE and Th profiles of a complete section concentrating on the cycles. This may allow a better of view of cyclicity which may be driven by large scale climatic influences. Fossils need to be analyzed in greater detail to understand how the water chemistry affects the concentrations. Does the depth of the water play a role? Phosphatic fossils found on the shoreline would be useful to examine because they would be assumed to be not affected by any harsh meromictic conditions. These are difficult to come by because of scavengers and degredation. Understanding more about the role of organics could be done by obtaining Fischer oil assays on the various facies and comparing that to the REE and Th concentrations. Once more understanding is done in Fossil Basin, it is reasonable to assume that the principles learned in a small basin can be applied to the other GRF basins.

Further micro-analysis could be done on the bone samples with the SEM, especially with EDX. Accurate analysis of the minerals contained in the bones may give clues about the environment of formation. Bone samples may have varying concentrations of elements throughout a cross section due to water chemistry changes over time. Sensitive analytical techniques may be able to see these varying changes and could lead to small scale water chemistry analysis. Employing synchrotron based XRF may be the best method for quantifying such small scale variations in the composition of the bones.

The area around Fossil Lake was tectonically uplifted by the Sevier Orogeny. The duration and timing of this event may have had substantial impact on the evolution of the basin geometry and depth over time. The effects of the elevation of the basin borders and shape of the basin may have played a key role in allowing the basin to remain fresh for a long period of time. Studies on oxygen isotopes were done to ascertain if the paleo-elevation of the surrounding mountains had influence on water inflow into the basin (Morrill and Koch 2002). It is still not yet clear how the elevation and geometry of the basin evolved over time and how accommodation space may have been affected.

The samples collected from Flaming Gorge are very anomalous and a closer analysis is needed to examine what makes these samples so high in many elements. An understanding of how these presumable “shales” can be so different from typical shales would tell a lot about the conditions that were found in the Wilkins Peak time and perhaps about the PETM.

Dating of the carbonate rocks is important to the understanding of process rates. This lake environment is believed by the author to contain samples that will prove to be useful for dating. Dating of the carbonates and phosphates can give a better understanding of rates of deposition and durations of cycles. This may help other workers to better understand climate dynamics.

References

Anderson, R. F., M. P. Bacon, et al. (1982). "Elevated Concentrations of Actinides in Mono Lake." Science **216**(4545): 514-516.

Banfield, J.F., B.F. Jones, and D. R. Veblen (1991). "An AEM-TEM study of Weathering and Diagenesis, Abert Lake Oregon: II. Diagenetic modification of the sedimentary assemblage." Geochemica et Cosmochemica Acta **55**: 2795-2810.

Banner, J.L., G.N. Hanson, and W.J. Meyers (1988). "Rare Earth Element and Nd Isotopic Variations in Regionally Extensive Dolomites from the Burlington-Koekuk Formation (Missippippian): Implications for REE Mobility during Carbonate Diagenesis" Journal of Sedimentary Petrology **58**: 415-432.

Barthelmy, D. (2004). "Mineralogy Database." < http://www.webmineral.com/> 2002-2004.

Boggs Jr., S (2001). Principles of Sedimentology and Stratigraphy 3rd Ed. Upper Saddle River, NJ, Prentice Hall.

Bradley, W. H. (1929). Algae Reefs and Oolites of the Green River Formation. US Geological Survey Professional Paper 154-G. Washington D.C.**:** 203-223.

Bradley, W. H. (1948). "Limnology and the Eocene lakes of the Rocky Mountain region." Geological Society of America Bulletin **59**(7): 635-648.

Bradley, W. H. (1963). Paleolimnology, in Frey, D. G. ed., Limnology in North America, University of Wisconsin Press, p. 621-652.

Bradley, W. H. and Eugster, H.P (1969). "Geochemistry and Paleolimnology of the Trona Deposits and Associated Minerals of the Green River Formation of Wyoming: US. " Geological Survey Professional Paper 803. 53p.

Buchardt, B., P Seaman, G Stockmann, et al. (1997). "Submarine Columns of Ikaite Tufa." Nature **390** (6656): 129-130, November 13.

Buchheim, H. P. and H. P. Eugster (1998). Eocene Fossil Lake; the Green River Formation of Fossil Basin, southwestern Wyoming. Modern & ancient lake systems; new problems and perspectives. J. K. Pitman and A. R. Carroll, Utah Geological Association Publication. **26:** 191-208.

Buchheim, H. P., R. W. e. Renaut, et al. (1994). "Eocene Fossil Lake, Green River Formation, Wyoming; a history of fluctuating salinity Sedimentology and geochemistry

of modern and ancient saline lakes." Sedimentary and paleolimnological records of saline lakes **50**: 239-247.

Buchheim, H. P., R. C. Surdam, et al. (1981). Paleoenvironments and fossil fishes of the Laney Member, Green River Formation, Wyoming Communities of the past. Second North American paleontology convention. Lawrence, KS, United States**:** 415-452.

Cohen, A. S. (2003). Paleolimnology: The history and evolution of lake systems. New York, New York, Oxford University Press.

Cohen, A. S., M. R. Palacaios-Fest, et al. (2000). "A paleoclimate record for the past 250,000 years from Summer Lake, Oregon, USA: II. Sedimentology, paleontology and gochemistry." Journal of Paleolimnology **24**: 151-182.

Cole, J. M., J. Nienstedt, et al. (2003). "Phosphor imaging as a tool for in situ mapping of ppm levels of uranium and thorium in rocks and minerals." Chemical Geology **193**(1-2): 127-136.

Cooper, J.J and D.L Koch (1984). “Limnology of a Desertic Terminal Lake, Walker Lake, Nevada, U.S.A.” Hydrobiologia **118**: 275-292.

Charlton, S. R., C. L. Macklin, et al. (1997). PHREEQCI; a graphical user interface for the geochemical computer program PHREEQC. Water-Resources Investigations - U. S. Geological Survey.

Christiansen, R. D. (2001). Wyoming Geologic Highway Map. Canton City, CO, GTR Mapping.

Dean, W. F., and T. D. Fouch (1983). "Carbonate Depositional Environments." AAPG Memoir 33: 98-130.

Deike, R. and B. Jones (1980). Provenance, Distribution and Alteration of Volcanic Sediments in a Saline Alkaline Lake. Hypersaline Brines and Evaporitic Environments. A. Nissenbaum. Amsterdam, Elsevier Scientific Publishing Co.

Demicco, R. V., T. K. Lowenstein, et al. (2003). "Atmospheric pCO_2 since 60 Ma from records of seawater pH, calcium, and primary carbonate mineralogy." Geology **31**(9): 793-796.

Desborough, G. A. (1978). "Biogenic-Chemical Stratified Lake Model for Origin of Oil-Shale of Green River Formation - Alternative to Playa-Lake Model." Geological Society of America Bulletin **89**(7): 961-971.

Ewing, R. C. and L. Wang (2002). Phosphates as Nuclear waste Forms. Phosphates: Geochemical, Geobiological, and Materials Importance. M. Kohn, Rakovan, J. and Hughes, J. Washington, DC, Mineralogical Society of America. **48:** 673-699.

Eugster, H. P. and L. A. Hardie (1975). "Sedimentation in an Ancient Playa-Lake Complex - Wilkins Peak Member of Green River Formation of Wyoming." Geological Society of America Bulletin **86**(3): 319-334.

Eugster, H. P. and R. C. Surdam (1973). "Depositional Environment of Green River Formation of Wyoming- Preliminary Report." Geological Society of America Bulletin **84**(4): 1115-1120.

Ferber, C. T. and N. A. Wells (1995). "Paleolimnology and taphonomy of some fish deposits in "Fossil" and "Uinta" Lakes of the Eocene Green River Formation, Utah and Wyoming." Palaeogeography, Palaeoclimatology, Palaeoecology **117**(3-4): 185-210.

Fischer, A. G. and L. T. Roberts (1991). "Cyclicity in the Green River Formation (Lacustrine-Eocene) of Wyoming." Journal of Sedimentary Petrology **63**: 333. **61**(7): 1146-1154.

Fuller, C. C., J. R. Bargar, et al. (2003). "Molecular-scale characterization of uranium sorption by bone apatite materials for a permeable reactive barrier demonstration." Environmental Science & Technology **37**(20): 4642-4649.

Grande, L. (1984). "Paleontology of the Green River Formation, with a review of the fish fauna; second edition." Bulletin - Geological Survey of Wyoming

Huh, C. (1995). "Th Isotopes in the Santa Monica Basin: Temporal Variation, Long-Term Mass Balance and Model Rate Constants." Journal of Oceanography **51**: 363-373.

Joâo, A., S. Bigot, et al. (1986). "Etude des carbonates complexes des elements IVB I-Determination de la constante de stabilite du pentacarbonatothorate (IV)." Bulletin de la Societe Chimique de France **1**: 42-44.

Johannesson, K. H. and W. B. Lyons (1994). "The Rare-Earth Element Geochemistry of Mono-Lake Water and the Importance of Carbonate Complexing." Limnology and Oceanography **39**(5): 1141-1154.

Johannesson, K. H., Lyons, W. Berry, Bird, David A. (1994). "Rare earth element concentrations and speciation in alkaline lakes from the Western U.S.A." Geophysical Research Letters **21**(9): 773-776.

Johnson D.M., P.R. Hooper, R.M. Conrey (1999). “XRF Analysis of Rocks and Minerals for Major and Trace Elements on a Single Low Dilution Li-tetraborate Fused Bead” Advances in X-Ray Analysis **41**:843-867.

LaFlamme, B. D. and J. W. Murray (1987). "Solid/solution interaction; the effect of carbonate alkalinity on adsorbed thorium." Geochimica et Cosmochimica Acta **51**(2): 243-250.

Lageson, D.R. and D.R. Spearing (1991). Roadside Geology of Wyoming 2nd Ed. Montana Press Publishing, Missoula, Montana.

Langmuir, D. and J. S. Herman (1980). "The Mobility of Thorium in Natural-Waters at Low-Temperatures." Geochimica Et Cosmochimica Acta **44**(11): 1753-1766.

Machlus, M., S. Hemming, et al. (2004). "Eocene calibration of geomagnetic polarity time scale reevaluated: Evidence from the Green River Formation of Wyoming." Geology **32**(2): 137-140.

McLennan, S. M. and S. R. Taylor (1979). "Rare earth element mobility associated with uranium mineralisation." Nature **282**(5736): 247-250.

McLennan, S. M. and S. R. Taylor (1980). "Geochemical Standards for Sedimentary-Rocks - Trace-Element Data for Usgs Standards Sco-1, Mag-1 and Sgr-1." Chemical Geology **29**(3-4): 333-343.

McLennan, S. M., W. B. Nance, and S. R. Taylor. (1980). "Rare-Earth Element-Thorium Correlations in Sedimentary-Rocks, and the Composition of the Continental Crust." Geochimica Et Cosmochimica Acta **44**(11): 1833-1839.

Milton, C. (1971). "Authigenic minerals of the Green River Formation Trona issue." Contributions to Geology **10**(1): 57-63.

"Profile of Monomixis and Meromixis." Monomixis and Meromixis at Mono Lake. Mono Basin Clearinghouse, 08 Jan. 2003 <http://www.monobasinresearch.org/timelines/meromixis.htm>

Morril, C and P.L. Koch (2002). "Elevation or Alteration? Evaluation of isotopic constraints on paleoaltitudes surrounding the Eocene Green River Basin." Geology **30**(2):151-154.

Osborne, R., G. Licari, and M.H Link (1982). "Modern Lacustrine Stromatolites, Walker Lake, Nevada." Sedimentary Geology **32**(1-2): 39-61.

Östhols, E., J. Bruno, et al. (1994). "On the Influence of Carbonate on Mineral Dissolution. 3. The solubility of Microcrystalline THO2 in CO2-H2O Media." Geochemica et Cosmochemica Acta **58**(2): 613-623.

Östhols, E. and M. Malmstrom (1995). "Dissolution Kinetics of ThO_2 in Acid and Carbonate Media." Radiochimica Acta **68**(2): 113-119.

Pan, Y. and M. E. Fleet (2002). Conpositions of the Apatite-Group Minerals: Substitution Mechanisms and Controlling Factors. Phosphates: Geochemical, Geobiological, and

Materials Importance. M. Kohn, Rakovan, J. and Hughes, J. Washington, DC, Mineralogical Society of America. **48:** 13-49.

Pearson, P. N. and M. R. Palmer (1999). "Middle eocene seawater pH and atmospheric carbon dioxide concentrations." Science **284**(5421): 1824-1826.

Pearson, P. N. and M. R. Palmer (2000). "Atmospheric carbon dioxide concentrations over the past 60 million years." Nature **406**(6797): 695-699.

Ramisch, F, M. Dittrich, C. Mattenberger, et al. (1999). “Calcite Dissolution in Two Deep Eutrophic Lakes.” Geochemica et Cosmochemica Acta **63**(19/20): 3349-3356.

Senko JM, Campbell BS, Henriksen JR, et al. “Barite deposition resulting from phototrophic sulfide-oxidizing bacterial activity.” Geochemica et Cosmochemica Acta 68 (4): 773-780 Feb 2004

Simpson, H. J., R. M. Trier, et al. (1982). "Radionuclides in Mono Lake, California." Science **216**(4545): 512-514.

Smith, M., B. Singer, et al. (2003). "Ar-40/Ar-39 geochronology of the Eocene Green River Formation, Wyoming." Geological Society of America Bulletin **115**(5): 549-565.

Surdam, R. C. and K. O. Stanley (1981). "Sedimentologic Framework of Green River Formation, Wyoming." Aapg Bulletin-American Association of Petroleum Geologists **65**(5): 1000-1000.

Surdam, R. C. and C. A. Wolfbauer (1975). "Green River Formation, Wyoming- A Playa Lake Complex." Geological Society of America Bulletin **86**(3): 335-345.

Tang, J and Johannesson, KA (2003). “Speciation of Rare Earth Elements in Natural Terrestrial Waters: Assessing the Role of Dissolved Organinc Matter From the Modeling Approach”. Geochemica et Cosmochemica Acta **67** (13): 2321-2339.

Taylor, S. and McLennan, SM (1985). The Continental Crust: its Composition and Evolution. Oxford, Blackwell Scientific Publications.

Trueman, C. N. and N. Tuross (2002). Trace elements in recent and fossil bone apatite. Phosphates: Geochemical, Geobiological, and Materials Importance. M. Kohn, Rakovan, J. and Hughes, J. Washington, DC, Mineralogical Society of America. **48:** 489-521.

Tuttle, M. L. and M. B. Goldhaber (1993). "Sedimentary Sulfur Geochemistry of the Paleogene Green River Formation, Western USA - Implications for Interpreting Depositional and Diagenetic Processes in Saline Alkaline Lakes." Geochimica Et Cosmochimica Acta **57**(13): 3023-3039.

Wetzel, R. G. (2001). Limnology: Lake and River Ecosystems. San Fransisco, CA, Academic Press.

Appendix A

REE Diagrams

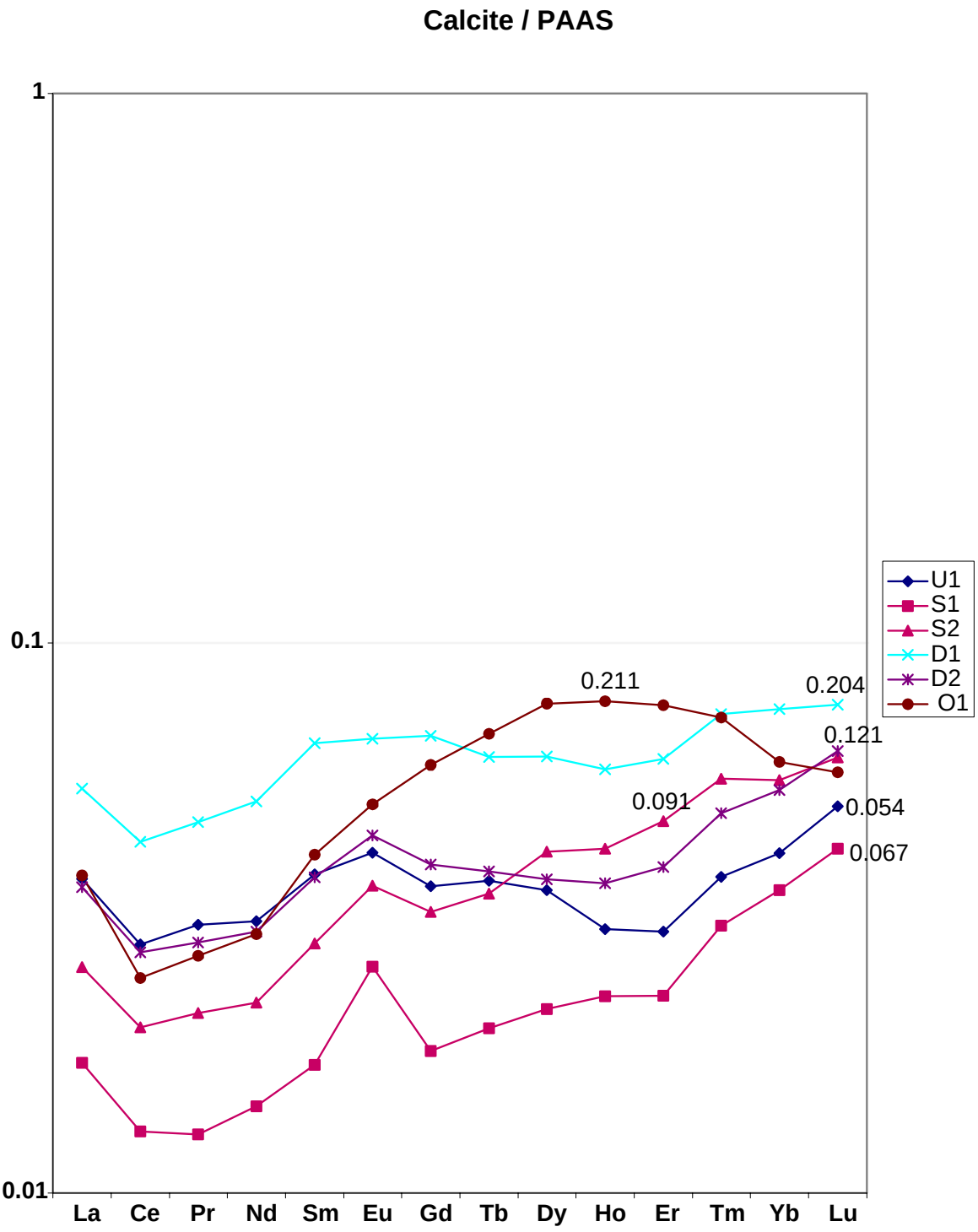

Figure A1. Calcite REE patterns normalized to PAAS (Post Archean Shale Composite). Numbers by each pattern represent the weight percent of phosphate in each sample.

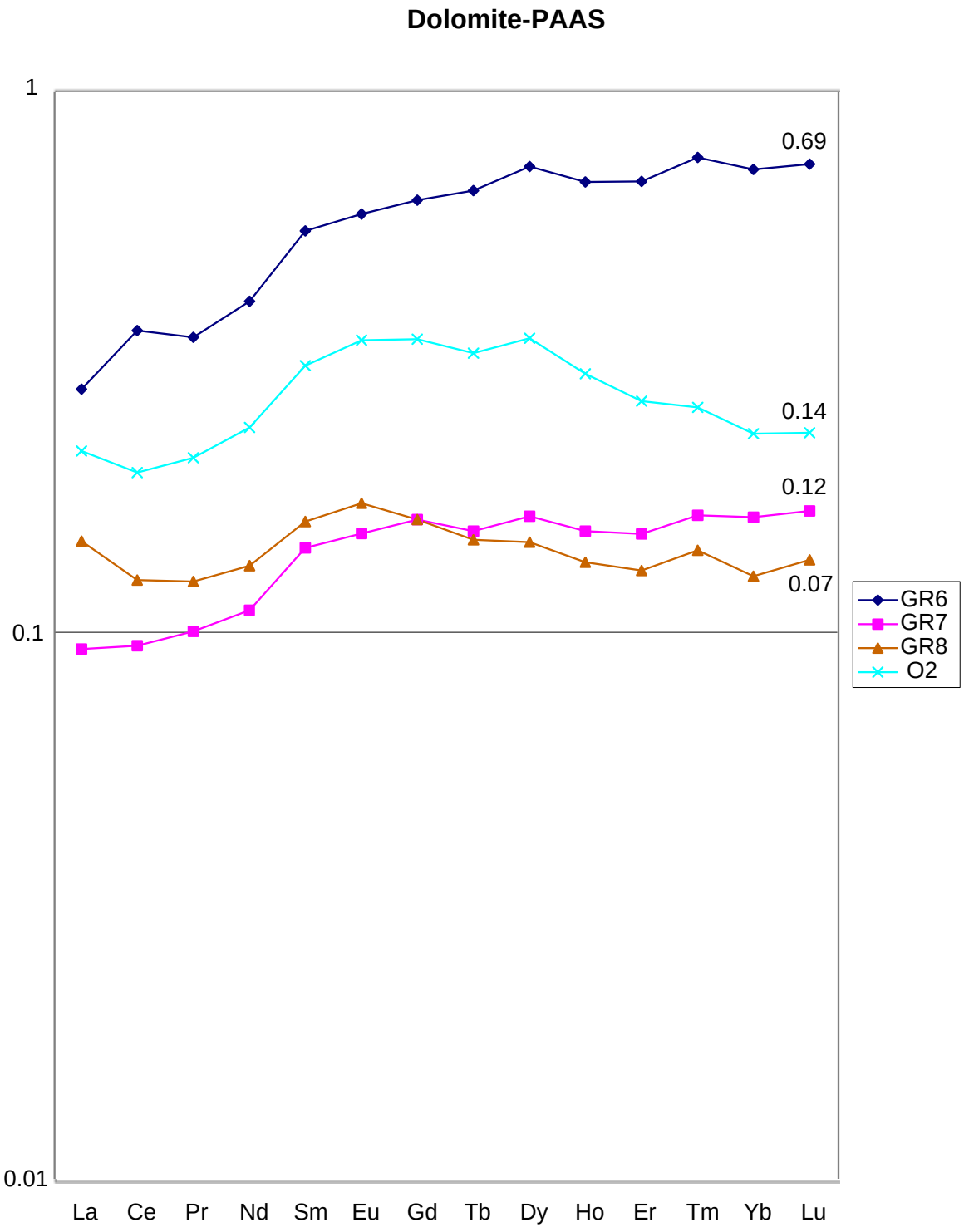

Figure A2. REE pattern showing dolomite samples normalized to PAAS. Numbers here represent the Th/Mg ratio.

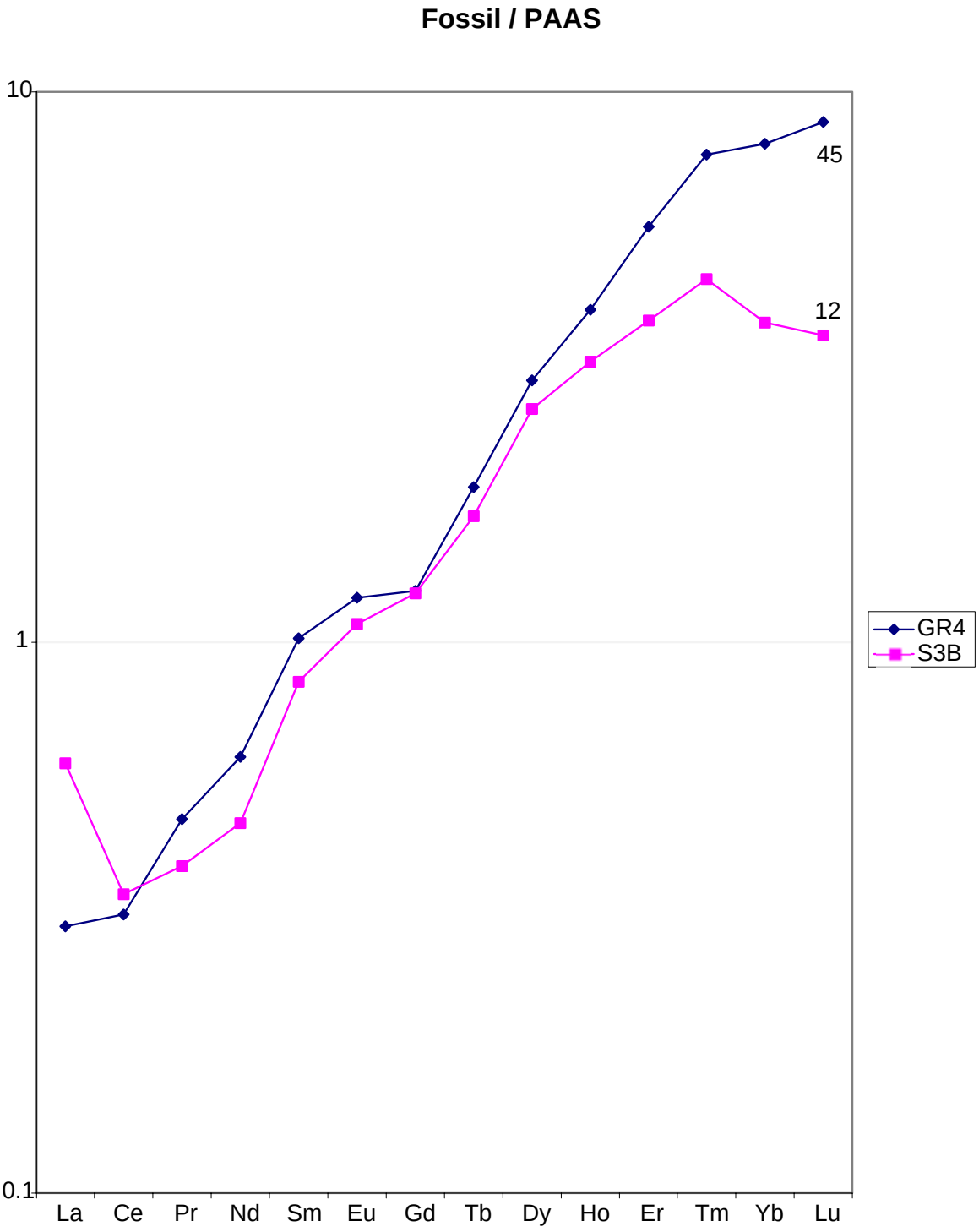

Figure A3. REE pattern showing phosphatic fossils normalized to PAAS. Numbers here are actual Th values in ppm.

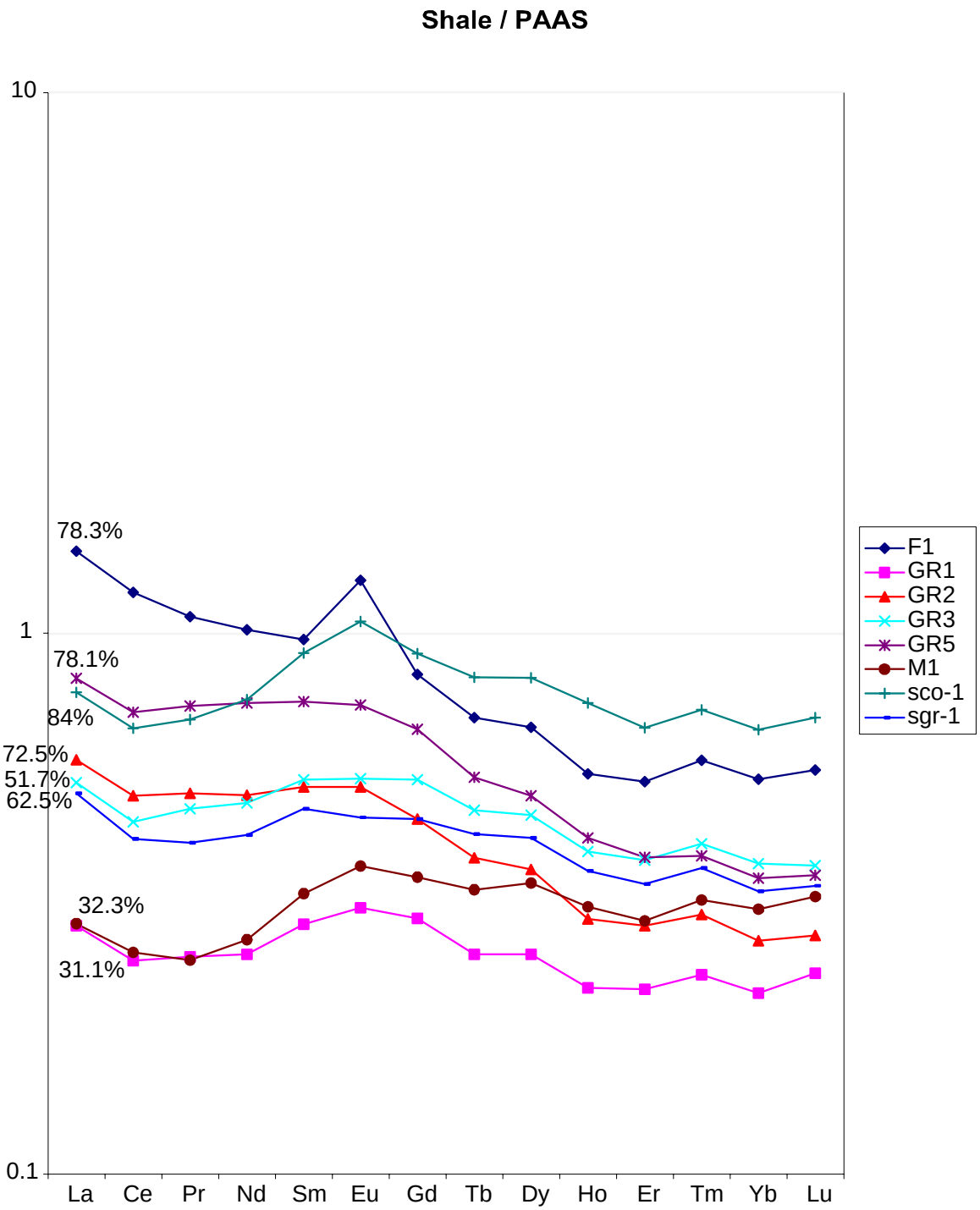

Figure A4. REE patterns of "shale" samples normalized to PAAS. Number here represent the normalized percentage of (Al_2O_3+SiO_2)

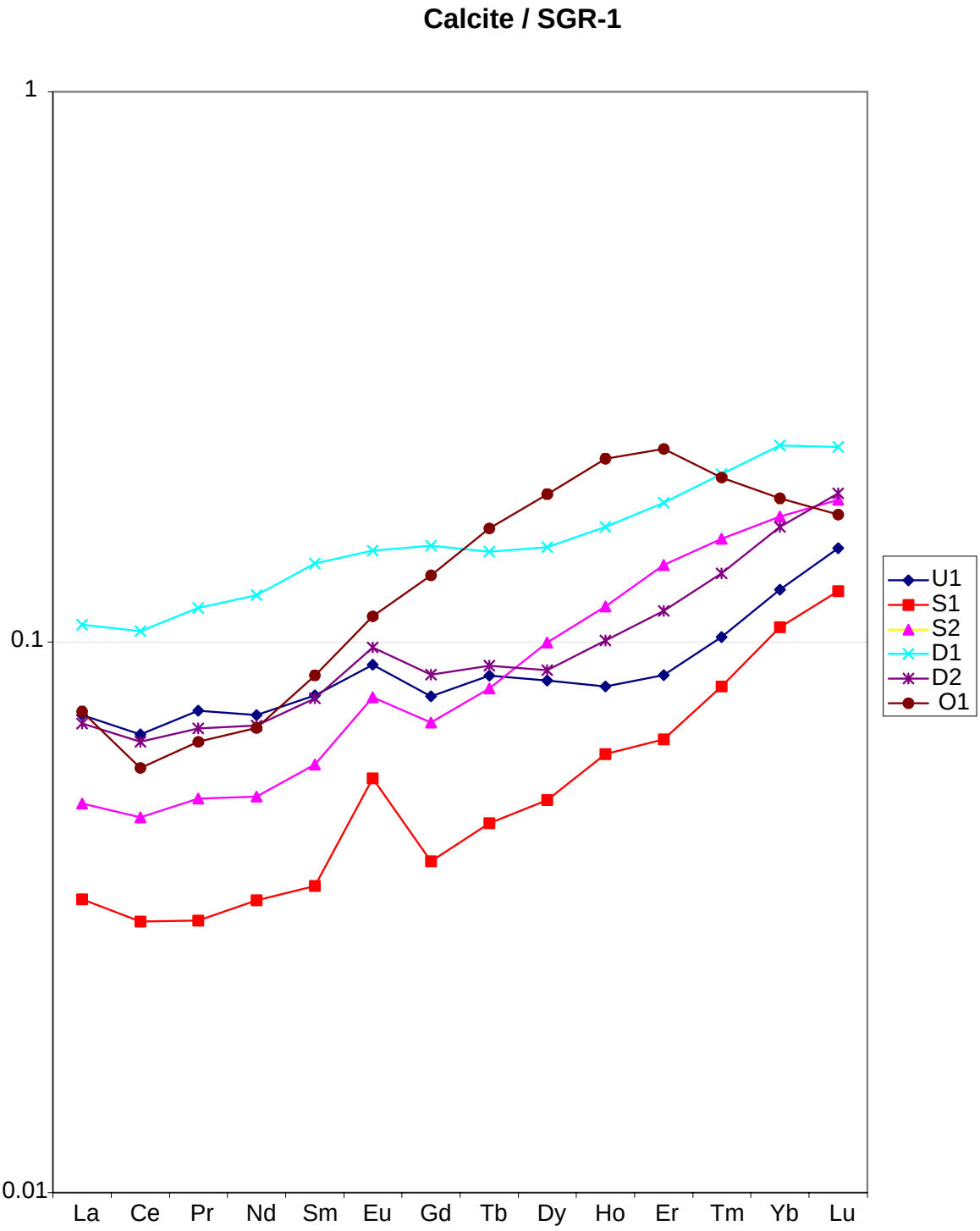

Figure A5. REE pattern showing Calcite rich samples normalized to SGR-1 (USGS standard for Green River Shale).

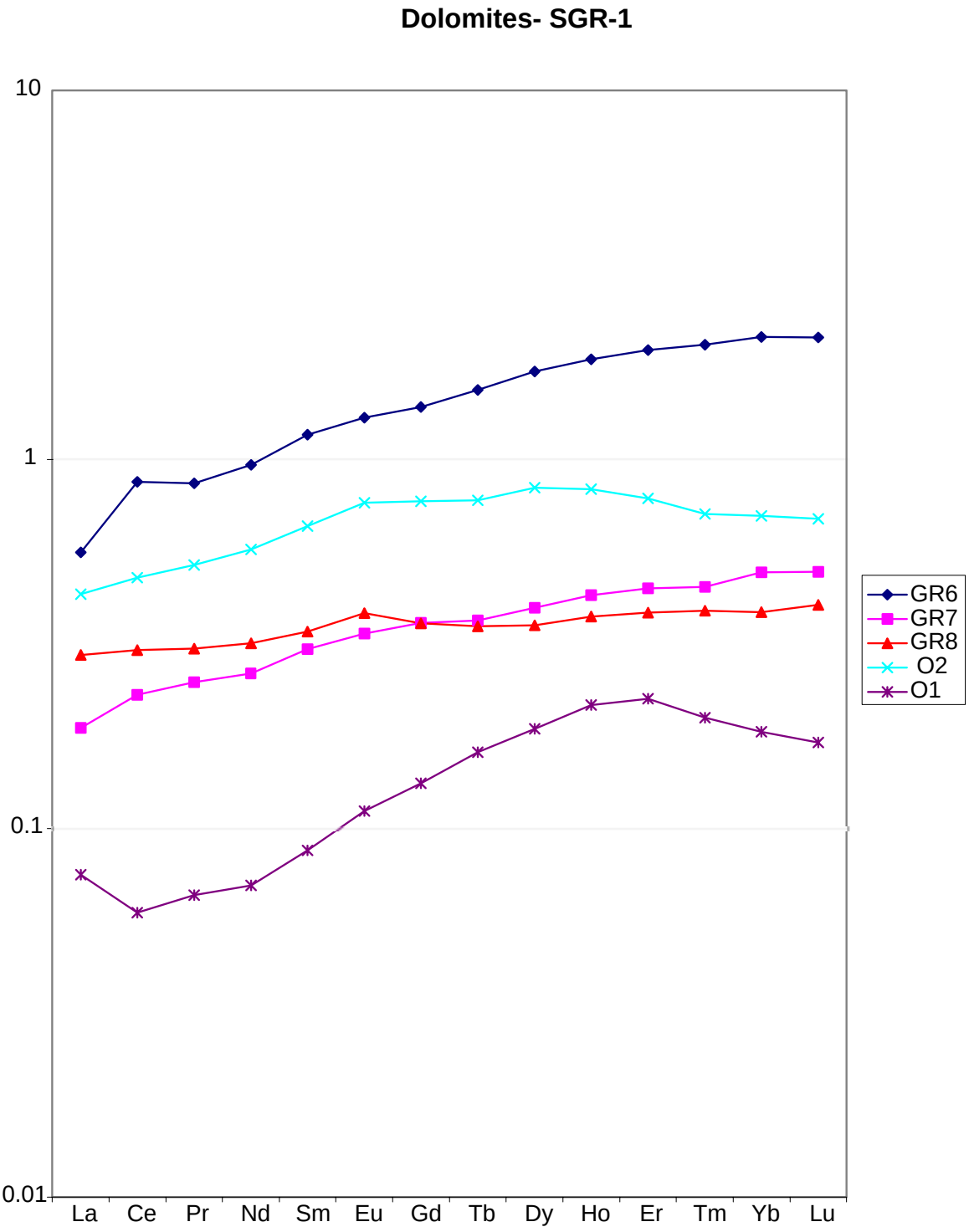

FigureA6. REE pattern showing dolomite samples normalized to SGR-1. O1 is an unusual calcite sample that is shown here for comparison.

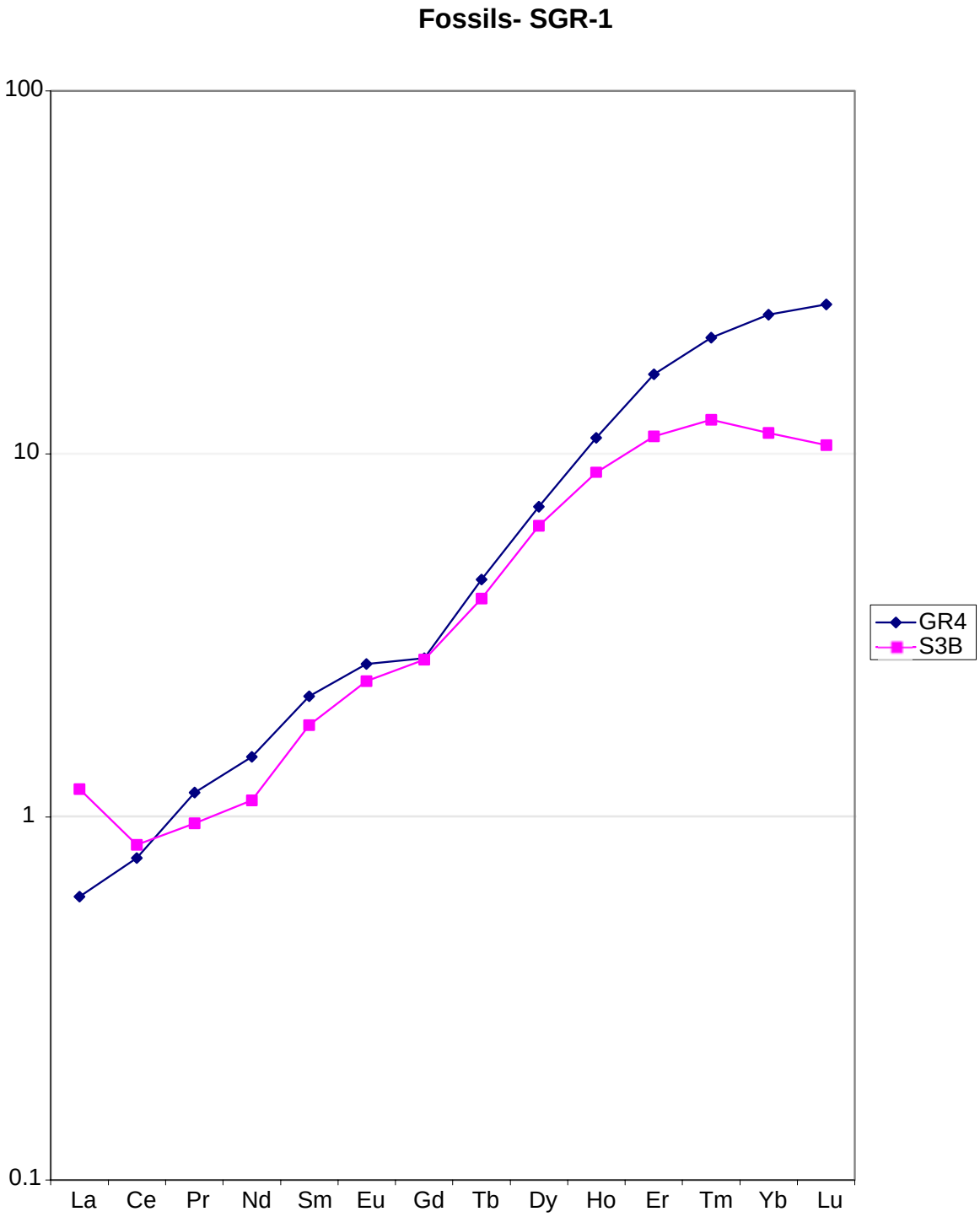

Figure A7. REE pattern of phosphatic fossil samples normalized to SGR-1.

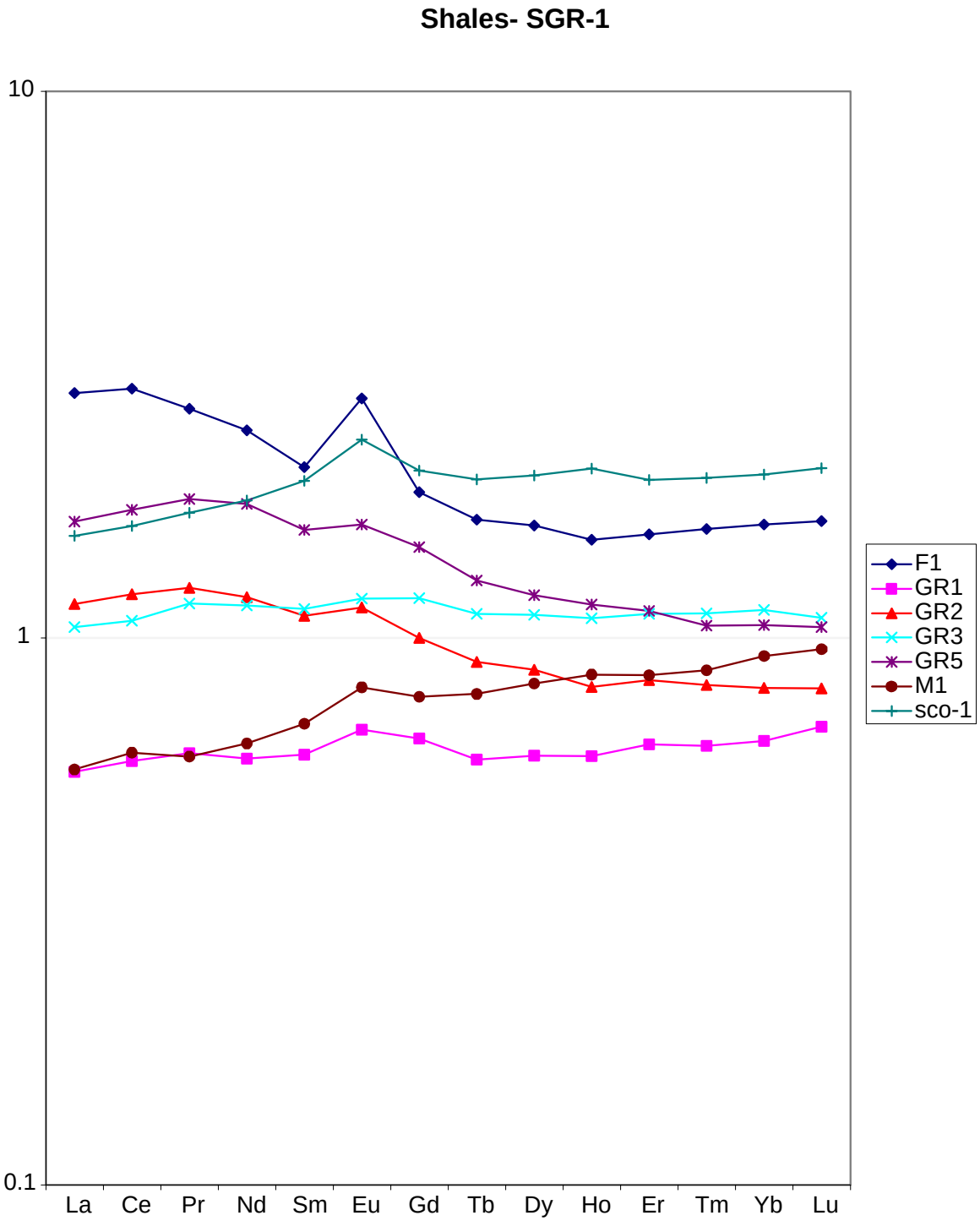

Figure A8. REE patterns of shale samples normalized to SGR-1.

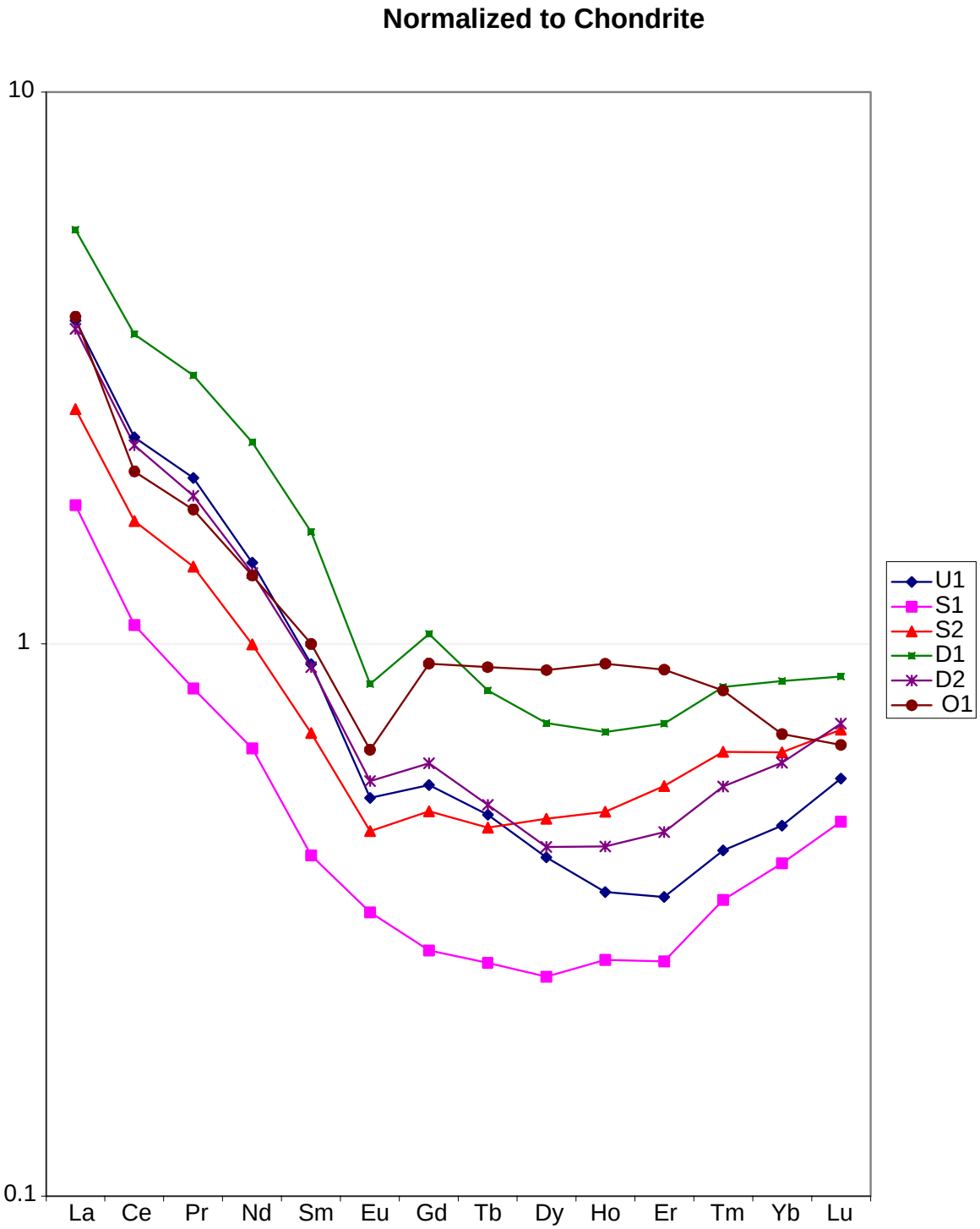

Figure A9. Calcite samples normalized to chondrite.

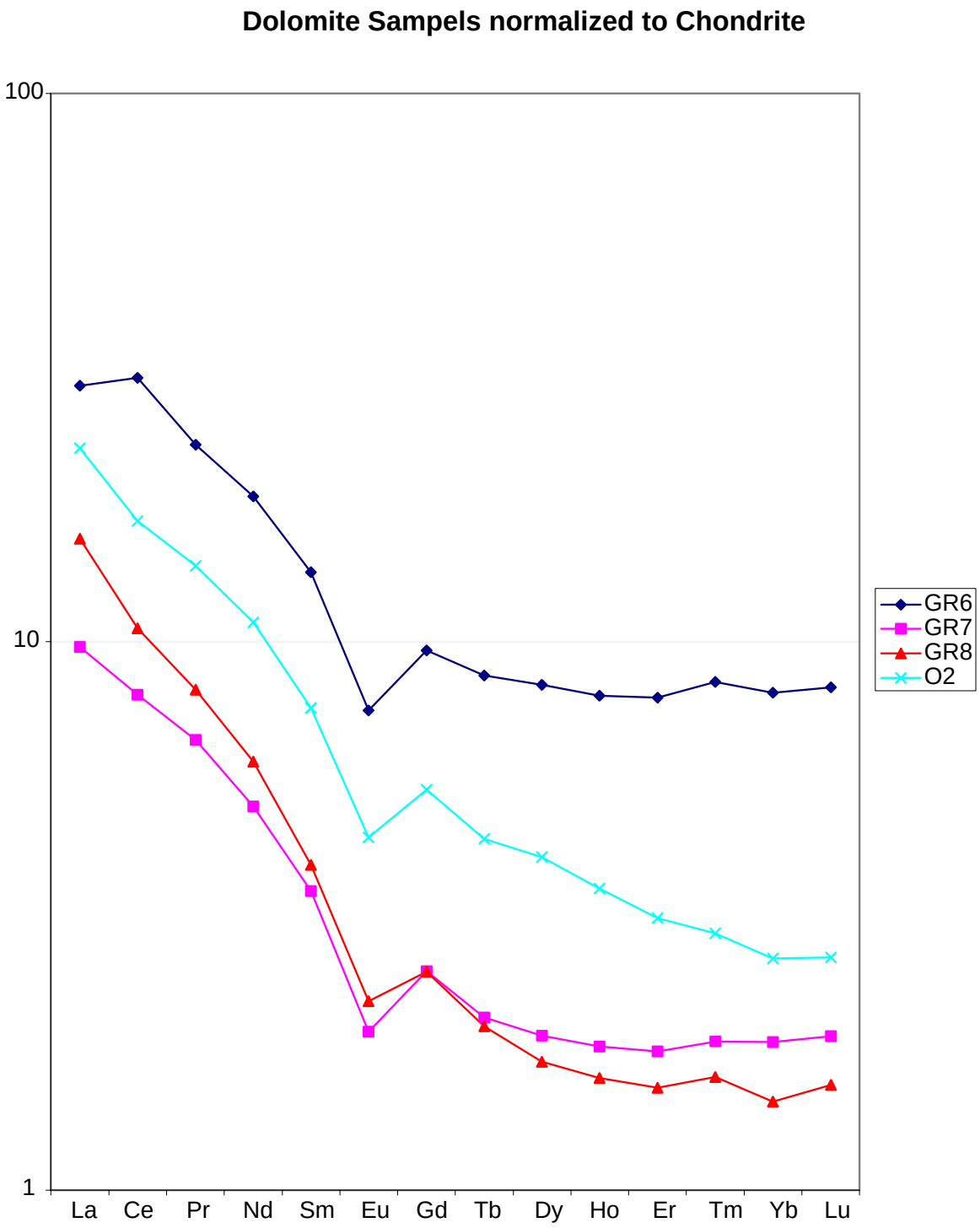

Figure A10. Dolomite samples normalized to chondrite.

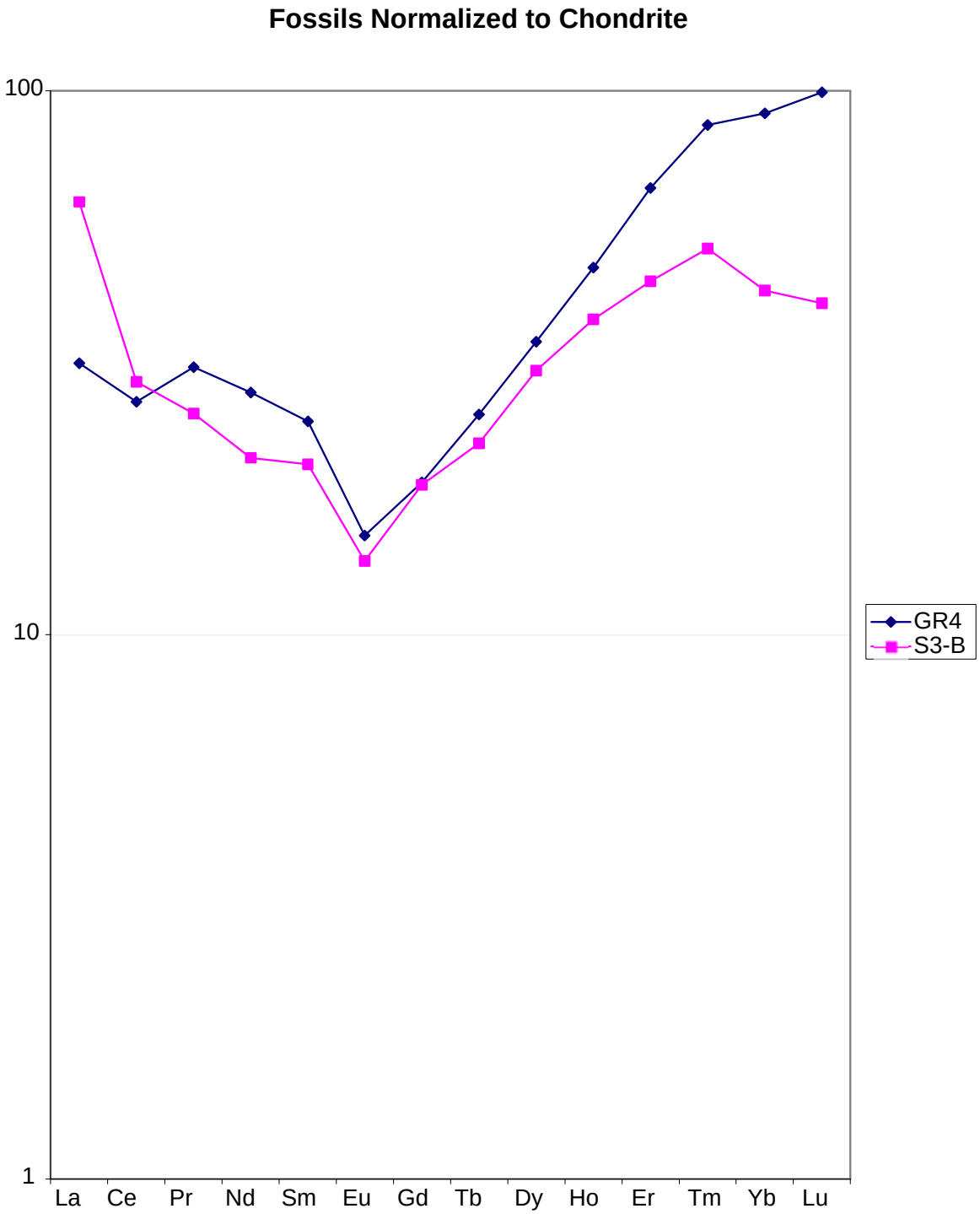

Figure A11. Phosphatic fossils normalized to chondrite.

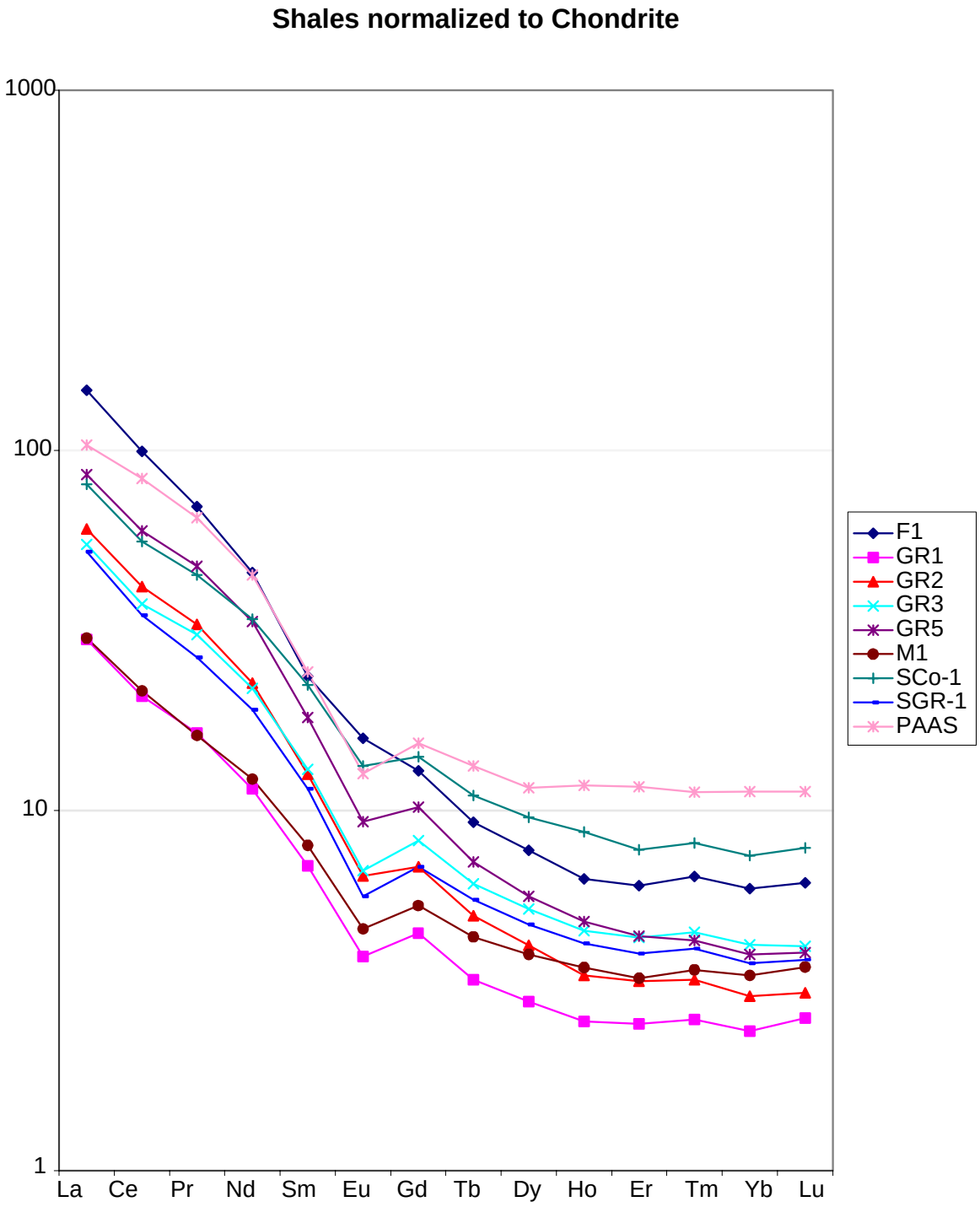

Figure A12. Shale samples normalized to chondrite.

Appendix B

Log K values for calculations in PHREEQCi. Log K data were collected from a variety of sources (Joao, Bigot and Fromage 1986, LaFlamme and Murray 1987, Östhols, Bruno, and Grenthe 1994, Östhols and Malmström 1995, Grenthe Personal Communication 2003) and added to the existing LLNL database provided with PHREEQCi. This table reflects values from all of these sources. Permission was granted to report values provided from Grenthe Personal Communication (2003).

Reaction	log_k
$Th^{4+} = Th^{4+}$	0
$2\ Th^{4+}\ 2\ H_2O\ + = Th_2(OH)_2^{6+} + 2\ H^+$	-6.4618
$4\ Th^{4+}\ 8\ H_2O\ + = Th_4(OH)_8^{8+} + 8\ H^+$	-21.7568
$6\ Th^{4+}\ 15\ H_2O\ + = Th_6(OH)_{15}^{9+} + 15\ H^+$	-37.7027
$Th^{4+} + CO_3^{2-} = Th(CO_3)^{2+}$	+11.03
$Th(OH)_4 + CO_3^{2-} = Th(OH)_4(CO_3)^{2-}$	+2.37
$Th^{4+} + 4\ OH^- + CO_3^{2-} = Th(OH)_3(CO_3)^-$	+41.5
$Th^{4+} + OH^- + 4\ CO_3^{2-} = Th(OH)(CO_3)_4^{4-}$	+35.8
$Th^{4+} + 2\ OH^- + 2CO_3^{2-} = Th(OH)_2(CO_3)_2^{2-}$	+37.0
$Th^{4+} + 2\ OH^- + CO_3^{2-} = Th(OH)_2(CO_3)$	+30.7
$Th^{4+} + 3\ OH^- + CO_3^{2-} = Th(OH)_3(CO_3)^-$	+38.5
$Th^{4+} + 4\ OH^- + CO_3^{2-} = Th(OH)_4(CO_3)^{2-}$	+40.7
$Th^{4+} + 5\ CO_3^{2-} = Th(CO_3)_5^{6-}$	+33.0
$2\ HPO_4^{2-} + 2\ H^+ + Th^{4+} = Th(H_2PO_4)_2^{2+}$	+23.2070
$2\ HPO_4^{2-} + Th^{4+} = Th(HPO_4)_2$	+22.6939
$3\ HPO_4^{2-} + Th^{4+} = Th(HPO_4)_3^{2-}$	+31.1894
$Th^{4+} + HPO_4^{2-} + H^+ = ThHPO_4^{3+}$	+11.7061
$Th^{4+} + HPO_4^{2-} + 2\ H^+ = ThH_3PO_4^{4+}$	+11.1197
$Th^{4+} + HPO_4^{2-} = ThHPO_4^{2+}$	+10.6799
$Th^{4+} + H_2O = ThOH^{3+}$	-3.8871
$2\ H_2O\ + Th^{4+} = Th(OH)_2^{2+} + 2\ H^+$	-7.1068
$3\ H_2O\ + Th^{4+} = Th(OH)_3^+ + 3\ H^+$	-11.8623
$4\ H_2O\ + Th^{4+} = Th(OH)_4 + 4H^+$	-16.0315

PHREEQCi input files for modeling

The following is the input file for Th speciation for figure 19.

```
DATABASE C:\Program Files\USGS\Phreeqc Interactive 2.6\llnl-Th.dat
SOLUTION 1
    temp      25
    pH        5
    pe        4
    redox     pe
    units     mol/kgw
    density   1
    Na        0.15
    Cl        0.15
    Th        1e-005
    -water    1 # kg
END

PHASES
        Fix_H+
        H+ = H+
        log_k  0.0

END

SELECTED_OUTPUT
    -file                 C:\Phreeqci\hydrox-fix pH_Th_CO3-T25.txt
    -reset                false
    -ph                   true
    -molalities           Th(HPO4)3-2  Th(HPO4)2  Th(OH)4
                          Th(OH)4(CO3)-2  Th(OH)3(CO3)-  Th(CO3)5-6  Th(CO3)+2
                          ThH2PO4+3  ThH3PO4+4  ThHPO4+2  Th2(OH)2+6
                          Th4(OH)8+8  Th(H2PO4)2+2  Th(OH)2+2  Th(OH)3+
                          ThOH+3  Th6(OH)15+9  Th(OH)2(CO3)2-2  Th(OH)2(CO3)
                          Th(OH)(CO3)4-5

USE solution 1
EQUILIBRIUM_PHASES 1
    Fix_H+    -5 NaOH      20
    Hydroxylapatite 0 10
    CO2(g)    -3.5 10
END

USE solution 1
EQUILIBRIUM_PHASES 1
      Fix_H+      -5.25 NaOH  20.0
      Hydroxylapatite 0 10
      CO2(g)    -3.5 10

END
USE solution 1
EQUILIBRIUM_PHASES 1
      Fix_H+      -5.50 NaOH  20.0
      Hydroxylapatite 0 10
      CO2(g)    -3.5 10

END
USE solution 1
EQUILIBRIUM_PHASES 1
      Fix_H+      -5.57 NaOH  20.0
      Hydroxylapatite 0 10
```

```
      CO2(g)    -3.5 10

END
USE solution 1
EQUILIBRIUM_PHASES 1
      Fix_H+      -6.0  NaOH  20.0
      Hydroxylapatite 0 10
      CO2(g)    -3.5 10

END
USE solution 1
EQUILIBRIUM_PHASES 1
      Fix_H+      -6.25 NaOH  20.0
      Hydroxylapatite 0 10
      CO2(g)    -3.5 10

END
USE solution 1
EQUILIBRIUM_PHASES  1
      Fix_H+      -6.50 NaOH  20.0
      Hydroxylapatite 0 10
      CO2(g)    -3.5 10

END
USE solution 1
EQUILIBRIUM_PHASES  1
      Fix_H+      -6.75 NaOH  20.0
      Hydroxylapatite 0 10
      CO2(g)    -3.5 10

END
USE solution 1
EQUILIBRIUM_PHASES  1
      Fix_H+      -7.0  NaOH  20.0
      Hydroxylapatite 0 10
      CO2(g)    -3.5 10

END
USE solution 1
EQUILIBRIUM_PHASES  1
      Fix_H+      -7.25 NaOH  20.0
      Hydroxylapatite 0 10
      CO2(g)    -3.5 10

END
USE solution 1
EQUILIBRIUM_PHASES  1
      Fix_H+      -7.50 NaOH  20.0
      Hydroxylapatite 0 10
      CO2(g)    -3.5 10

END
USE solution 1
EQUILIBRIUM_PHASES  1
      Fix_H+      -7.75 NaOH  20.0
      Hydroxylapatite 0 10
      CO2(g)    -3.5 10

END
USE solution 1
EQUILIBRIUM_PHASES  1
      Fix_H+      -8.0  NaOH  20.0
      Hydroxylapatite 0 10
      CO2(g)    -3.5 10

END
USE solution 1
EQUILIBRIUM_PHASES  1
      Fix_H+      -8.25 NaOH  20.0
      Hydroxylapatite 0 10
      CO2(g)    -3.5 10

END
USE solution 1
EQUILIBRIUM_PHASES  1
      Fix_H+      -8.50 NaOH  20.0
      Hydroxylapatite 0 10
      CO2(g)    -3.5 10

END
USE solution 1
EQUILIBRIUM_PHASES  1
      Fix_H+      -8.75 NaOH  20.0
      Hydroxylapatite 0 10
      CO2(g)    -3.5 10

END
USE solution 1
EQUILIBRIUM_PHASES  1
      Fix_H+      -9.0  NaOH  20.0
      Hydroxylapatite 0 10
      CO2(g)    -3.5 10

END

USE solution 1
EQUILIBRIUM_PHASES  1
      Fix_H+      -9.25 NaOH  20.0
      Hydroxylapatite 0 10
      CO2(g)    -3.5 10

END

USE solution 1
EQUILIBRIUM_PHASES  1
      Fix_H+      -9.5  NaOH  20.0
      Hydroxylapatite 0 10
      CO2(g)    -3.5 10

END

USE solution 1
EQUILIBRIUM_PHASES  1
      Fix_H+      -9.75 NaOH  20.0
```

```
      Hydroxylapatite 0 10
      CO2(g)    -3.5 10

END

USE solution 1
EQUILIBRIUM_PHASES  1
      Fix_H+      -10.0 NaOH  20.0
      Hydroxylapatite 0 10
      CO2(g)    -3.5 10

END

USE solution 1
EQUILIBRIUM_PHASES  1
      Fix_H+      -10.25      NaOH  20.0
      Hydroxylapatite 0 10
      CO2(g)    -3.5 10

END

USE solution 1
EQUILIBRIUM_PHASES  1
      Fix_H+      -10.5 NaOH  20.0
      Hydroxylapatite 0 10
      CO2(g)    -3.5 10

END

USE solution 1
EQUILIBRIUM_PHASES  1
      Fix_H+      -10.75      NaOH  20.0
      Hydroxylapatite 0 10
      CO2(g)    -3.5 10

END

USE solution 1
EQUILIBRIUM_PHASES  1
      Fix_H+      -11.0 NaOH  20.0
      Hydroxylapatite 0 10
      CO2(g)    -3.5 10

END

USE solution 1
EQUILIBRIUM_PHASES  1
      Fix_H+      -11.25      NaOH  20.0
      Hydroxylapatite 0 10
      CO2(g)    -3.5 10

END

USE solution 1
EQUILIBRIUM_PHASES  1
      Fix_H+      -11.5 NaOH  20.0
      Hydroxylapatite 0 10


      CO2(g)    -3.5 10

END

USE solution 1
EQUILIBRIUM_PHASES  1
      Fix_H+      -11.75      NaOH  20.0
      Hydroxylapatite 0 10
      CO2(g)    -3.5 10

END

USE solution 1
EQUILIBRIUM_PHASES  1
      Fix_H+      -12.0 NaOH  20.0
      Hydroxylapatite 0 10
      CO2(g)    -3.5 10

END
```

The following is the input file for REE speciation for figure 20.

```
SOLUTION 1
    temp      25
    pH        7
    pe        4
    redox     pe
    units     mol/l
    density   1
    Ce        0.0001
    Er        0.0001
    Dy        0.0001
    Eu        0.0001
    Gd        0.0001
    La        0.0001
    Lu        0.0001
    Nd        0.0001
    Pr        0.0001
    Sm        0.0001
    Tb        0.0001
    Ho        0.0001
    Tm        0.0001
    Yb        0.0001
    Na        0.1
    Cl        0.1
    -water    1 # kg
PHASES
        Fix_H+
        H+ = H+
        log_k  0.0
end
use solution 1
EQUILIBRIUM_PHASES 1
    Fix_H+    -5 NaOH      10
    CO2(g)    -3.5 10
end
use solution 1
EQUILIBRIUM_PHASES 1
        Fix_H+   -6   NaOH    10.0
        CO2(g) -3.5  10
end
use solution 1
EQUILIBRIUM_PHASES 1
        Fix_H+   -7   NaOH    10.0
        CO2(g) -3.5  10
end
use solution 1
EQUILIBRIUM_PHASES 1
        Fix_H+   -8   NaOH    10.0
        CO2(g) -3.5  10
end
use solution 1
EQUILIBRIUM_PHASES 1
        Fix_H+   -9   NaOH    10.0
        CO2(g) -3.5  10
end
use solution 1
EQUILIBRIUM_PHASES 1
        Fix_H+   -10   NaOH    10.0
        CO2(g) -3.5  10
end
use solution 1
EQUILIBRIUM_PHASES 1
        Fix_H+   -11   NaOH    20.0
        CO2(g) -3.5  10
end
use solution 1
EQUILIBRIUM_PHASES 1
        Fix_H+   -12   NaOH    20.0
        CO2(g) -3.5  10
```

The following is the input file for REE speciation for figure 12.

```
DATABASE C:\Program Files\USGS\Phreeqc Interactive 2.8\llnl.dat
SOLUTION 1
   temp      35
   pH        9.8
   pe        4
   redox     pe
   units     mol/kgw
   density   1
   Ca        0.03 mMol/kgw
   Mg        0.6 mMol/kgw
   Na        617 mMol/kgw
   K         16.6 mMol/kgw
   S(6)      58 mMol/kgw
   Cl        293.4 mMol/kgw
   Alkalinity 319.5 meq/kgw
   Fe        3.67 uMol/kgw
   Ba        19 uMol/kgw
   P         450 uMol/kgw
   La        1.3e-007
   Ce        6.42e-007
   Pr        1.14e-007
   Nd        6.03e-007
   Sm        2.39e-007
   Eu        5.3e-008
   Gd        4.39e-007
   Tb        1.26e-007
   Dy        1.188e-006
   Ho        3.33e-007
   Er        1.208e-006
   Tm        1.95e-007
   Yb        1.289e-006
   Lu        2.06e-007
   -water    1 # kg

SELECTED_OUTPUT
   -file              selected-35-red.txt
   -molalities        Ce(CO3)2-  Ce(PO4)2-3  CeH2PO4+2  CeHCO3+2
                      CeHPO4+  CePO4  Ce(HPO4)2-  DyCO3+
                      DyH2PO4+2  DyHCO3+2  DyHPO4+  DyPO4
                      Dy(CO3)2-  Dy(HPO4)2-  Dy(PO4)2-3  Er(CO3)2-
                      Er(HPO4)2-  Er(PO4)2-3  ErH2PO4+2  ErHCO3+2
                      ErHPO4+  ErPO4  Eu(CO3)2-  Eu(CO3)3-3
```

Eu(HPO4)2- Eu(OH)2CO3- Eu(PO4)2-3 EuCO3+
EuH2PO4+2 EuHCO3+2 EuHPO4+ EuOH(CO3)2-2
EuOHCO3 EuPO4 Gd(CO3)2- Gd(HPO4)2-
Gd(PO4)2-3 GdCO3+ GdH2PO4+2 GdHCO3+2
GdHPO4+ GdPO4 La(CO3)2- La(HPO4)2-
La(PO4)2-3 LaCO3+ LaH2PO4+2 LaHCO3+2
LaHPO4+ LaPO4 Lu(CO3)2- Lu(HPO4)2-
Lu(PO4)2-3 LuH2PO4+2 LuHCO3+2 LuCO3+
LuHPO4+ LuPO4 Nd(CO3)2- Nd(HPO4)2-
Nd(PO4)2-3 NdCO3+ NdH2PO4+2 NdHCO3+2
NdHPO4+ NdPO4 Pm(HPO4)2- Pm(CO3)2-
Pm(PO4)2-3 PmCO3+ PmH2PO4+2 PmHCO3+2
PmIIPO4+ PmPO4 Pr(CO3)2- Pr(IIPO4)2-
Pr(PO4)2-3 PrCO3+ PrH2PO4+2 PrHCO3+2
PrHPO4+ PrPO4 Sm(CO3)2- Sm(HPO4)2-
Sm(PO4)2-3 SmH2PO4+2 SmHCO3+2 SmHPO4+
SmPO4 Tb(CO3)2- Tb(HPO4)2- Tb(PO4)2-3
TbCO3+ TbH2PO4+2 TbHCO3+2 TbHPO4+
TbPO4 Tm(CO3)2- Tm(HPO4)2- Tm(PO4)2-3
TmCO3+ TmH2PO4+2 TmHCO3+2 TmHPO4+
TmPO4 Yb(CO3)2- Yb(HPO4)2- Yb(PO4)2-3
YbCO3+ YbH2PO4+2 YbHCO3+2 YbHPO4+
YbPO4 Ho(CO3)2- Ho(HPO4)2- Ho(PO4)2-3
HoH2PO4+2 HoHCO3+2 HoHPO4+ HPO4-2
HoPO4

Appendix C
ICP-MS and XFR analysis

Sample ID	La	Ce	Pr	Nd	Sm	Eu	Gd	Tb	Dy	Ho	Er	Tm	Yb	Lu
S1	0.65	1.04	0.11	0.46	0.10	0.03	0.09	0.02	0.10	0.02	0.07	0.01	0.10	0.02
S2	0.98	1.60	0.19	0.71	0.16	0.04	0.15	0.03	0.18	0.04	0.14	0.02	0.16	0.03
S4	0.91	1.50	0.18	0.67	0.15	0.03	0.14	0.03	0.17	0.04	0.12	0.02	0.15	0.03
S-4 ®	0.93	1.53	0.17	0.69	0.15	0.04	0.16	0.03	0.17	0.04	0.12	0.02	0.16	0.03
D1	2.06	3.48	0.42	1.65	0.37	0.07	0.32	0.05	0.27	0.06	0.18	0.03	0.21	0.03
D2	1.37	2.19	0.25	0.96	0.21	0.05	0.19	0.03	0.16	0.04	0.11	0.02	0.15	0.03
O1	1.44	1.97	0.24	0.95	0.23	0.06	0.28	0.05	0.34	0.08	0.22	0.03	0.17	0.03
O2	8.27	15.90	1.88	7.70	1.75	0.38	1.64	0.25	1.54	0.30	0.78	0.10	0.66	0.10
O3	8.07	15.51	1.83	7.40	1.73	0.38	1.62	0.25	1.50	0.29	0.78	0.11	0.67	0.10
O2 ®	8.18	15.57	1.85	7.52	1.73	0.37	1.64	0.25	1.51	0.29	0.78	0.11	0.64	0.10
S3B	22.92	27.90	3.49	15.04	4.75	1.19	5.77	1.31	11.66	3.24	11.13	1.83	10.65	1.55
M1	11.04	20.56	2.21	8.68	1.85	0.41	1.66	0.26	1.52	0.31	0.85	0.13	0.86	0.14
Sco-1*	29.54	53.39	6.17	24.14	5.15	1.16	4.31	0.64	3.64	0.74	1.94	0.29	1.86	0.30
SGR-1*	19.21	33.30	3.64	13.54	2.65	0.50	2.13	0.33	1.84	0.36	1.00	0.15	0.93	0.15
F1	53.86	95.12	9.56	32.50	5.45	1.38	3.94	0.54	2.95	0.55	1.54	0.23	1.50	0.24
U1	1.41	2.26	0.27	1.00	0.21	0.05	0.17	0.03	0.16	0.03	0.09	0.02	0.12	0.02
GR1	10.94	19.85	2.25	8.15	1.62	0.34	1.40	0.20	1.12	0.22	0.64	0.09	0.60	0.10
GR2	22.18	40.04	4.51	16.07	2.91	0.57	2.13	0.30	1.61	0.30	0.83	0.12	0.76	0.12
GR3	20.11	35.80	4.22	15.52	3.00	0.59	2.52	0.36	2.03	0.39	1.10	0.16	1.05	0.16
GR4	11.58	25.66	4.25	19.83	5.70	1.32	5.83	1.47	13.16	4.02	16.51	3.08	22.53	3.79
GR5	31.37	57.15	6.54	23.80	4.18	0.81	3.12	0.42	2.20	0.42	1.12	0.16	0.99	0.15
GR6	10.76	28.96	3.13	13.09	3.09	0.65	2.95	0.50	3.18	0.68	1.97	0.30	2.00	0.31
GR7	3.59	7.66	0.91	3.56	0.81	0.17	0.77	0.12	0.73	0.16	0.45	0.07	0.46	0.07
GR8	5.66	10.12	1.12	4.29	0.91	0.19	0.77	0.12	0.65	0.14	0.38	0.06	0.36	0.06
Sco-1**	30.30	55.30	6.75	25.28	5.12	1.07	4.17	0.63	3.49	0.66	1.97	0.29	1.95	0.31
SGR-1**	18.92	33.22	3.84	13.85	2.58	0.47	2.04	0.30	1.69	0.33	0.92	0.14	0.89	0.15
AL1***	3.10	6.16	0.71	2.97	0.73	0.14	0.67	0.10	0.59	0.12	0.30	0.04	0.27	0.04
AU1***	3.81	7.66	0.90	3.77	0.82	0.15	0.63	0.08	0.42	0.08	0.20	0.03	0.16	0.02
FG-A15***	24.90	47.83	5.81	23.59	5.12	1.04	4.55	0.98	8.89	2.48	8.85	1.53	9.62	1.36
FB-B2***	74.95	171.25	21.95	91.98	20.26	3.70	16.00	2.40	12.71	2.20	5.20	0.67	3.76	0.53

Table C1. ICP-MS REE data for collected samples as collected by Washington State University. Notes:* USGS standards taken in Dec. 2002. **USGS Standards taken on Jan. 2004. ***samples analyzed but not included in this study. ®replicate samples.

Sample ID	Ba	Th	Nb	Y	Hf	Ta	U	Pb	Rb	Cs	Sr	Sc	Zr
S1	95	0.16	0.20	0.71	0.07	0.02	1.79	0.65	1.51	0.09	1055	0.49	2.26
S2	111	0.31	0.49	1.25	0.15	0.03	2.66	0.78	3.31	0.19	1044	0.68	4.82
S4	103	0.31	0.50	1.20	0.13	0.03	2.47	0.77	3.21	0.17	1001	0.80	4.67
S-4 ®	106	0.30	0.52	1.22	0.14	0.03	2.52	0.73	3.15	0.17	982	0.83	4.57
D1	270	0.72	1.17	1.87	0.16	0.07	9.53	2.05	8.97	0.29	1224	0.93	5.65
D2	159	0.41	0.54	1.16	0.10	0.04	5.01	1.16	4.60	0.18	1270	0.81	3.36
O1	103	0.17	0.20	3.64	0.08	0.02	9.04	7.08	1.04	0.06	504	0.31	4.92
O2	85	2.94	1.72	8.85	0.40	0.09	7.26	10.53	9.05	0.53	779	1.61	16.62
O3	83	2.81	1.73	9.04	0.43	0.08	6.93	10.59	9.07	0.53	790	1.62	18.17
O2 ®	83	2.86	1.74	8.93	0.43	0.09	6.92	10.54	8.94	0.53	779	1.72	16.63
S3B	27656	12.04	0.10	117.49	0.48	0.01	267.89	13.20	0.10	0.01	7363	5.75	36.01
M1	669	4.00	3.57	9.66	0.80	0.23	4.79	7.06	42.28	1.17	1446	5.12	32.47
Sco-1*	563	9.30	11.42	20.08	2.52	0.86	2.64	30.74	110.08	7.62	166	13.69	89.98
SGR-1*	274	4.56	6.56	10.90	0.95	0.46	4.62	44.74	79.60	5.23	396	5.90	31.05
F1	834	8.18	35.14	17.55	4.78	1.37	2.40	26.71	79.89	5.03	418	10.88	179.20
U1	129	0.36	0.51	1.20	0.07	0.03	2.68	1.29	2.87	0.21	957	0.73	2.03
GR1	915	2.79	3.32	7.81	0.89	0.22	4.67	9.10	38.51	1.60	1510	4.30	31.38
GR2	1255	5.59	15.32	9.29	1.50	0.47	6.18	30.06	110.85	5.20	532	6.56	72.72
GR3	592	5.05	7.63	13.19	1.15	0.45	3.74	18.81	100.62	1.48	1097	6.51	37.87
GR4	5115	45.30	1.28	144.93	0.67	0.04	122.83	9.05	5.70	0.22	6588	14.20	153.95
GR5	406	8.49	14.94	13.51	1.58	0.94	4.91	31.77	113.41	11.18	386	4.87	45.55
GR6	728	10.90	1.56	22.52	0.65	0.10	3.76	11.88	8.42	0.48	1562	6.60	19.52
GR7	273	1.69	0.61	5.70	0.13	0.04	0.85	18.17	3.06	0.31	980	0.84	5.31
GR8	967	1.17	0.20	4.75	0.08	0.01	2.32	1.82	0.77	0.12	1477	2.32	4.88
Sco-1*	568	8.12	12.24	21.46	2.89	0.86	2.42	31.06	115.97	7.85	180	12.65	97.61
SGR-1*	262	4.02	6.55	10.46	1.00	0.44	4.09	45.82	79.43	5.36	394	5.45	30.96
AL1**	275	0.65	6.15	3.00	2.92	0.80	8.34	8.50	66.38	0.10	50	0.71	77.72
AU1**	482	0.45	4.55	2.16	2.43	0.60	2.83	19.00	64.52	0.54	170	0.56	71.43
FG-A15**	531	158.69	7.53	84.97	1.77	0.60	21.83	11.49	75.96	4.31	1023	12.80	60.80
FB-B2**	441	77.74	14.22	68.10	3.09	0.98	13.60	19.72	121.74	6.34	510	12.80	104.16

Table C2. Trace elements analyzed by ICP-MS at Washington State University. See table caption forC1 for note descriptions

	S1	S2	AL1	AU1	D1	D2	D3B	S3B	O1	O2	FGA15
Date	25-Jan-04	25-Jan-04	25-Jan-04	25-Jan-04	25-Jan-04	25-Jan-04	25-Jan-04	25-Jan-04	27-Jan-04	27-Jan-04	25-Jan-04
Unnormalized Major Elements (Weight %):											
SiO2	0.00	0.49	61.23	62.19	3.61	1.71	3.81	0.00	0.00	5.19	43.76
TiO2	0.022	0.035	0.248	0.084	0.097	0.045	0.026	0.028	0.021	0.094	0.420
Al2O3	0.35	0.69	16.16	15.62	1.33	0.77	2.25	0.12	0.20	1.43	9.66
FeO*	0.00	0.00	5.60	1.49	0.03	0.00	0.00	0.00	0.00	1.12	2.77
MnO	0.004	0.005	0.003	0.007	0.006	0.005	0.042	0.003	0.405	0.153	0.139
MgO	0.88	1.28	0.12	0.18	5.34	3.71	0.34	0.42	0.90	31.79	7.03
CaO	73.35	73.47	1.37	4.25	66.34	71.22	48.99	41.02	71.98	45.78	25.72
Na2O	0.18	0.40	14.28	13.48	0.73	0.36	0.06	0.00	0.05	0.30	2.89
K2O	0.00	0.00	0.14	0.53	0.15	0.11	1.74	0.39	0.03	0.36	2.82
P2O5	0.084	0.120	0.116	0.188	0.293	0.162	21.035	22.320	0.274	0.149	0.882
Total	**74.88**	**76.49**	**99.27**	**98.00**	**77.93**	**78.08**	**78.29**	**64.31**	**73.86**	**86.36**	**96.09**
LOI (%)	**40.23**	**41.83**	**10.95**	**3.57**	**45.31**	**41.14**	**19.24**	**9.85**	**43.11**	**43.85**	**22.30**
Major and trace elements normalized to 100-LOI (Weight %, ppm):											
SiO2	0.00	0.37	54.87	61.12	2.52	1.28	3.87	0.00	0.00	3.37	35.27
TiO2	0.018	0.026	0.222	0.082	0.068	0.034	0.026	0.035	0.016	0.061	0.338
Al2O3	0.28	0.52	14.48	15.35	0.93	0.58	2.28	0.16	0.15	0.92	7.79
FeO*	0.00	0.00	5.02	1.46	0.02	0.00	0.00	0.00	0.00	0.72	2.23
MnO	0.003	0.004	0.003	0.007	0.005	0.004	0.042	0.004	0.311	0.099	0.112
MgO	0.70	0.97	0.11	0.18	3.73	2.78	0.35	0.54	0.70	20.62	5.66
CaO	58.37	55.71	1.23	4.18	46.35	53.47	49.80	52.49	55.33	29.70	20.73
Na2O	0.14	0.30	12.79	13.25	0.51	0.27	0.06	0.00	0.04	0.19	2.33
K2O	0.00	0.00	0.13	0.52	0.10	0.08	1.77	0.50	0.03	0.24	2.27
P2O5	0.067	0.091	0.104	0.185	0.204	0.121	21.382	28.560	0.211	0.096	0.711
sum	**59.59**	**58.00**	**88.97**	**96.32**	**54.44**	**58.63**	**79.58**	**82.29**	**56.78**	**56.01**	**77.45**

Table C3. XRF data from Washington State University Geoanalytical Lab. Unnormalized data are above and data normalized to LOI is below.

	S1	S2	AL1	AU1	D1	D2	D3B	S3B	O1	O2	FGA15
Date	25-Jan-04	25-Jan-04	25-Jan-04	25-Jan-04	25-Jan-04	25-Jan-04	25-Jan-04	25-Jan-04	27-Jan-04	27-Jan-04	25-Jan-04
Ni	0	0	23	14	0	0	0	0	0	0	16
Cr	2	2	6	7	3	2	4	0	1	7	43
Sc	0	0	1	3	2	1	7	9	0	4	13
V	16	20	96	27	76	63	32	57	9	15	59
Ba	133	136	277	508	351	218	5148	63119	210	123	588
Rb	4	7	65	71	13	8	12	15	5	13	80
Sr	1678	1451	56	193	1894	1973	5987	14799	792	1039	1121
Zr	29	31	85	179	30	28	158	123	37	58	112
Y	3	2	5	4	3	1	157	193	9	12	85
Nb	0.0	0.0	5.4	4.6	0.0	0.0	0.0	0.0	0.2	0.9	6.3
Ga	1	2	17	20	3	2	1	4	0	0	10
Cu	0	0	82	24	9	0	0	54	0	4	21
Zn	8	5	107	51	17	11	103	67	36	12	65
Pb	6	3	10	24	1	3	8	16	4	11	6
La	1	7	9	0	6	5	21	38	1	10	26
Ce	7	15	20	14	15	9	35	0	2	28	52
Th	2	1	1	0	2	0	50	51	0	4	188
sum tr.	1892	1683	864	1144	2423	2325	11724	78546	1107	1342	2491
in %	0.19	0.17	0.09	0.11	0.24	0.23	1.17	7.85	0.11	0.13	0.25
sum m+t	59.77	58.17	89.05	96.43	54.69	58.86	80.76	90.15	56.89	56.15	77.70
sum LOI+m+t	100.00	100.00	100.00	100.00	100.00	100.00	100.00	100.00	100.00	100.00	100.00

Table C4. XRF data from Washington State University Geoanalytical Lab continued for samples above.

	F1	U1	GR1	GR2	GR3	GR4	GR5	GR6	GR7	GR8	SCo-1 298A	Working Values	SGR-1 298A	Working Values
Date	14-Dec-02	14-Dec-02	14-Dec-02	14-Dec-02	14-Dec-02	14-Dec-02	14-Dec-02	14-Dec-02	14-Dec-02	14-Dec-02	14-Dec-02	(Gov,89)	15-Dec-02	(Gov,95)
LOI (%)	7.18	42.78	38.03	38.01	28.36	17.53	17.47	42.14	43.54	45.67	8.77	8.77	44.42	44.42
100-LOI:	92.82	57.22	61.97	61.99	71.64	82.47	82.53	57.86	56.46	54.33	91.24	91.23	55.58	55.58
	Unnormalized Major Elements (Weight %):										SCo-1	SCo-1	SGR-1	SGR-1
SiO2	60.13	4.43	24.25	56.31	40.82	4.62	60.14	12.60	7.13	3.79	67.92	62.78	48.38	28.24
Al2O3	17.24	0.94	5.83	12.32	9.86	1.07	16.45	1.87	1.42	0.66	15.01	13.67	11.28	6.52
TiO2	0.609	0.044	0.194	0.487	0.370	0.087	0.568	0.105	0.036	0.010	0.638	0.628	0.419	0.264
FeO*	5.38	0.28	1.95	5.20	3.40	1.90	4.62	3.94	3.08	2.06	5.34	4.67	4.59	2.73
MnO	0.061	0.008	0.136	0.075	0.044	0.027	0.032	0.141	0.211	0.100	0.055	0.053	0.055	0.034
CaO	3.23	92.05	58.60	8.32	25.72	45.46	3.99	51.71	60.22	59.31	2.82	2.62	14.46	8.38
MgO	3.43	2.36	2.40	5.39	11.14	3.04	2.68	26.80	25.43	32.58	2.98	2.72	7.63	4.44
K2O	2.79	0.37	1.96	4.56	5.74	0.26	4.99	0.40	0.15	0.04	2.98	2.77	2.70	1.66
Na2O	5.71	0.10	1.23	1.66	0.94	1.33	4.46	0.60	0.62	0.50	1.00	0.90	5.05	2.99
P2O5	0.226	0.096	0.318	0.371	0.085	24.590	0.208	0.072	0.093	0.066	0.224	0.206	0.478	0.328
Total	98.80	100.68	96.86	94.70	98.12	82.39	98.13	98.24	98.39	99.11	98.97	91.02	95.04	55.58
	Major and trace elements normalized to 100-LOI (Weight %, ppm):													
SiO2	56.36	2.51	15.45	36.70	29.71	4.53	50.49	7.39	4.08	2.07	62.51	62.82	28.23	28.24
Al2O3	16.16	0.53	3.71	8.03	7.18	1.05	13.81	1.10	0.81	0.36	13.81	13.68	6.58	6.52
TiO2	0.571	0.025	0.124	0.317	0.269	0.085	0.477	0.062	0.021	0.005	0.587	0.628	0.245	0.264
FeO*	5.04	0.16	1.24	3.39	2.48	1.87	3.87	2.31	1.76	1.12	4.92	4.67	2.68	2.73
MnO	0.057	0.005	0.087	0.049	0.032	0.026	0.027	0.083	0.121	0.055	0.051	0.053	0.032	0.034
CaO	3.03	†52.22	†37.32	5.42	†18.7	†44.6	3.35	†30.32	†34.5	†32.4	2.60	2.62	8.44	8.38
MgO	3.22	1.34	1.53	3.51	8.11	2.98	2.25	15.71	14.56	17.78	2.74	2.72	4.45	4.44
K2O	2.62	0.21	1.25	2.97	4.18	0.25	4.19	0.23	0.09	0.02	2.74	2.77	1.58	1.66
Na2O	5.35	0.06	0.78	1.08	0.68	1.30	3.74	0.35	0.35	0.27	0.92	0.90	2.95	2.99
P2O5	0.212	0.054	0.203	0.242	0.062	†24.1	0.175	0.042	0.053	0.036	0.206	0.206	0.279	0.328
sum	92.61	57.12	61.70	61.73	71.43	80.79	82.38	57.60	56.33	54.09	91.08	91.07	55.46	55.58
	Total Fe is expressed as FeO. "†" denotes values >120% of our highest standard.													

Table C5. XRF data from Washington State University Geoanalytical Lab. Unnormalized data are above and data normalized to LOI is below.

	FGB2	M1	TS1	S4	O3	SGR-1 298A	SGR1 2-98A	Working Values	SCo-1 298A	SCO1 2-98A	Working Values
Date	25-Jan-04	25-Jan-04	25-Jan-04	25-Jan-04	28-Jan-04	14-Dec-98	24-Jan-04	(Gov,95)	13-Dec-98	24-Jan-04	(Gov,89)
Ni	32	6	0	0	0	25	31	29	29	30	27
Cr	57	18	1	2	9	32	30	30	64	69	68
Sc	13	7	5	1	5	0	6	5	13	11	11
V	135	82	12	20	18	114	125	128	122	131	131
Ba	485	829	4529	145	111	286	301	290	574	574	570
Rb	124	55	8	4	13	76	81	83	115	111	112
Sr	546	2016	9732	1472	1085	392	450	420	170	171	174
Zr	173	74	70	31	60	48	56	53	167	167	160
Y	66	12	278	3	13	11	11	13	26	25	26
Nb	14.0	3.5	0.0	0.0	1.2	7.0	7.3	5.2	12.5	11.3	11.0
Ga	16	8	0	2	2	9	9	11	18	18	15
Cu	17	23	0	0	5	59	68	66	29	32	29
Zn	91	37	53	6	12	70	75	74	98	102	103
Pb	18	11	21	2	14	14	18	38	29	32	31
La	75	18	93	0	11	13	20	20	28	31	30
Ce	180	31	315	13	29	40	39	36	61	55	62
Th	83	6	14	1	6	4	6	5	9	9	10
sum tr.	2126	3237	15130	1703	1393	1200	1333	1306	1565	1577	1570
in %	0.21	0.32	1.51	0.17	0.14	0.12	0.13	0.13	0.16	0.16	0.16
sum m+t	87.37	64.27	84.65	58.39	56.55	55.58	55.58	55.71	91.23	91.23	91.23
sum LOI+m+t	100.00	100.00	100.00	100.00	100.00	100.00	100.00	100.00	100.00	100.00	100.00

Table C6. XRF data from Washington State University Geoanalytical Lab continued for samples above.

Appendix D

Sample Photos/Autoradiography

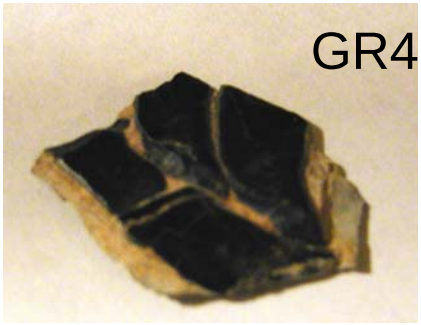

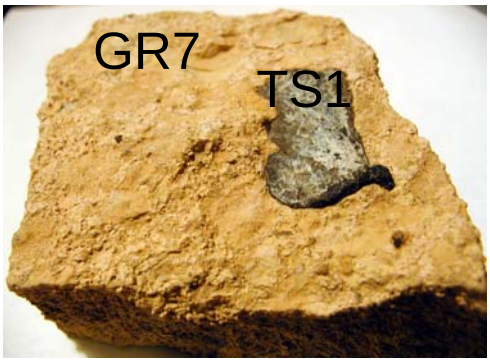

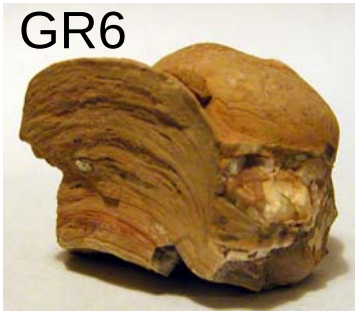


U1
GR5
SB-3 (bone)

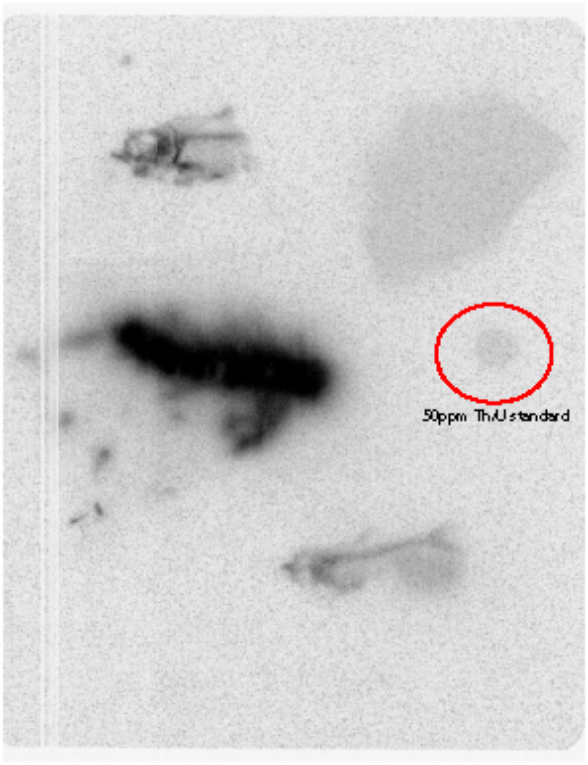
50ppm Th/U standard

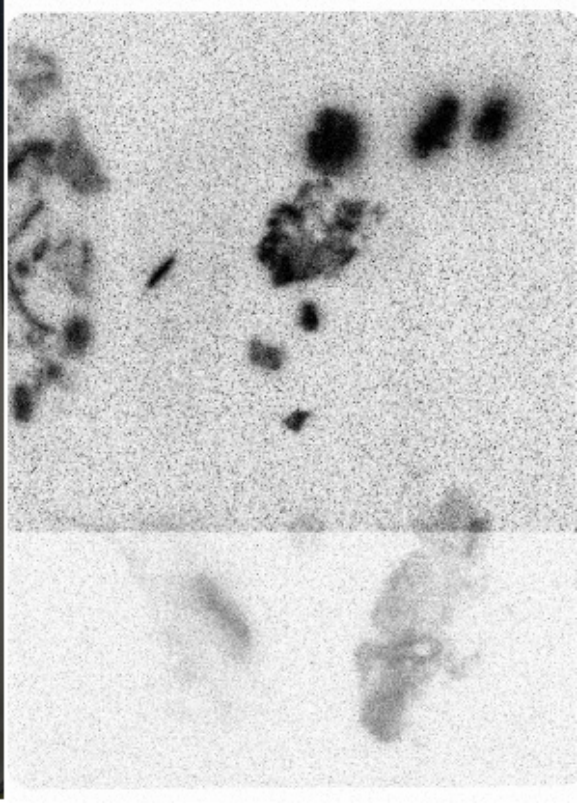

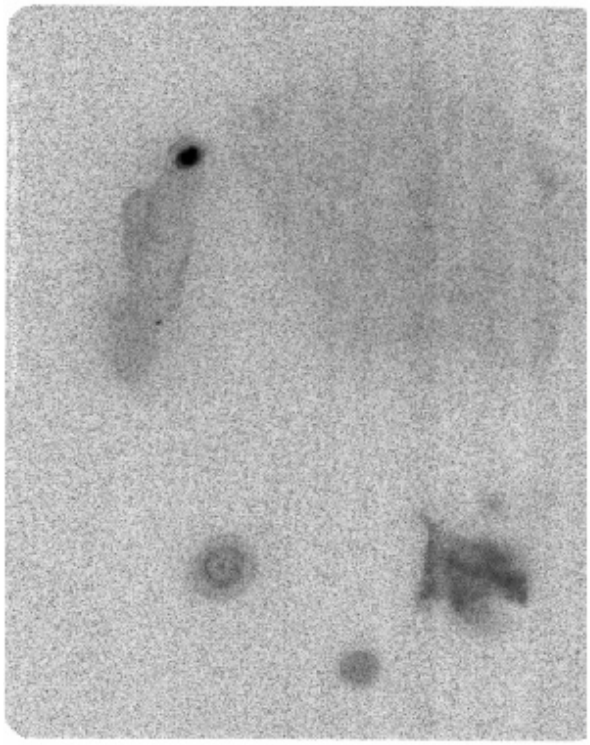

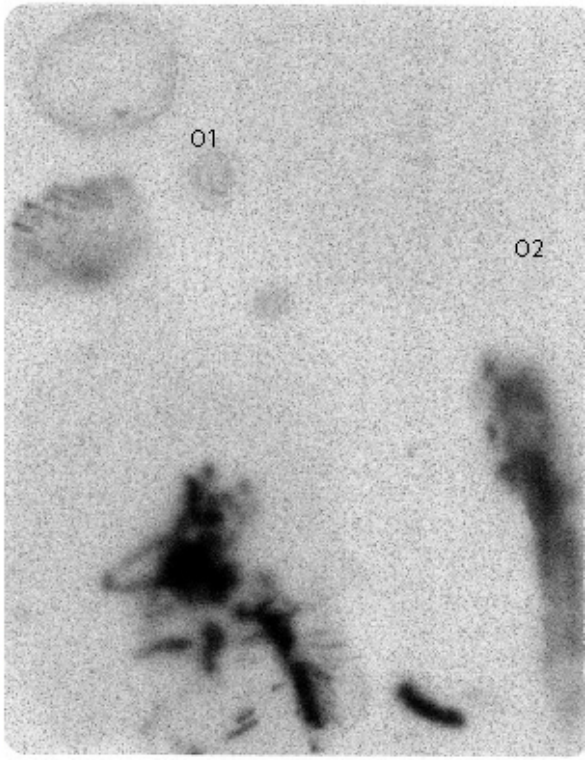
O1
O2

Appendix E

Simplified type section of east end of Fossil Butte National Monument (after Buchheim and Eugster 1998).